

**SCAFFOLD-FREE TISSUE ENGINEERING
FOR ARTICULAR CARTILAGE REPAIR**

By

Devon E. Anderson

A DISSERTATION

Presented to the Department of Biomedical Engineering
and the Oregon Health & Science University
School of Medicine

in partial fulfillment of
the requirements for the degree of

DOCTOR OF PHILOSOPHY

August 2016

School of Medicine
Oregon Health & Science University

CERTIFICATE OF APPROVAL

This is to certify that the PhD dissertation of
Devon Eric Anderson
has been approved

Brian Johnstone, PhD (Mentor/Advisor)

Monica Hinds, PhD (Dissertation Advisory Committee Chair)

Xiaolin Nan, PhD

Carmem Pfeifer, DDS, PhD

Hans Peter Bächinger, PhD

Owen McCarty, PhD

TABLE OF CONTENTS

LIST OF FIGURES	iv
LIST OF TABLES.....	v
LIST OF ABBREVIATIONS.....	vi
ACKNOWLEDGEMENTS.....	viii
ABSTRACT.....	xi
CHAPTER 1: INTRODUCTION & BACKGROUND	1
1.1 Articular Cartilage in Health.....	1
1.1.1 Joint, Bone, & Articular Cartilage Development.....	2
1.1.2 Articular Cartilage Structure.....	8
1.1.3 Articular Cartilage Function	11
1.2 Articular Cartilage in Disease.....	16
1.2.1 Focal Cartilage Lesions.....	17
1.2.2 Degenerative Joint Disease.....	19
1.3 Articular Cartilage Therapies.....	20
1.4 Tissue Engineering for Articular Cartilage Repair	25
1.4.1 Cells	26
1.4.1.1 Chondrocytes	27
1.4.1.2 Mesenchymal Stem Cells.....	29
1.4.1.3 Articular Cartilage Progenitor Cells	32
1.4.2 Scaffolds	34
1.4.2.1 Biomaterial-Based Tissue Engineering.....	34
1.4.2.2 Scaffold-Free Tissue Engineering.....	36
1.4.3 Signals.....	38
1.4.3.1 Growth Factors.....	39
1.4.3.2 Oxygen Tension.....	40
1.4.3.3 Mechanical Stimulation	42
1.5 Dissertation Objective & Aims.....	44
CHAPTER 2: MATERIALS & METHODS.....	47
2.1 Cell & Tissue Culture	47
2.1.1 Cell Harvest & Isolation:	47
2.1.2 Pellet Culture:	48
2.1.3 Tissue Culture:	49
2.2 Tissue Analysis.....	50

2.2.1	Biochemical Analysis:	50
2.2.2	Biomechanical Analysis:	51
2.2.3	Gene Expression Analysis:	52
2.2.4	Histology & Immunohistochemistry:	53
2.2.5	Western Blotting:	55
2.3	Statistical Analysis:.....	55
CHAPTER 3: PROGENITOR CELL CHONDROGENICITY.....		56
3.1	Abstract:	57
3.2	Introduction:.....	58
3.3	Materials & Methods:	62
3.4	Results:.....	65
3.5	Discussion:.....	75
3.6	Conclusions:.....	81
CHAPTER 4: SCAFFOLD-FREE NEOCARTILAGE IN PHYSIOXIA		83
4.1	Abstract:.....	84
4.2	Introduction:.....	85
4.3	Materials & Methods:	88
4.4	Results:.....	94
4.5	Discussion:.....	105
4.6	Conclusions:.....	110
CHAPTER 5: DYNAMIC COMPRESSIVE STIMULATION OF NEOCARTILAGE.....		111
5.1	Abstract:.....	112
5.2	Introduction:.....	113
5.3	Materials & Methods:	117
5.4	Results:.....	123
5.5	Discussion:.....	135
5.6	Conclusions:.....	140
CHAPTER 6: CONCLUSIONS & FUTURE DIRECTIONS.....		141
6.1	Cell Chondrogenicity	142
6.1.1	Articular Cartilage Progenitor Cells	143
6.2	Scaffold-Free Tissue Engineering.....	149
6.2.1	Culture Duration	150
6.2.2	In Vivo Implantation.....	154
6.3	Stimulating Factors for Tissue Maturation	156
6.3.1	Mechanical Stimulation	157
6.3.2	Advanced Microscopy	158
6.4	Final Remarks.....	163

APPENDIX A: CHONDROPLASTY	164
APPENDIX B: NEOCART	167
APPENDIX C: CELL DENSITY & MEDIA VOLUME	172
APPENDIX D: MESENCHYMAL STEM CELL-DERIVED NEOCARTILAGE	175
REFERENCES.....	178

LIST OF FIGURES

CHAPTER 1: INTRODUCTION & BACKGROUND

FIGURE 1.1 – SYNOVIAL JOINT MORPHOGENESIS.....	4
FIGURE 1.2 – ENDOCHONDRAL OSSIFICATION.....	6
FIGURE 1.3 – CHONDROGENIC DIFFERENTIATION OF MESENCHYMAL STEM CELLS.....	8
FIGURE 1.4 – ANISOTROPIC ORGANIZATION OF ARTICULAR CARTILAGE.....	10
FIGURE 1.5 – TERRITORIAL ORGANIZATION OF ARTICULAR CARTILAGE.....	11
FIGURE 1.6 – BULK BIOMECHANICAL PROPERTIES OF ARTICULAR CARTILAGE.....	13
FIGURE 1.7 – LOCALIZED BIOMECHANICAL PROPERTIES OF ARTICULAR CARTILAGE.....	15
FIGURE 1.8 – DISEASE PROGRESSION AFTER FOCAL DAMAGE TO ARTICULAR CARTILAGE..	19
FIGURE 1.9 – SURGICAL THERAPIES TO TREAT ARTICULAR CARTILAGE DISEASE.....	22
FIGURE 1.10 – THE TISSUE ENGINEERING TRIAD.....	26
FIGURE 1.11 – ADVANTAGES OF SCAFFOLD-FREE TISSUE ENGINEERING.....	38
FIGURE 1.12 – HIF REGULATION AND SIGNALING.....	42
FIGURE 1.13 – BIOREACTORS IN ARTICULAR CARTILAGE TISSUE ENGINEERING.....	44

CHAPTER 3: PROGENITOR CELL CHONDROGENICITY

FIGURE 3.1 – BIOCHEMICAL ANALYSIS OF PROGENITOR CELL CHONDROGENESIS.....	67
FIGURE 3.2 – THRESHOLD FOR PROTEOGLYCAN PRODUCTION.....	68
FIGURE 3.3 – QUALITATIVE ANALYSIS OF PROTEOGLYCAN PRODUCTION.....	68
FIGURE 3.4 – DIFFERENTIAL GENE EXPRESSION BASED ON CHONDROGENICITY.....	70
FIGURE 3.5 – OXYGEN-DEPENDENT GENE EXPRESSION.....	71
FIGURE 3.6 – GENE EXPRESSION OF HIGHLY CHONDROGENIC PROGENITOR CELLS.....	72
FIGURE 3.7 – QUALITATIVE IMMUNOHISTOCHEMICAL ANALYSIS OF COLLAGENS.....	74
FIGURE 3.8 – TYPE X COLLAGEN WESTERN BLOTS FOR CHONDROPROGENITORS.....	75

CHAPTER 4: SCAFFOLD-FREE NEOCARTILAGE IN PHYSIOXIA

FIGURE 4.1 – SCHEMATIC OF NEOCARTILAGE SELF-ORGANIZATION.....	95
FIGURE 4.2 – COMPARISON OF SCAFFOLD-FREE SYSTEMS.....	96
FIGURE 4.3 – DEVELOPMENT OF SCAFFOLD-FREE NEOCARTILAGE OVER TIME.....	97
FIGURE 4.4 – CELL VIABILITY WITHIN SCAFFOLD-FREE NEOCARTILAGE.....	98
FIGURE 4.5 – BIOCHEMICAL ANALYSIS OF SCAFFOLD-FREE NEOCARTILAGE.....	99
FIGURE 4.6 – BIOMECHANICAL ANALYSIS OF SCAFFOLD-FREE NEOCARTILAGE.....	100
FIGURE 4.7 – CHONDROGENIC GENE EXPRESSION OF SCAFFOLD-FREE NEOCARTILAGE....	101
FIGURE 4.8 – COLLAGEN ANALYSIS OF SCAFFOLD-FREE NEOCARTILAGE.....	103
FIGURE 4.9 – LOCALIZED MOLECULES OF SCAFFOLD-FREE NEOCARTILAGE.....	104

CHAPTER 5: DYNAMIC COMPRESSIVE STIMULATION OF NEOCARTILAGE

FIGURE 5.1 – BIOREACTOR FOR DYNAMIC MECHANICAL STIMULATION.	119
FIGURE 5.2 – BIOREACTOR SOFTWARE GRAPHICAL USER INTERFACE.....	120
FIGURE 5.3 – BIOREACTOR VALIDATION WITH AGAROSE HYDROGELS.	124
FIGURE 5.4 – PROTEOGLYCAN DISTRIBUTION IN STIMULATED NEOCARTILAGE.	125
FIGURE 5.5 – BIOCHEMICAL ANALYSIS OF STIMULATED NEOCARTILAGE.	126
FIGURE 5.6 – BIOMECHANICAL ANALYSIS OF STIMULATED NEOCARTILAGE.....	127
FIGURE 5.7 – CHONDROGENIC GENE EXPRESSION OF STIMULATED NEOCARTILAGE.	129
FIGURE 5.8 – CHONDROGENIC GENE EXPRESSION CLUSTERING.....	129
FIGURE 5.9 – PROTEIN ANALYSIS FOR FGF SIGNALING.	130
FIGURE 5.10 – COLLAGEN ANALYSIS OF STIMULATED NEOCARTILAGE.	132
FIGURE 5.11 – EXTRACELLULAR MATRIX MOLECULES OF STIMULATED NEOCARTILAGE.	134

CHAPTER 6: CONCLUSIONS & FUTURE DIRECTIONS

FIGURE 6.1 – WNT HOMEOSTASIS.....	146
FIGURE 6.2 – EFFECT OF ADDING GROWTH FACTORS DURING EXPANSION.....	147
FIGURE 6.3 – EFFECT OF EXTENDED CULTURE DURATION.	151
FIGURE 6.4 – TRADEOFF BETWEEN MATURITY AND INTEGRATION.	154
FIGURE 6.5 – PRINCIPLES OF SUPER-RESOLUTION MICROSCOPY.	160
FIGURE 6.6 – SUPER-RESOLUTION MICROSCOPY OF THE PERICELLULAR MATRIX.	161
FIGURE 6.7 – SUPER-RESOLUTION MICROSCOPY EXPERIMENTAL DESIGN.	161
FIGURE 6.8 – SECOND HARMONIC GENERATION MICROSCOPY OF CARTILAGE.....	163

APPENDICES

FIGURE C.1 – EFFECT OF CELL NUMBER PER MEDIA VOLUME ON CHONDROGENESIS.....	174
FIGURE D.1 – MESENCHYMAL STEM CELL-BASED SCAFFOLD-FREE NEOCARTILAGE.	177

LIST OF TABLES

TABLE 1.1 – OXYGEN TENSION WITHIN HUMAN TISSUES.....	41
TABLE 2.1 – TAQMAN PRIMERS.....	52
TABLE 2.2 – PRIMARY ANTIBODIES AND ANTIGEN RETRIEVAL METHODS.....	54
TABLE 2.3 – SECONDARY ANTIBODIES.....	54
TABLE 4.1 – PARAMETERS FOR OPTIMIZATION OF THE SCAFFOLD-FREE SYSTEM	89
TABLE 4.2 – CELL SEEDING DENSITY	90
TABLE 4.3 – MARKERS OF SCAFFOLD-FREE TISSUE MATURATION	97
TABLE 5.1 – DYNAMIC STIMULATION EXPERIMENTAL DESIGN.....	118
TABLE 6.1 –LONG-TERM CULTURE DURATION EXPERIMENTAL DESIGN.....	158

LIST OF ABBREVIATIONS

AC	Articular chondrocyte
ACI	Autologous Chondrocyte Implantation
ACP	Articular Cartilage Progenitor
ADAMTS	A Disintegrin and Metalloproteinase with Thrombospondin Motifs
BCA	Bicinchoninic Acid
BMP	Bone Morphogenetic Protein
BSA	Bovine Serum Albumin
CAM	Cell Adhesion Molecule
CD	Classification Determinant
DAPI	4',6-diamidino-2-phenylindole
DMEM	Dulbecco's Modified Eagle Medium
DMMB	1,9-Dimethylmethylene Blue
DNA	Deoxyribonucleic Acid
ECM	Extracellular Matrix
ELISA	Enzyme-linked Immunosorbent Assay
ERK	Extracellular-Regulated Kinase
FBS	Fetal Bovine Serum
FDA	Food and Drug Administration
FFPE	Formalin Fixed Paraffin Embedded
FGF	Fibroblast Growth Factor
FGFRI	FGF Receptor Inhibitor
GAG	Glycosaminoglycan
GDF	Growth and Differentiation Factor
GUI	Graphical User Interface
HA	Hyaluronic Acid
HIF	Hypoxia Inducible Factor
HOX	Homeobox
HP	Hydroxylysyl-Pyridinoline
HRP	Horseradish Peroxidase
IGF	Insulin-like Growth Factor
Ihh	Indian Hedgehog
IRB	Institutional Review Board
LOX	Lysyl Oxidase
LP	Lysyl-Pyridinoline

MACI	Matrix-Associated Chondrocyte Implantation
MAPK	Mitogen-Activated Protein Kinase
MHC	Major Histocompatibility Complex
MMP	Matrix Metalloproteinase
MRI	Magnetic Resonance Imaging
MSC	Mesenchymal Stem Cell
NGS	Normal Goat Serum
NHS	National Health Service
OA	Osteoarthritis
OCA	Osteochondral Allograft
OHSU	Oregon Health & Science University
PAGE	Polyacrylamide Gel Electrophoresis
PBS	Phosphate Buffered Saline
PCM	Pericellular Matrix
PCR	Polymerase Chain Reaction
PRO	Patient Reported Outcome
P/S	Penicillin-Streptomycin
PTHrP	Parathyroid Hormone Related Peptide
PTOA	Post-Traumatic Osteoarthritis
PVDF	Polyvinylidene Difluoride
RNA	Ribonucleic Acid
SDS	Sodium Dodecyl Sulfate
SHG	Second Harmonic Generation
shh	Sonic Hedgehog
SOX	Sry-related HMG Box
SRM	Super-Resolution Microscopy
STORM	Stochastic Optical Reconstruction Microscopy
STRING	Search Tool for the Retrieval of Interacting Genes/Proteins
TE	Tissue Engineering
TGF- β	Transforming Growth Factor β
TIMP	Tissue Inhibitor of Metalloproteinase

ACKNOWLEDGEMENTS

At each checkpoint on the long journey to becoming a physician-scientist, I am reminded of not only the support, but also the trust, given to me by the individuals who have realized my intent and potential to bring innovative therapies from the laboratory to the operating room. As I finish graduate school, I am especially grateful to my advisor, Dr. Brian Johnstone, who has supported my large and expensive engineering endeavors, trained me as a competent matrix and stem cell biologist, and facilitated my tenuous balance of goals in science and medicine. When I entered his laboratory, Brian was aware of my career intentions, and he immediately embraced and championed the need for surgeon-scientists in our field. His mentorship and friendship over the years have strengthened my passions in both orthopaedic research and academic medicine.

Brian is joined by many other academic mentors in supporting my goals unconditionally. I would like to thank my dissertation advisory committee members Drs. Monica Hinds, Xiaolin Nan, Carmem Pfiefer, and Hans Peter Bächinger, who have each advanced my education by introducing me to topics that not only challenged, but continually excited, me throughout my doctoral research. Thank you to Drs. Owen McCarty and David Jacoby, who recruited me to OHSU and have continued to support my non-traditional goals in engineering and medicine each day since. I am also grateful to my clinical mentors, Drs. Dennis Crawford and Jung Yoo, who have afforded me unique opportunities as an MD/PhD student and have offered invaluable career advice as surgeon-scientists themselves. This research would not have been possible without the generosity and mentorship of Drs. Rob Mauck and Alice Huang, who went out of their way to welcome me into the greater orthopaedic research community and provided me the

engineering training that I needed throughout graduate school. I am forever thankful to my undergraduate advisors Drs. Doug Van Citters, John Collier and Vince Watts, who ignited my strongest passions in engineering, orthopaedic research, and medicine.

This doctoral dissertation is not only an academic pursuit but also a life pursuit during which I am constantly supported by and thankful to my wife, Abigail. When I selfishly dragged her West, Abigail prioritized my career, and I am grateful every day to be married to such a strong, intelligent, and adventurous woman. My parents, Lynn and Dennis, spurred my respective passions in medicine and engineering, and I am thankful for the world of opportunity they have already, and continue to provide, along this endless journey of learning. I am so proud to share my pursuit of a doctorate in parallel with my mother, who impresses me daily as she fulfills her life dream of attaining a doctorate later in life. So too am I humbled by and proud of my father, whose lifelong entrepreneurship and innovation are truly inspirational to a young engineer like myself. I am thankful to my sister, Chelsea, who keeps me grounded in clinical medicine and continually keeps my ego in check. I feel truly fortunate to have such close friends from all stages of my life, and I especially appreciate the comradery of Sarah, Trevor, Drew, Rob, and John as we marched through graduate school together.

This research would not have been possible without the scientific advising, technical support, and daily friendship of lab mates including Dr. Brandon Markway, Dr. Paul Holden, Holly Cho, My Vu Nguyen, Cat Moscibrocki, Paul Jones, Derek Bond, Connie Pritchard, Daniel Simmons, and Ken Weekes. I am especially thankful to Brandon, who has been a constant friend and mentor during graduate school and who also challenged me daily to become a more thoughtful and thorough scientist. I am so grateful for the huge

amount of work that Derek, Connie, and Ken undertook for this dissertation research, and I appreciate that they endured and tolerated my early experiences of being a mentor myself. I am thankful to many individuals at the Shriners Hospital for Children in Portland and at the McKay Orthopaedic Research Laboratories at the University of Pennsylvania; each welcomed me into larger musculoskeletal research communities and provided me the tools and resources I needed to conduct a large portion of this dissertation research. Finally, I am thankful to the OHSU MD/PhD Program, the ARCS Foundation Oregon, the Drinkwards, and the Barnes, who offered not only financial, but also moral, support throughout graduate school.

ABSTRACT

Articular cartilage is the tissue at the junction of bones where its highly organized anisotropic structure facilitates its biomechanical function during skeletal motion. The complex architecture and lack of a blood supply, however, limit the intrinsic ability of cartilage to regenerate following injury. Without repair of focal defects resulting from acute traumatic injury, cartilage progresses toward chronic degeneration and causes significant disability. To date, neither current strategies for surgical repair of focal defects nor biomaterial-based tissue engineering approaches to generate a replacement tissue have successfully reproduced the structural organization or functional mechanical properties of native articular cartilage. The limitations in current approaches to focal cartilage repair demand innovative strategies to generate neocartilage.

Tissue engineering is characterized by a triad consisting of [1] cells that reside within a [2] scaffold and that respond to [3] signals from the culture environment. The overall objective of my dissertation research was to develop a novel scaffold-free tissue engineering approach to generate large-scale mature neocartilage tissues from a single human adult-derived progenitor cell. Unlike biomaterial-based systems, scaffold-free tissue engineering relies on cells to secrete and organize the extracellular matrix over time and in response to environmental signals. Over the course of this dissertation research, I worked within the framework of the tissue engineering triad to: [1] characterize the chondrogenic differentiation capacity (chondrogenicity) of multiple cell types derived from adult human donors; [2] develop a scaffold-free system for large-scale tissue production; and [3] define the role of stimuli representative of the native joint environment, including low oxygen (physioxia) and dynamic mechanical compression, in driving

maturation of scaffold-free tissues. Specifically, I hypothesized that physioxia would stimulate biochemical anabolism of extracellular matrix molecules, and mechanical stimulation would induce structural reorganization toward anisotropy in scaffold-free tissues.

I found that there exists a wide range of baseline chondrogenicity among cells derived from different humans and among clonal populations of cells derived from a single human. Consequently, variation in chondrogenicity influenced gene and protein expression in response to culture in altered oxygen tension. Utilizing bone marrow-derived mesenchymal stem cells (MSCs), articular cartilage derived progenitor cells (ACPs), and articular chondrocytes (ACs) of high chondrogenicity, I developed a novel scaffold-free system with which I generated large neocartilage tissues and investigated the role of both oxygen tension and dynamic compression on tissue maturation. Regardless of environment, MSCs produced hypertrophic cartilage. In physioxia, ACPs produced tissue with significantly enhanced mechanical properties and collagen content relative to AC-derived neocartilage. ACP-derived tissue exhibited a pericellular matrix approaching that of native articular cartilage; however, only ACs produced lubricin. Relative to free-swelling controls, dynamic compression for 14 days did not enhance the biochemical or biomechanical properties of AC- or ACP-derived neocartilage, nor did it influence localization of extracellular matrix molecules. Tissue reorganization in the mechanical environment may require a longer time scale. Ultimately, the ability to generate tissues of the mature articular cartilage phenotype utilizing a scaffold-free approach from a single cell origin may improve the functional properties and therapeutic potential of neocartilage destined for autologous repair.

CHAPTER 1: INTRODUCTION & BACKGROUND

1.1 ARTICULAR CARTILAGE IN HEALTH

Hyaline cartilage, which is also referred to as articular cartilage when it covers the articulating surfaces of long and sesamoid bones within synovial joints, is a highly organized skeletal tissue that functions to transmit and translate loads throughout the skeleton during motion. Hyaline cartilage is also found in the larynx, trachea, nasal septum and sternocostal joints where it provides structural support of the respiratory tract. It is one of three types of cartilage; the others include elastic cartilage and fibrocartilage (1). Each type of cartilage is defined by distinct structure composed of extracellular matrix (ECM) that is suited for its function. Elastic cartilage contains abundant elastin fibers within a dense collagen matrix to function as a flexible support for soft tissue structures of the external ear, the larynx, the eustachian tube, and the epiglottis. Fibrocartilage, which includes the meniscus of the knee, the annulus fibrosis of the intervertebral disc and the temporomandibular disc, lacks elastin and has a predominance of large-fiber type I collagen. Fibrocartilage functions to support a combination of compressive and tensile loads and to distribute loads radially from the axial loading plane. Although all three types of cartilage are prone to structural damage and subsequent loss of function, the focus of this dissertation is limited to tissue engineering strategies for the repair of articular cartilage of synovial joints. In its native and healthy state, articular cartilage resides within the framework of a classical structure-function relationship: the complex tissue structure dictates its biomechanical properties, and the functional environment drives structural organization.

1.1.1 JOINT, BONE, & ARTICULAR CARTILAGE DEVELOPMENT

Articular cartilage coats the bearing surfaces of two opposing bones within synovial joints, which are enclosed within a membrane lined with highly vascularized synovial tissue. In addition to bone, cartilage, and synovium, joints also contain ligamentous and fibrocartilaginous tissues to facilitate specific motion. Embryologic development of synovial joints occurs in a sequence of coordinated processes known as joint specification and cavitation that coincide with development of skeletal bones through endochondral ossification. Formation of all skeletal tissues begins with condensation of mesenchymal cells that subsequently differentiate toward connective tissue lineages. In the early embryo, cells within the mesoderm condense in a process mediated by cell-cell interactions through cadherins and cell adhesion molecules (CAMs), and cells form a pre-cartilaginous matrix with which they establish cell-matrix interactions through CD44 and integrins (2). Cells within the condensation subsequently proliferate in response to fibroblast growth factors (FGF); pattern under the control of sonic hedgehog (shh), homeobox (HOX) transcription factors, and wnt-signaling pathways; and differentiate toward a chondrogenic lineage through transforming growth factor-beta (TGF- β) induction of Sry-related HMG Box (SOX) transcription factors (3). Chondrogenic cells secrete extracellular matrix, and the resultant cartilaginous tissue establishes a template, or anlagen, for formation of bones, cartilage, and joints of the skeleton. Although the initiating mechanism is unknown, coordination of signals within the cartilage template drives the formation and stabilization of an interzone, which marks the future site of a joint by separation of a cartilage anlagen into adjacent parts (Figure 1.1). Canonical Wnt signaling, specifically by Wnt9A, induces chondrocyte dedifferentiation, promotes production of growth and differentiation factor 5

(Gdf5), and inhibits bone morphogenetic proteins (BMPs) through induction of BMP antagonists chordin and noggin (2-4). These signals stabilize the specified cell population of the interzone for subsequent cavitation. Cavitation is characterized by extracellular matrix remodeling and induced, in part, by mechanical forces (5). There is a marked increase in hyaluronic acid (HA) within the developing joint cavity, and HA subsequently acts not only as a lubricant within the extracellular matrix but also as a mediator of cell signaling through interaction with CD44 on interzone cells (3,6). In a positive feedback loop, HA facilitates physical separation of adjacent tissues while mechanical forces—generated by muscles in response to separation—stimulate HA production (2). Mechanical action is necessary for cavitation, and joints fail to fully develop with induced neuromuscular paralysis prior to cavitation (7,8). However, exact mechanotransduction signaling mechanisms that mediate joint development remain unknown, for there are myriad potential pathways and cell-matrix interactions that act within the complex system (9). Following joint specification and cavitation, the adjacent cartilage anlagen on either side provide the template for subsequent bone development through endochondral ossification and articular cartilage formation through mechanisms as yet incompletely understood (10).

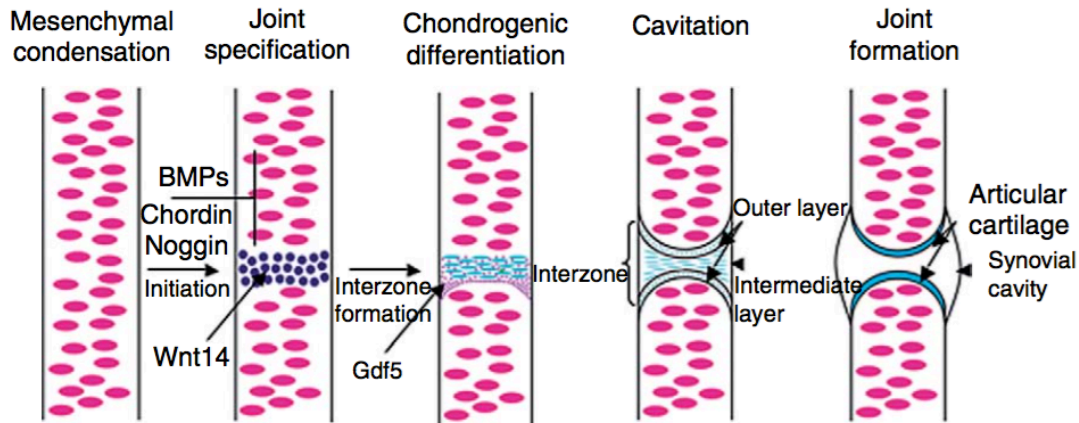


FIGURE 1.1 – SYNOVIAL JOINT MORPHOGENESIS.

Within an initial mesenchymal condensation, an unknown trigger stimulates Wnt14 (now termed Wnt9A) expression at the site of incipient joint formation. Thereafter, Gdf5 is expressed, and the cells take on an elongated morphology and significantly reduce *sox9* and collagen type II expression. BMP antagonists chordin and noggin are expressed in the interzone cells and act to stabilize joint-inducing positional cues. The interzone adopts a three-layered structure (in the case of long bone elements) that undergoes separation or cavitation on mechanically induced synthesis of hyaluronan. The morphogenesis of the functional joint organ results in articular cartilage lining the ends of skeletal elements, which are bathed in synovial fluid, produced by a synovial membrane, and encased within a fibrous capsule. Reproduced with permission from Khan et al. © 2007, Elsevier (3).

Endochondral ossification is a dynamic process for development of bones of the axial and appendicular skeleton (Figure 1.2). Chondrocytes within the elongated cartilage anlagen reorganize into two distinct populations—rounded cells of low proliferation remain at the distal ends and highly proliferative central chondrocytes organize into columns (5). Indian hedgehog (*Ihh*) and parathyroid hormone related peptide (PTHrP) promote differential chondrocyte proliferation rates and organization (11). Central chondrocytes subsequently exit the cell cycle and become hypertrophic, with expression of type X collagen and matrix metalloproteinase 13 (MMP13) at the gene and protein level (5). Hypertrophic chondrocytes undergo apoptosis for replacement with osteoblasts from the neighboring perichondrium; however, increasing evidence indicates that at least some

hypertrophic chondrocytes transdifferentiate directly to osteoprogenitor cells within the endochondral center (12,13). As the cartilaginous matrix is concurrently degraded through catabolic MMP activity and mineralized by hypertrophic chondrocytes, Ihh promotes the transcription factor Runx2 to drive downstream osteogenic differentiation of invading and transdifferentiating osteoprogenitors. Runx2 also promotes vascular invasion into this primary ossification center (14). As the cartilage template is gradually replaced by bone and bone marrow at the primary ossification center, the proliferative chondrocytes at the distal ends remain intact to allow for longitudinal growth *in utero*. Near term or following birth—depending on the specific bone—secondary ossification centers form within the distal portions of the cartilage anlagen, giving rise to distinct regions, which include the metaphysis that separates the ossified diaphysis at the middle of the bone and the epiphysis at the distal ends (5,11). The pool of proliferative chondrocytes within the epiphyseal plate, also known as the growth plate, facilitate longitudinal bone growth throughout adolescence under FGF and Ihh/PTHrP signaling control (11). While regulation of bone formation from a cartilage anlage is well characterized, the development of articular cartilage is not fully understood.

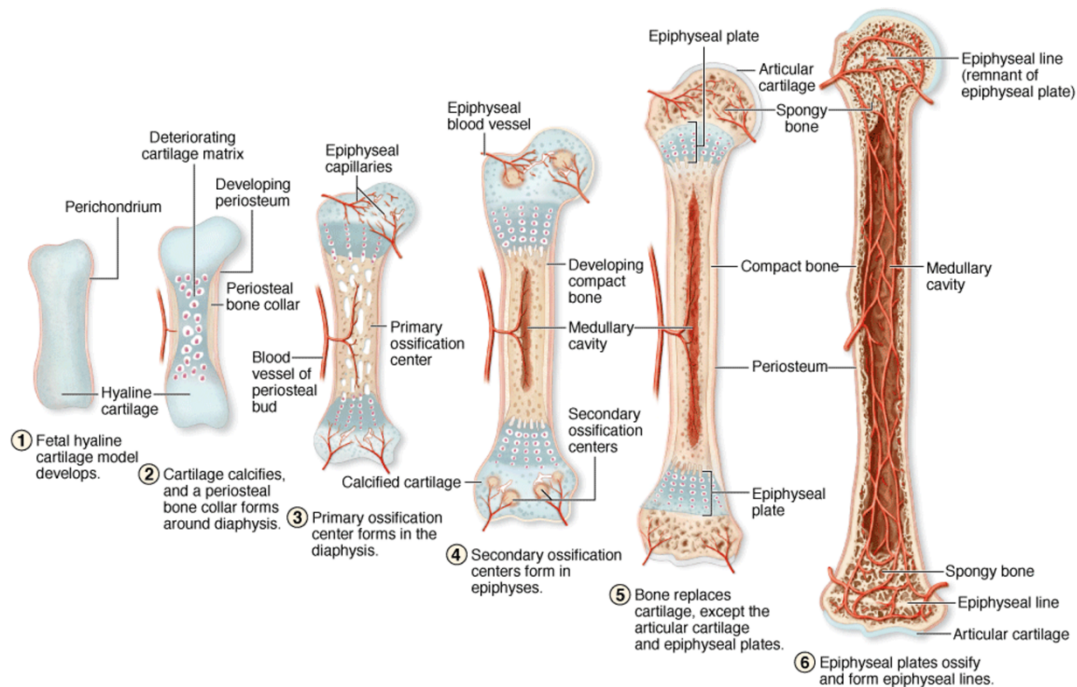


FIGURE 1.2 – ENDOCHONDRAL OSSIFICATION.

[1] The process by which most bones form initially begins with embryonic models of the skeletal elements made of hyaline cartilage. [2] A bone collar develops beneath the perichondrium, causing chondrocyte hypertrophy in the underlying cartilage. [3] Capillaries and osteoprogenitor cells invade from what is now the periosteum to produce a primary ossification center in the diaphysis. [4] Osteoblasts deposit osteoid, which undergoes calcification and is then remodeled as compact bone. Secondary ossification centers begin to develop by a similar process in the bone's epiphyses. [5] The primary and secondary ossification centers gradually come to be separated only by the epiphyseal plate which provides for continued bone elongation. [6] The two ossification centers merge when the epiphyseal plate disappears. Reproduced with permission from Mescher, AL. © 2016, Elsevier (1).

Articular cartilage covers the epiphysis at the distal surfaces of the developed bone, but its embryonic origin is distinct from the cartilage formed by the chondrocytes within the bulk of the anlage. Unlike transient chondrocytes that undergo programmed proliferation, hypertrophy, and death (or transdifferentiation) during programmed endochondral ossification, articular chondrocytes are stable from development into adulthood and do not undergo hypertrophy. Chondrogenic differentiation from a

mesenchymal progenitor cell toward a hypertrophic chondrocyte is under the control of various growth factors and transcription factors that drive progression through stages defined by extracellular matrix molecule production (Figure 1.3). Stable articular chondrocytes first arise during joint specification and are believed to be formed by remnant interzone cells at the surface layer following cavitation (2-4). The transcription factor ERG has been implicated in driving interzone cells toward the stable cartilaginous phenotype; neighboring transient chondrocytes from mesenchymal condensation lack this transcription factor (15). During later stages of development, when the articular cartilage layer is distinguishable from epiphyseal bone, chondrocytes proliferate in an appositional pattern from the surface inward as opposed to localized proliferation of each cell in an interstitial pattern (16). Accordingly, the surface of articular cartilage is thought to contain a progenitor cell population with high colony forming efficiency via self-renewal, extended expansion potential through reduced telomerase activity, and plasticity to differentiate toward multiple connective tissue lineages (17,18). Articular cartilage progenitor cells (ACPs) reside not only in developing articular cartilage but also in stable adult human tissue. ACPs can be distinguished from the total chondrocyte population *in vitro* through cell surface markers and differential adhesion to fibronectin (19); however, identification of progenitor cells *in situ* remains a challenge. Most recently, lineage tracing to identify the origin of chondrocytes during embryonic development of murine articular cartilage confirmed appositional growth from potential progenitors in the superficial zone (20); although, the gene locus chosen to trace tissue development co-localizes to the superficial zone but has not been identified as specific or exclusive to ACPs (21). Following tissue formation *in utero*, articular cartilage is relatively immature and isotropic with respect to

the extracellular matrix. During post-natal development, mechanical forces drive tissue reorganization toward the structural anisotropy characteristic of articular cartilage (22,23).

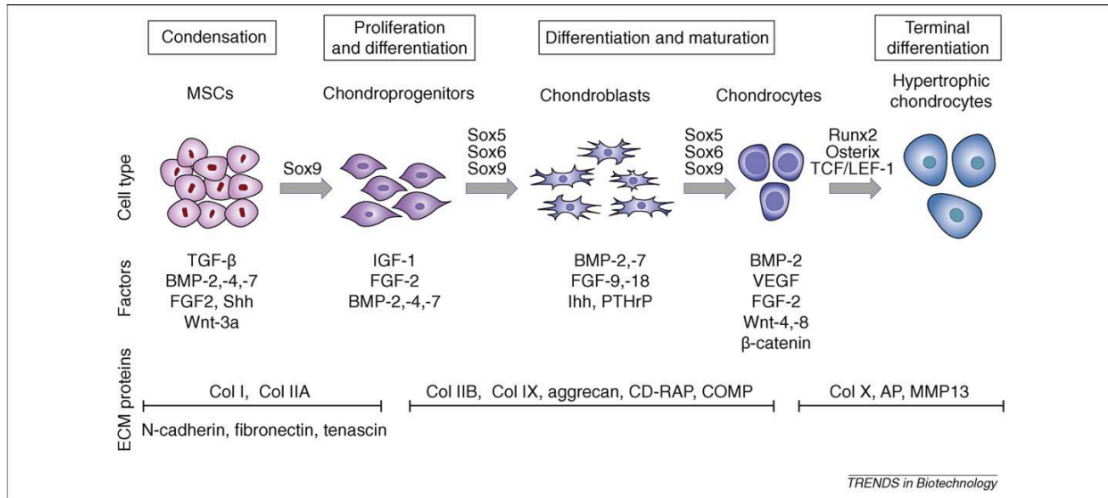


FIGURE 1.3 – CHONDROGENIC DIFFERENTIATION OF MESENCHYMAL STEM CELLS.

The different stages of chondrogenesis are schematically represented. The temporal expression profiles of the different growth and differentiation factors are shown below and the main transcription factors involved in each step are indicated. Proteins that are characteristic of the extracellular matrix (ECM) for the various stages are also highlighted in the lower part of the figure. Abbreviations: AP, alkaline phosphatase; CD-RAP, cartilage-derived retinoic acid-sensitive protein; Col, collagen; COMP, cartilage oligomeric protein; MMP, matrix metalloproteinase; VEGF, vascular endothelial growth factor. Reproduced with permission from Vinatier et al. © 2009, McGraw-Hill (24).

1.1.2 ARTICULAR CARTILAGE STRUCTURE

Articular cartilage is composed of chondrocytes and chondroprogenitors housed within a dense extracellular matrix consisting primarily of type II collagen, aggrecan, and water. At the bulk level, the tissue is composed of 65-85% water, 10-20% collagen (wet weight), and 5-10% proteoglycans (wet weight) (25). The collagenous network of articular cartilage is predominantly fibril-forming type II collagen that is built upon a type XI collagen core and crosslinks with fibril-associated type IX collagen to form heterofibrils.

Articular cartilage has minimal type I collagen and elastin in contrast to fibro- and elastic cartilages (26).

Proteoglycans are macromolecules consisting of a protein core to which polyanionic glycosaminoglycan (GAG) side chains are covalently attached. Among many others, aggrecan is the principle proteoglycan of articular cartilage. Aggrecan forms large aggregates as it decorates the non-sulfated GAG hyaluronan through noncovalent interactions, which are stabilized by link protein (27). The high fixed charge density of GAGs within the matrix generates large repulsive electrochemical forces that avidly attract and hold water (26), and tissue swelling is balanced by elastic resistance of the collagens (28).

While type II collagen and aggrecan are distributed throughout the bulk of the tissue, mature articular cartilage is characterized by both depth-dependent anisotropy and territorial organization from the cell outward with respect to chondrocyte morphology, collagen orientation, and extracellular matrix distribution (Figure 1.4) (29). The superficial zone contains abundant type II collagen oriented parallel to the tissue surface to resist tensile and shear stress, flattened cells in high density, and a unique superficial zone protein (lubricin), which acts as a boundary lubricant. The middle zone exhibits randomly oriented type II collagen fibrils with a high density of proteoglycans, primarily aggrecan. The deep zone contains type II collagen oriented perpendicular to the tissue surface and vertical columns of chondrocytes to resist compressive stresses. A calcified zone marks the transition to bone with hypertrophic cells and an increasing ratio of type X to type II collagen (28,30,31). All zones also exhibit cell-outward anisotropy with distinct regional matrices (Figure 1.5). The pericellular matrix (PCM) contains abundant network-forming

type VI collagen, perlecan, and fibronectin; the cell and its surrounding PCM comprise a chondron (32). The territorial matrix exhibits matrilins and increasing amounts of type II collagen organized in radial bundles. The interterritorial zone, which is furthest from cell, contains densely packed type II collagen bundles that demonstrate radial alignment into arcades spanning the tissue depth (32,33). To accommodate mechanical compressive resistance and viscoelasticity, the tissue is avascular and aneural.

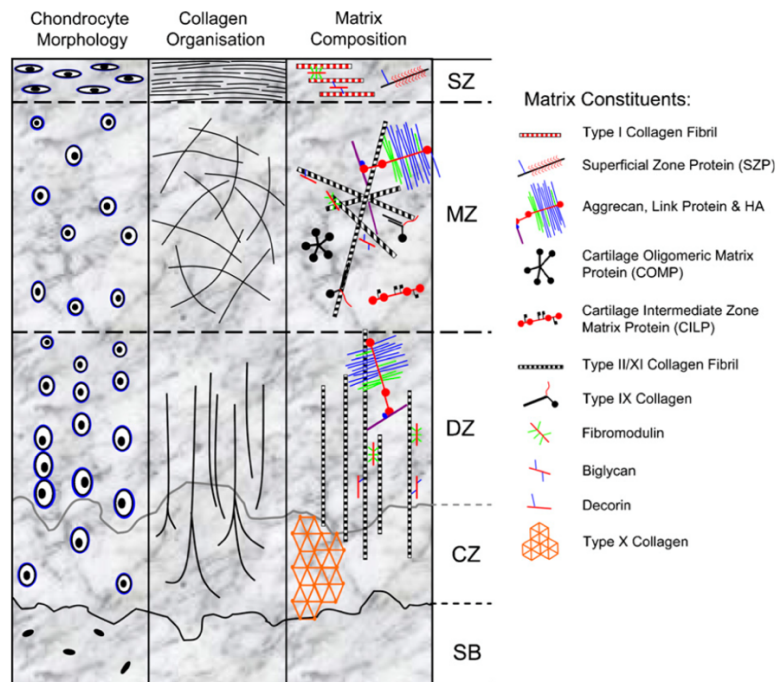


FIGURE 1.4 – ANISOTROPIC ORGANIZATION OF ARTICULAR CARTILAGE.

Articular cartilage consists of four distinct zones: superficial (SZ); middle (MZ), deep (DZ), and a zone of calcified cartilage matrix (CZ), below which is the subchondral bone (SB). Each zone is distinct in terms of its cell morphology (left panel), collagen fiber organization (middle panel), and the biochemical composition of its extracellular matrix (ECM) (right panel). Matrix constituents of each cartilage zone are presented as molecular schematics. Reproduced with permission from Hayes et al. © 2007, Sage (31).

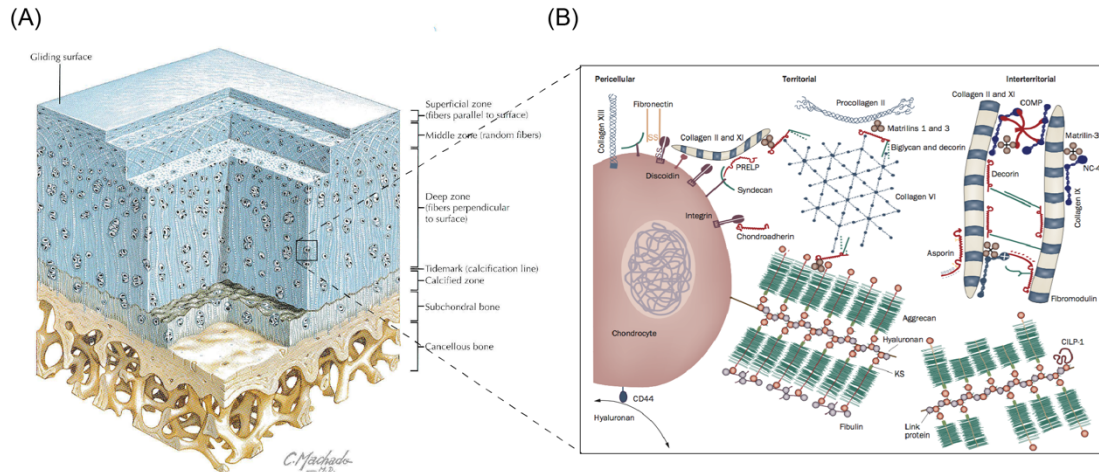


FIGURE 1.5 – TERRITORIAL ORGANIZATION OF ARTICULAR CARTILAGE.

(A) Three-dimensional organization of articular cartilage. (B) The cartilage matrix surrounding chondrocytes in healthy articular cartilage is arranged into territories defined by their distance from the cell. The pericellular matrix lies immediately around the cell and is the zone where molecules that interact with cell surface receptors are located; for example, hyaluronan binds the receptor CD44. Next to the pericellular matrix, slightly further from the cell, lies the territorial matrix. At largest distance from the cell is the interterritorial matrix. The types of collagens and the collagen-binding proteins that form the matrices are different in each zone. Abbreviations: CILP-1, cartilage intermediate layer protein 1; COMP, cartilage oligomeric matrix protein; CS, chondroitin sulfate; KS, keratan sulfate; PRELP, proline-arginine-rich end leucine-rich repeat protein. Reproduced with permission from Thompson, JC. © 2010, Elsevier (34), and Hinegård et al. © 2010, Nature Publishing Group (35).

1.1.3 ARTICULAR CARTILAGE FUNCTION

The primary functions of articular cartilage are to transfer compressive loads between adjacent bones and to translate shear loads between adjacent bearing surfaces for efficient skeletal motion in multiple planes. At the bulk level, articular cartilage demonstrates unique biomechanical properties attributed to biphasic viscoelasticity—a model that accounts for the dynamic and non-linear behavior associated with compression of a composite material consisting of two incompressible and immiscible phases (Figure 1.6). The two phases of viscoelastic behavior include: [1] a fluid phase in which

redistribution of fluid throughout a porous solid matrix generates frictional drag in compression, and [2] the intrinsic viscoelastic nature of the solid constituents of the extracellular matrix in compression (25). The fluid phase is primarily composed of water attracted to and trapped within the dense proteoglycan-rich matrix, where fluid redistribution generates significant swelling pressures. Thus, proteoglycans, and the water they trap, provide the majority of compressive stiffness to the tissue. In confined compression, native articular cartilage has an aggregate modulus from 0.5 to 0.9MPa (36). While proteoglycans provide resistance to compressive strain, collagens of the extracellular matrix resist tensile, shear, and dynamic strains. The Young's modulus for cartilage in tension is 5 to 25MPa depending on axis and location of measurement (28), while the average equilibrium shear modulus for human patellar cartilage is 0.23MPa (25). Articular cartilage is subject to high shear loading at both the bearing surface and at the tidemark where cartilage is anchored to subchondral bone, which is substantially stiffer. At the bearing surface, shear loads are minimized by the inherent low-friction interface between opposing surfaces, boundary lubrication from macromolecules of the synovial fluid, and fluid exudation surface under compression (26). Through these mechanisms, the coefficient of friction (~ 0.0005) at the articular interface of cartilage is the lowest of any known bearing, synthetic or biologic (25). While these represent general biomechanical properties of adult articular cartilage, tissue stiffness under any loading regime is dependent on both tissue maturity and physical location within a joint (23,37). In a classical structure-function relationship, structural anisotropy defines the biomechanical properties at any point within the tissue, and the mechanical environment drives tissue maturation toward depth-dependent and territorial anisotropy (23,38,39).

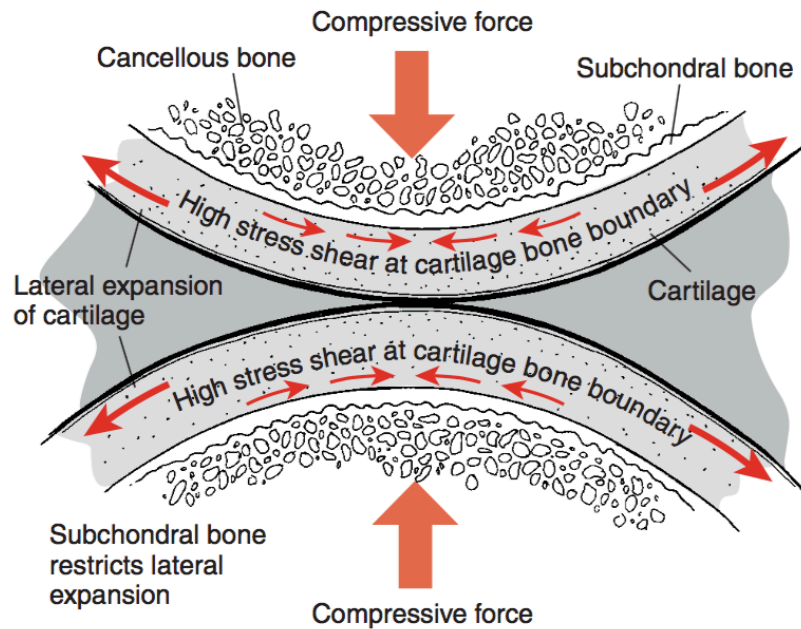


FIGURE 1.6 – BULK BIOMECHANICAL PROPERTIES OF ARTICULAR CARTILAGE.

Under compressive loads, articular cartilage experiences a relatively large lateral displacement due to its high Poisson's ratio, and the tissue displays biphasic viscoelasticity with contributions from both fluid redistribution and ECM molecules. This expansion is restrained by the much stiffer subchondral bone, causing a high shear stress at the cartilage bone interface. Reproduced with permission from Mansour, JM © 2003, Wolters Kluther Health (36).

Each zone throughout the depth of articular cartilage is organized for response to the biomechanical environment at that location (Figure 1.7). During physiologic loading, the superficial zone experiences high fluid flow and exudation, large consolidative compressive strains, and substantial shear and tensile strains (40). As a result, the superficial zone has low GAG content but high collagen content. Collagen is aligned parallel to the bearing surface—an orientation that both maximizes tissue strength in tension and shear and is driven by the predominance of these strains. The superficial zone also represents the bearing surface, and a specialized proteoglycan, lubricin, is produced

by superficial chondrocytes and acts as a boundary lubricant at the tissue and synovial fluid interface (41). The middle zone experiences less bulk fluid flow within the GAG-rich extracellular matrix, and the randomly oriented collagen network provides resistance to high fluid pressures from all directions. The deep zone has the least fluid flow and the highest fluid pressurization. Compressive strains moving through the bulk of the tissue drives type II collagen fibers, which are anchored in subchondral bone, to align perpendicular to the bearing surface. The tidemark at the deepest region represents the transition of cartilage to bone where the matrix is both calcified and rich in network-forming type X collagen; these matrix elements minimize shear strains by creating a gradual stiffness gradient between cartilage and subchondral bone (28). Just as each zone throughout the tissue depth, from superficial to deep, is uniquely structured for function, so too are the territorial zones from the cell outward organized in response to and structured to facilitate biomechanical loading.

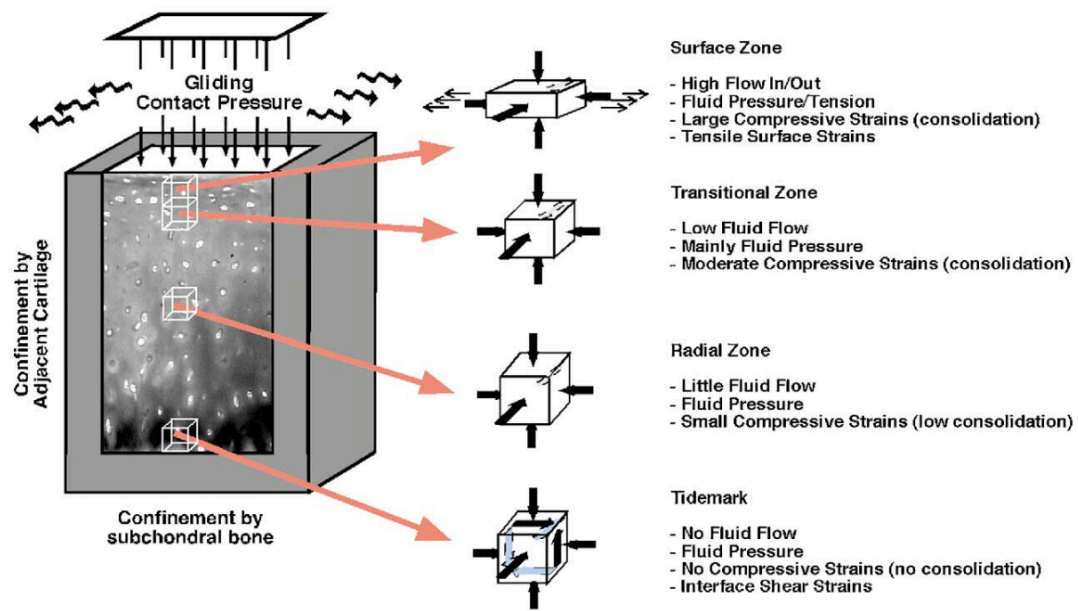


FIGURE 1.7 – LOCALIZED BIOMECHANICAL PROPERTIES OF ARTICULAR CARTILAGE.

Schematic representation of the in vivo mechanical environment at each zone throughout the depth of articular cartilage under intermittent joint loading and motion. Reproduced with permission from Wong et al. © 2003, Elsevier (40).

The chondron consists of each chondrocyte in its immediately surrounding pericellular matrix (PCM). Chondrocytes are suspended within the dense extracellular matrix through connections to individual molecules that support and distribute loads around the cell and transmit mechanical signals that can be converted to chemical signals at the cell surface. Throughout the bulk of the tissue, chondrons function as distinct mechanical units that compact under compression, distort under lateral and shear forces, and recover when unloaded (32). Type VI collagen, a network-forming collagen, completely surrounds the cell to function as a three-dimensional basement membrane equivalent, along with fibronectin and laminin. Perlecan, a large heparan sulfate proteoglycan, colocalizes to the PCM with type VI collagen, and these two molecules collectively contribute to elastic stiffness and hydration to protect the cell under load

(42,43). In addition to its mechanical properties, the PCM facilitates mechanotransduction through chemical signals; heparan sulfate side-chains of perlecan act as a reservoir for growth factors that are released and signal to the adjacent cell under load (44,45). Similar to development of depth-dependent anisotropy, molecules of the PCM, including type VI collagen, perlecan, and laminin are redistributed from the bulk of the immature tissue to the pericellular matrix in response to mechanical conditioning in the post-natal period (43,46). There is also depth-dependent variation in cell morphology in response to regional loading (47). Moving out from each cell, the extracellular matrix is organized into territorial followed by interterritorial zones. The territorial matrix is indistinct but marks a transition from type VI to type II collagen, which creates another stiffness gradient from the relatively fragile cell to the more stiff extracellular matrix (48). During post-natal tissue maturation, organization and orientation of densely packed type II collagen fibers in the interterritorial zones is driven by loads distributed across the bulk of the depth-dependent zones (23).

The structure of articular cartilage across all length scales, from total tissue organization to the morphology of each chondron, is suited for complex mechanical function. Further, the biomechanical environment in which the tissue resides dictates the development and maintenance of tissue structure, but it can also lead to breakdown of structural organization in trauma or chronic disease.

1.2 ARTICULAR CARTILAGE IN DISEASE

The structural organization and avascular nature of articular cartilage permit its mechanical function but limit its regenerative capacity in pathologic conditions. Among

developed nations, musculoskeletal conditions represent the leading contribution to the global burden of disease and total years lost to disability (49). Musculoskeletal diseases are common among both men and women across all ages and socio-demographic strata; although, the prevalence is higher for women and increases significantly with age (50). Musculoskeletal disability and pain lead to a further reduction in the overall health of individuals and populations as patients experience progressive inability to maintain cardiovascular and mental health with impaired physical function (49). The economic burden of musculoskeletal conditions worldwide is immense with contributions from direct health care costs, long-term treatment sequelae, and loss of productivity (50,51). In the United States alone, the overall cost of musculoskeletal disease was estimated at \$873.8 billion in 2011, representing 5.73% of the gross domestic product (52). Among all musculoskeletal conditions, damage to articular cartilage, including from both acute traumatic injury and chronic degeneration, represents the most common cause of disability in the United States (53).

1.2.1 FOCAL CARTILAGE LESIONS

During supra-physiologic or aberrant loading, articular cartilage is subject to mechanical failure, which includes cracking, fibrillation, and wear (36). Impact, repetitive loading, torsional loading, joint malalignment, and foreign bodies within the synovial joint are all potential mechanisms for focal cartilage injury (28). Articular cartilage can also fail when a focal area of subchondral bone loses its blood supply (through an unknown mechanism) in a disease known as osteochondritis dessicans, which primarily affects adolescents (54). Under physiologic loading regimes during activities of daily living,

articular cartilage is suited to sustain substantial forces, which have been estimated between 1.7 and 4.3, but as high as 7.1, times body weight for walking (55). For running, forces at the knee produce a typical stress rate on the order of 100MPa/s (28). Cartilage, however, is subject to instantaneous failure under either impact or torsion dependent on both the magnitude and the rate of loading according to the following criteria: (1) loading rate greater than 100kN/s, (2) stress rate greater than 1000MPa/s, or (3) strain rate greater than 500/s (56). These parameters are easily achieved through blunt trauma in motor vehicle accidents, sporting injuries, or even ground level falls. Repetitive loading or joint malalignment can also cause tissue failure through wear under substantially smaller loading parameters sustained over a longer period. Focal trauma to articular cartilage is common in the general population; the mean annual incidence of patients undergoing surgical repair of articular cartilage is 90 per 10,000 patients with an annual incidence increase of 5% from 2000 to 2010 (57); however, this incidence only represents patients who sought treatment for symptomatic cartilage lesions. The prevalence of chondral injuries among all individuals receiving a knee arthroscopy has been consistently reported around 60%, but fewer than 30% of these patients underwent surgery for a known cartilage injury while the remainder were found to have incidental cartilage pathology with known ligamentous or meniscal injury (58,59). The overall prevalence of full-thickness chondral injuries for athletes is nearly twice that of the general population at 36% and reported as high as 56% for asymptomatic basketball players and runners (60). Following acute injury, focal damage to articular cartilage leads to a substantial decrease in patient reported quality of life comparable to disability experienced from chronic osteoarthritis (61). If left unrepaired, focal cartilage defects lead to altered joint biomechanics and initiate long-term sequelae

including degeneration because of the inability for self-repair despite the presence of resident progenitor cells (Figure 1.8).

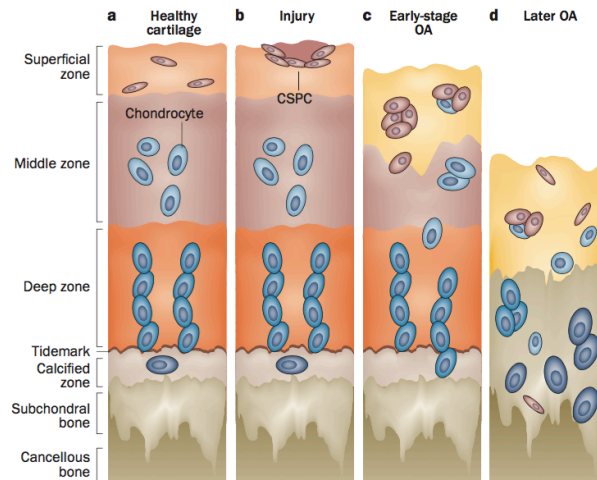


FIGURE 1.8 – DISEASE PROGRESSION AFTER FOCAL DAMAGE TO ARTICULAR CARTILAGE.

(a) In normal adult cartilage, cartilage specific progenitor cells (CSPCs) probably reside in the superficial zone. (b) In response to injury, cartilage CSPCs appear and migrate to the injury site. (c) In early osteoarthritis (OA), characterized by loss of the superficial zone and changes to the internal structure of articular cartilage, cells express distinct surface markers and cell clusters emerge. (d) In late-stage OA, characterized by continued ECM loss and chondrocyte hypertrophy, CSPCs seem to migrate throughout the articular cartilage. Reproduced with permission from Jiang et al. © 2014, Nature Publishing Group (62).

1.2.2 DEGENERATIVE JOINT DISEASE

Osteoarthritis (OA) is a chronic disease of the entire joint characterized by progressive loss, or degeneration, of articular cartilage with remodeling of the underlying bone. In the United States, arthritis is the leading cause of disability (53), with an estimated 23% of the population having doctor-diagnosed arthritis and 42% of those patients reporting limitations to activities attributed to arthritis (63). Based on longitudinal studies in the US population, there is a 1 in 2 and a 1 in 4 lifetime risk for developing osteoarthritis of the knee and hip, respectively (64,65). The etiology for the majority of osteoarthritis

cases remains unknown as the disease arises from a complex interplay of structural, mechanical, genetic, environmental, and inflammatory factors (66); although, known non-modifiable risk factors include increased age and female sex (67). Modifiable risk factors include those that compromise the structural and mechanical integrity of the joint such as obesity, malalignment, acute injury, repetitive loading, and muscle imbalance (67). Degeneration arising secondarily to a specific traumatic injury is known as post-traumatic osteoarthritis (PTOA) and accounts for approximately 12% of the overall prevalence of symptomatic OA of the hip, knee, shoulder, and ankle (68). PTOA arises following either traumatic injury to intra-articular soft tissues—meniscus, ligaments, synovium, or cartilage—or following total joint perturbations such as dislocation, intra-articular fracture, or instability. Though surgical repair of the primary injury can delay the onset or slow the progression of chronic degeneration, PTOA remains an inevitable outcome (69). Ultimately, both the initial traumatic injury and subsequent surgical intervention alter joint biomechanics to produce an aberrant loading environment under which articular cartilage fails. In the case of focal cartilage injuries, the goal of surgical repair is to restore both tissue structure and function to that of the pre-injured native cartilage to prevent, or at least delay, progression toward chronic degeneration.

1.3 ARTICULAR CARTILAGE THERAPIES

Without early intervention, injury to articular cartilage will progress toward osteoarthritis. Total joint arthroplasty is the standard therapy for end-stage osteoarthritis of the knee, hip, shoulder, and ankle, but the polymer, ceramic and metal materials employed in total joint replacements are subject to mechanical failure within a finite period (70). As

life expectancy of the population rises and as our understanding of post-traumatic osteoarthritis informs us that younger patients are at risk of developing OA, it is essential to surgically restore the structure of articular cartilage and the function of joint before the onset of cartilage degeneration that requires total joint replacement. Similarly, when structures other than cartilage are damaged, surgical intervention may serve a chondroprotective role through improved stability or restored biomechanics; these operations may include reduction of intra-articular fractures, corrective osteotomy for joint realignment, meniscal repair or replacement, and ligament reconstruction (71). Surgical interventions to address cartilage specific injuries can be classified as palliative, reparative, and restorative (Figure 1.9). The degree of repair and type of surgical intervention is dependent on both injury-specific parameters such as lesion size, lesion location, and concurrent pathology and patient-specific parameters such as age, activity-level, and surgical history (72).

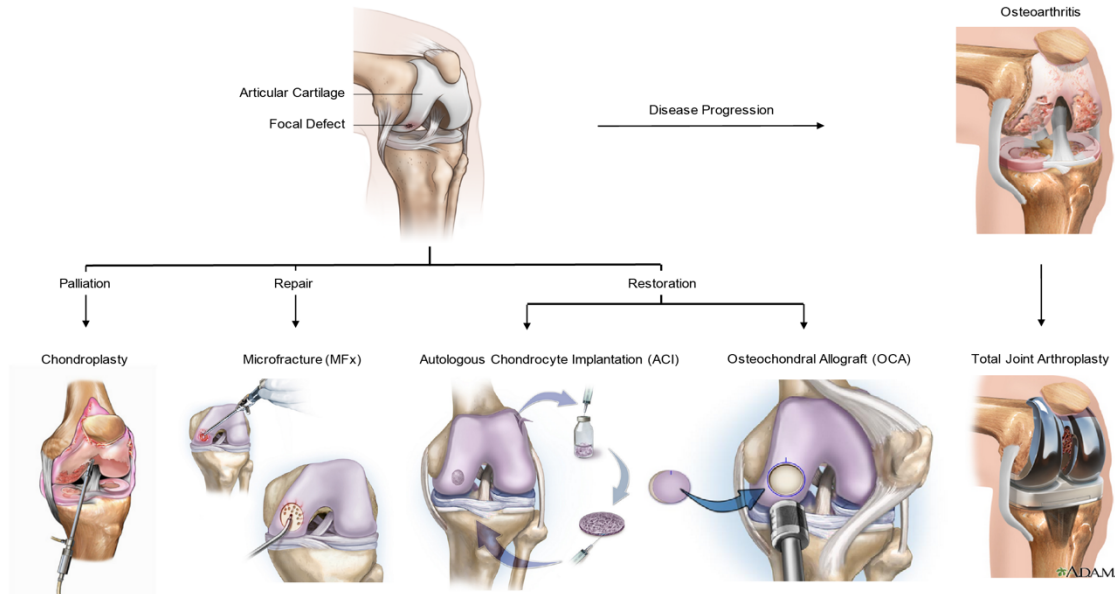


FIGURE 1.9 – SURGICAL THERAPIES TO TREAT ARTICULAR CARTILAGE DISEASE.

Surgical treatment of focal articular cartilage damage can be classified as palliative, reparative, and restorative. Selection of a given surgical approach is informed by both patient and lesion characteristics. The standard of care for treatment of osteoarthritis is a total joint replacement. Portions reproduced from Nucleus Medical Art, A.D.A.M. Education, and Histogenics. Portions adapted with permissions from © 2013, IONMedicalDesigns.

Palliative therapies such as arthroscopic debridement, termed chondroplasty, are techniques utilized to alleviate pain, mechanical symptoms, and recurrent effusions associated with symptomatic focal articular cartilage lesions (73). Currently, arthroscopic chondroplasty represents the vast majority of all cartilage procedures performed in the United States (74). Of the roughly 300,000 total patients who underwent surgery for focal cartilage disease in the United States in 2010, an estimated 220,000 patients underwent arthroscopic chondroplasty (57). Chondroplasty includes a spectrum of techniques specific to individual surgical practices ranging from radiofrequency thermal ablation to subchondral abrasion to mechanical chondroplasty. The latter, which is the least invasive and most common, consists of debriding the unstable cartilage tissue to a stable rim.

Despite the high prevalence, limited outcomes data exist regarding short- and long-term results following chondroplasty. To date, the procedure has only been characterized as a primary treatment for osteoarthritis (OA) or with concurrent surgical intervention, most commonly sub-total menisectomy (75-80). Heavily cited studies have investigated the effect of debridement and lavage in subjects with osteoarthritis, demonstrating limited benefit (75,81). While investigation into the efficacy of this procedure as a primary treatment for OA was warranted, a majority of patients receiving chondroplasty are younger and do not have evidence of joint disease beyond a focal cartilage lesion (74). The lack of outcomes data on chondroplasty in patients without evidence of osteoarthritis, meniscal injury, or concomitant ligament tear prompted our clinical investigation (Appendix A) into the efficacy of this commonly performed procedure in the general population and in isolation from other surgical intervention.

Performed about half as often as palliative chondroplasty, reparative techniques are employed to stabilize a focal cartilage defect by filling it with a substitute tissue. In marrow stimulation techniques, which include microfracture, communication between the cartilage defect and the underlying bone marrow is created by drilling holes or tapping small fractures (microfracture) through the subchondral bone. Subsequently, marrow elements form a clot that serves as a structural scaffold into which progenitor cells from the marrow migrate, differentiate, and create a tissue—the resultant tissue is fibrocartilaginous with mixed cartilage and fibrous tissue elements (82). Microfracture remains the standard of care for small lesions in less active patients (72); and significantly improves knee function up to two years following surgery (83). Long-term clinical efficacy, however, is limited by high incidence of resultant subchondral pathology (84), inability to control repair tissue

volume, functional mismatch between fibrocartilage and adjacent articular cartilage, and high failure rates in athletes (83).

Restorative techniques for articular cartilage repair include transplantation of autologous or allogeneic cells or tissues to restore the defect with a cartilaginous substitute. In autologous chondrocyte implantation (ACI), tissue is harvested from a non-weight bearing articular surface, cells are isolated and expanded *ex vivo*, and a high-density cell suspension is injected under a periosteal or collagen flap. This procedure has shown durable clinical benefit up to ten years following intervention for larger unipolar lesions (85); however, ACI is limited by the need for two surgical interventions, long recovery time for improved functional outcomes, and the production of a fibrocartilaginous tissue following chondrocyte de-differentiation *ex vivo* (86). Next-generation techniques, termed matrix-associated chondrocyte implantation (MACI), utilize a scaffold upon which to seed chondrocytes prior to or upon implantation in an attempt to improve the structural and mechanical properties of ACI tissue. Over the past decade, a variety of collagen- and hyaluronan-based MACI products have demonstrated significant benefit in comparison with microfracture or ACI in clinical trials in Europe (87). NeoCart, which consists of autologous chondrocytes seeded in a collagen matrix and cultured in a bioreactor prior to implantation, is currently the only MACI therapeutic under investigation in comparison with microfracture in the United States (88,89). Clinical and radiographic outcomes from the US Food and Drug Administration (FDA) Phase II clinical trial results are promising at five-year follow-up—studies for which I helped to analyze and report the data (Appendix B). Along with the same limitations as those for ACI, MACI products are further hindered by a long and expensive path to regulatory approval. A final category of restorative

techniques includes transplantation of osteochondral tissues to fill focal defects in articular cartilage and underlying bone. Autologous transplants from another articular surface are associated with high donor-site morbidity. Living osteochondral tissues from allogeneic donors, however, successfully restore the defect with a tissue that is of native structure, that anchors and integrates into surrounding osseous tissue, and that functions properly in the mechanical environment. Osteochondral allografts (OCA) have demonstrated “good-to-excellent” clinical outcomes over long-term follow-up, especially for large unipolar lesions on load-bearing surfaces (90); however, there is a limited supply of allografts needed to restore articular cartilage for the large population suffering from focal cartilage damage.

Focal cartilage repair has evolved from minimally invasive palliative procedures to multi-step cell-based therapies over the past three decades; however, all cartilage repair and restoration techniques, aside from OCA, are limited by the inability to reproduce the architecture of native cartilage necessary for proper function in the mechanical environment. Widespread application of OCA is limited by availability of resources amid a substantial and growing population that needs focal cartilage repair to prevent progression to chronic degeneration. The lack of a widely available tissue that can fulfill the structural and functional requirements of articular cartilage demands a tissue engineering approach to produce a tissue suited for focal cartilage repair.

1.4 TISSUE ENGINEERING FOR ARTICULAR CARTILAGE REPAIR

The traditional paradigm for tissue engineering consists of a triad encompassing [1] a scaffold that houses [2] cells that respond to [3] signals from the culture environment

(Figure 1.10). While each component of the triad represents an independent variable for tissue engineering, the interactions among these three components contribute to a complex system that can potentially be tuned to produce tissues of a favorable phenotype. Specifically, cells build and remodel the extracellular scaffold or matrix over time in response to signals, the scaffold facilitates delivery of signaling molecules and transmits mechanical stimuli to cells, and signals regulate cell cycle, differentiation, and extracellular matrix metabolism (91).

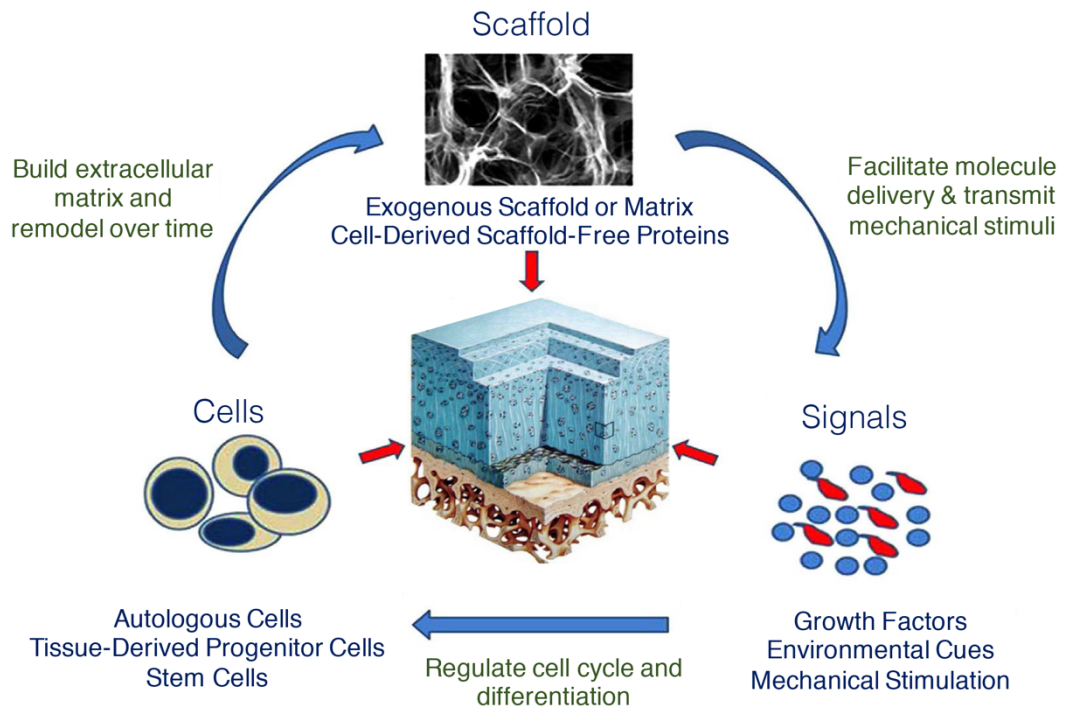


FIGURE 1.10 – THE TISSUE ENGINEERING TRIAD.

Schematic of the three elements—cells, scaffold, and signals—that contribute to a tissue engineering system. Adapted with permission from Murphy et al. © 2013, eCM (91).

1.4.1 CELLS

Cells of a chondrocyte phenotype and cells with chondrogenic differentiation potential represent potential cell sources for articular cartilage tissue engineering and

specifically include: primary or expanded articular chondrocytes (ACs) derived from autologous or allogeneic sources; adult bone marrow-derived mesenchymal stem cells (MSCs); induced pluripotent stem cells (iPSCs); adipose-derived stem cells (ASCs); embryonic stem cells; and adult tissue-derived progenitor cells, which are termed articular cartilage progenitor cells (ACPs) when isolated from hyaline cartilage. Adult human-derived ACs, MSCs, and ACPs were used throughout the work presented in subsequent chapters, and each of these cell types present benefits and limitations in cartilage tissue engineering application and clinical practice.

1.4.1.1 CHONDROCYTES

Within adult articular cartilage, chondrocytes reside at low density (5-10% total tissue volume) in an extensive extracellular matrix that they build and maintain through a balance of anabolic and catabolic control (92). As described in the clinical approaches to focal cartilage repair, autologous chondrocytes are widely used in clinical restoration procedures including ACI; although, to achieve sufficient cell numbers to fill a focal defect with autologous cells seeded in a scaffold or in suspension, chondrocytes must be expanded *in vitro*. Monolayer expansion of chondrocytes, however, induces modulation of the articular chondrocyte phenotype in a process known as dedifferentiation, which is characterized by decreased extracellular matrix synthesis (93), a shift from expression of type II to type I collagen at both the gene and protein level (94), loss of gene expression for aggrecan and lubricin (95), changes to the integrin profile on the cell surface (96), and differential expression of metabolic mediators and growth factors that regulate extracellular matrix homeostasis (97,98). Though the mechanism for phenotypic

modulation is not entirely known, the presence of serum in cell propagation and a two-dimensional growth environment facilitate these changes (99). Upon *in vitro* expansion, chondrocytes further experience telomere erosion and consequential replicative senescence, which has been estimated to artificially age chondrocytes by up to 30 years for an 8-10 fold expansion (100,101). Ultimately, dedifferentiation promotes a phenotype similar to that of a fibrochondrocyte; thus, tissues generated following ACI and MACI procedures are fibrocartilaginous. Following dedifferentiation, chondrocytes may regain the articular chondrocyte phenotype through redifferentiation in serum-free medium supplemented with growth factors and in three-dimensional culture, either within a hydrogel or in high cell density pellets (93,102).

While chondrocytes are stable throughout much of adult life, *in vitro* redifferentiation capacity of adult-human derived chondrocytes is significantly reduced with age and highly varied among human donors (101,103). Further, juvenile human-derived and expanded chondrocytes demonstrate significantly higher redifferentiation capacity with respect to extracellular matrix production, chondrogenic gene expression, and neocartilaginous tissue formation when compared with chondrocytes derived from adult humans (104). Juvenile cells, thus, represent a potential cell population with which to generate tissue engineered cartilage from an allogeneic source and are the basis for an ongoing clinical trial utilizing minced juvenile articular cartilage implanted into focal cartilage defects (105). Since chondrocytes are physically separated from both the blood supply and other cell types by the dense extracellular matrix *in situ*, they lack constitutive major histocompatibility complex (MHC) cell surface receptors for T-cell immunogenic

responses and actively express negative regulators of the immune response (106), thus, allowing for potential allogeneic transplantation.

To reduce the potential for phenotypic modulation during expansion, primary chondrocytes from large animal sources have been studied as cell source for tissue engineering; however, the availability of primary cells from humans is limited similar to transplant tissues. A majority of animal studies have employed primary chondrocytes derived from neonatal or juvenile bovine tissues. These cells have high anabolic capacity to produce robust cartilaginous tissues (31,107), yet unlike allogeneic human cells, xenogeneic chondrocyte-derived tissues evoke an innate immune response in the host characterized by natural killer cells, monocytes, and macrophages (108-110). While animal studies utilizing primary chondrocytes have provided invaluable insight to chondrocyte biology and tissue engineering methods, clinical application of xenograft tissues is unlikely due to potential for immune rejection. The limitations associated with chondrocyte-based tissue engineering, especially phenotypic modulation and cell availability, have generated significant interest in identifying stem and progenitor cell populations for articular cartilage tissue engineering.

1.4.1.2 MESENCHYMAL STEM CELLS

Stem cells represent naïve cells that differentiate to specific tissue lineages during development, but they also reside within tissue compartments to replenish cell populations over the lifetime of the individual. Mesenchymal stromal/stem cells (MSCs) have been extensively characterized over the past three decades following identification and isolation of this cell population from bone marrow aspirates. MSCs exhibit the following properties

in vitro: adherence to plastic; the ability to form single-colony forming units-fibroblastic (CFU-F); expression of the cell surface antigens CD105, CD73, and CD90; lack of cell surface antigens CD45, CD34, CD14, CD11b, CD79 α , CD19, or HLA-DR; and potential to differentiate toward bone marrow stromal, chondrogenic, osteogenic, and adipogenic lineages (111-115). In addition to providing a pool of progenitor cells with which to regenerate tissues, MSCs create a unique niche in bone marrow to support hematopoiesis, and they secrete trophic factors to promote tissue repair following injury (114). Not only are MSCs immunoprivileged with low MHC expression similar to chondrocytes, but they also modulate the local immune environment through suppression of immune cell proliferation and cytokine release (114,116). MSCs represent 2-3% of the nucleated cell fraction of a bone marrow aspirate and can be isolated from the total cell population by selective adherence to tissue culture plastic (111,117). The MSC population derived from bone marrow aspirate of an adult human is highly heterogeneous with respect to cell surface markers (making isolation based on cell surface marker expression difficult) and differentiation capacity, such that individual cells may be lineage restricted (115,118). MSCs also reside within connective tissues throughout the body (114); these too are heterogeneous populations that exhibit preferential differentiation toward the tissue from which they were derived (119,120). Though MSCs are characterized by CFU-F capacity *in vitro*, clonal populations derived from self-renewing populations lose multipotent differentiation capacity and undergo replicative senescence with expansion due to lack of telomerase (121,122), which calls into question the true stemness of this cell population. More recent work suggests that MSCs are likely progenitor, not true stem, cells derived from a common pericyte stem cell lineage (123,124). As pericytes arise from both neural

crest cells of the ectoderm and directly from the mesoderm, the diverse developmental pathways for this common cell pool may explain heterogeneity among populations of mesenchymal progenitor cells that were historically all considered equivalent based on *in vitro* criteria (114).

Regardless of developmental origin, MSCs represent a potential cell source for engineering connective tissues based on both multipotential differentiation capacity and relatively easy harvest from a bone marrow aspirate for autologous application. With regard to articular cartilage tissue engineering, bone marrow-derived MSCs undergo chondrogenesis *in vitro* when cultured in three-dimensions and in the presence of necessary growth factors and supplements. Priming MSCs with fibroblast growth factor 2 (FGF2) during monolayer expansion delays replicative senescence, promotes cell proliferation, and enhances subsequent chondrogenesis (125-128). To initiate chondrogenesis, MSCs must be transferred into a 3D culture system, either seeded into an exogenous scaffold or centrifuged into a high cell density pellet to facilitate cell condensation. Exogenous addition of transforming growth factor-beta (TGF- β) is necessary to initiate *in vitro* chondrogenic differentiation through upregulation of Sox9, the master transcriptional regulator of chondrogenesis (129,130). The synthetic glucocorticoid dexamethasone is another necessary mediator of *in vitro* chondrogenic differentiation and enhances TGF- β activity through unknown mechanisms (129,131). With chondrogenic induction, MSCs elaborate proteins of the articular cartilage tissue including type II collagen and aggrecan; however, they also produce abundant type X collagen and have high alkaline phosphatase activity, which are both markers of chondrocyte hypertrophy in the endochondral ossification pathway (129,130). Since the mechanisms that maintain the articular

chondrocyte phenotype *in situ* remain unknown, we are presently unable to modulate *in vitro* chondrogenesis toward a stable cell phenotype. The recent identification and characterization of a tissue-derived progenitor cell population that resides within adult articular cartilage may offer a cell source to overcome limitations of MSC differentiation toward hypertrophic chondrocytes destined for endochondral ossification. *This is the basis for the hypothesis that I tested in the work presented in Chapter 3 of this dissertation.*

1.4.1.3 ARTICULAR CARTILAGE PROGENITOR CELLS

Presently, articular cartilage is believed to originate from the interzone during joint specification and to be maintained by a progenitor cell population that resides within the superficial zone throughout adulthood. Articular cartilage progenitor cells (ACPs) were first identified as a stable and slowly proliferating cell population that fail to form the full tissue when cell cycle progression is inhibited (16). Subsequently, these cells were localized *in situ* in juvenile mammalian cartilage by a unique integrin signature and Notch 1 expression (17,132). When isolated from the total chondrocyte population through differential adhesion to fibronectin based on integrin density (133), ACPs exhibit high colony-forming efficiency and phenotypic plasticity toward multiple connective tissue lineages when engrafted into chick embryos (17). Characterization of ACPs derived from adult humans revealed that they differentially express CD49e, $\alpha 5$ integrin, from the total chondrocyte population, and regardless of donor age they maintain phenotypic plasticity as well as karyotype with extended population doublings due to enhanced telomerase activity (19). Further studies have shown that ACPs persist in osteoarthritic tissue despite fibrillation and degeneration of the articular surface (134,135), and they migrate to sites of

injury where they differentiate and modulate tissue repair (136,137). As articular cartilage lacks the ability for intrinsic regeneration, these cells are likely more supportive than regenerative in osteoarthritis, especially as the deranged biomechanical environment limits structural reorganization of the tissue. Most recently, lineage tracing studies corroborated that a group of cells near the articular surface undergo proliferation in an appositional growth mechanism during tissue development (20); although, the cell marker was not necessarily specific to the ACP population (21). Further investigation into distinct markers for ACPs will hopefully finalize the mechanism for not only development but also maintenance of the mature tissue.

The role of ACPs *in situ* remains controversial as they have not been definitively identified and they do not effectively repair damaged tissue; however, ACPs are a promising cell source for *in vitro* tissue engineering. First, ACPs retain chondrogenic differentiation capacity following extensive expansion from clonal populations (19), which may overcome challenges of chondrocyte dedifferentiation to achieve sufficient cell numbers for autologous tissue repair. Second, ACPs may be preferentially committed to the chondrogenic lineage, similar to the preference of bone marrow-derived MSCs and adipose-derived stem cells (ASCs) to the osteogenic and adipogenic lineages, respectively (138). The initial characterization of both human- and horse-derived ACPs showed that the cells, in contrast to MSCs, do not undergo hypertrophy following chondrogenic differentiation (19,139). Thus, ACPs may overcome the main limitation of MSCs based on the potential to generate a stable articular cartilage tissue phenotype. Despite a promising cellular phenotype following differentiation, ACPs generated a fibrocartilage tissue when seeded into a fibrin scaffold and implanted into a focal cartilage defect in the first tissue

engineering application (140). The benefits over alternative cell sources, however, warrant further investigation into the use of ACPs in tissue engineering systems for focal articular cartilage repair. *This is the basis for the hypothesis that I tested in the work presented in Chapter 4 of this dissertation.*

1.4.2 SCAFFOLDS

While cells within tissue engineered neocartilage define phenotype, the scaffold surrounding those cells provides structure that dictates tissue function. The ideal scaffold for articular cartilage is that of the native and mature extracellular matrix, and tissue engineering strategies seek to reproduce comparable tissue structure that can function in the native biomechanical environment. Fundamentally, a scaffold should: consist of an interconnected porous network to allow for diffusion of nutrients and wastes; be biocompatible and bioresorbable with a degradation rate that matches tissue growth rate; facilitate cell attachment, proliferation, and differentiation; and possess material properties suited for the biomechanical environment (28). The field of articular cartilage tissue engineering has historically employed exogenous biomaterial-based scaffolds with which to build tissues *in vitro*; however, an emergence of scaffold-free tissue engineering techniques over the past decade has enabled the production of tissues utilizing cell-derived extracellular matrix molecules as a scaffolding.

1.4.2.1 BIOMATERIAL-BASED TISSUE ENGINEERING

There are two major categories of biomaterials used for soft tissue engineering: natural polymers, either protein- or carbohydrate-based, produced by living organisms or

synthetic polymers produced through chemical reactions (28). Scaffolds derived from natural polymers are generally biocompatible, non-toxic to cells, and exhibit material properties similar to the extracellular matrix. For instance, fibrous polymeric biomaterials composed of collagen, silk, or cellulose have similar mechanical properties to the solid phase of articular cartilage while hydrogel polymers composed of agarose, alginate, or hyaluronic acid tightly hold water and behave similarly to the fluid phase of native tissue. Overall, natural polymers are limited by difficult manufacturing processes, high variation among batches, and relative mechanical inferiority to both native tissue and synthetic polymers (141). Synthetic polymers such as poly-glycolic acid (PGA), poly-lactic acid (PLA), poly-caprolactone (PCL), and poly-ethylene glycol (PEG) can be manufactured to meet specifications including porosity for cell infiltration, bioresorption rate to accommodate tissue growth, and mechanical stiffness to support mechanical loads. These properties, however, can also be detrimental as the biomaterial may influence cell phenotype, degradation products may be toxic to cells, and stiff substrates may shield cells from mechanotransduction signals (142). Composites that combine multiple scaffold materials, either natural or synthetic, offer additive benefits from individual constituents, but they also increase complexity and variation to the fabrication process (141). To date, biomaterial-based tissue engineering has failed to produce a cell-based therapeutic that meets the structure or functional demands of native articular cartilage, and alternative strategies are warranted.

1.4.2.2 SCAFFOLD-FREE TISSUE ENGINEERING

In the absence of cues from an initial extracellular framework, cells drive formation and maturation of a three-dimensional tissue composed of extracellular matrix molecules. Scaffold-free tissues may offer advantages over biomaterial-based tissue engineering at all stages from cell seeding through implantation (Figure 1.11). Scaffold-free cartilage tissue engineering first emerged as an *in vitro* method to study developmental processes of chondrogenesis in coalescing limb bud mesenchymal cells (143-145). Subsequently, an *in vitro* model system to study chondrogenic differentiation was developed by centrifuging mesenchymal stem cells at high density into micromass culture (129,146,147). Scalable scaffold-free techniques to create large cartilaginous tissues for potential cartilage repair emerged independently by Hu et al. (2006), Novotny et al. (2006) and Hayes et al. (2007), and each showed that neonatal mammalian primary chondrocytes build robust tissues with characteristics of the articular cartilage tissue phenotype (31,148,149). Scaffold-free tissue engineering methods are categorized by two models: self-assembling and self-organizing, which differ based on cell seeding methods.

Self-assembled tissues form through cell condensation in the absence of external stimuli (142). In what is known as the differential adhesion hypothesis of tissue formation, cells in suspension will minimize free energy by binding in direct cell-cell contact, which decreases the surface tension across the entire cell population (150). When suspended into non-adherent culture *in vitro*, neighboring cells bind and organize through N-cadherin cell surface receptors, similar to initial events of mesenchymal cell condensation that precede chondrogenesis (142). Following condensation and given the correct differentiation signals, chondrogenic cells secrete and model the extracellular matrix in a sequential and

spatial pattern representative of the pre-cartilaginous matrix during development (46,151,152). Cartilage tissue formation through self-assembly has been extensively characterized utilizing primary chondrocytes harvested from neonatal or juvenile animals (148,149,152-155), as well as with expanded adult human-derived articular chondrocytes (HACs) and bone marrow-derived mesenchymal stem cells (MSCs), although each from a single donor (156). In contrast to cell-mediated self-assembly, self-organizing models of scaffold-free tissue engineering employ external cues to guide the cells toward condensation. Specifically, cells are centrifuged from suspension into an aggregate pellet or onto a substrate, including polymer membranes (157) or protein-coated membranes (31,158-160), to define tissue dimensions. Culture on an adherent substrate constrains the bottom cell layer through cell surface attachments; although, neighboring cells interact through cell-cell attachments similar to the self-assembling process. Unlike self-assembly, self organization can be manipulated to create tissues of complex geometries (161,162). Scaffold-free methods for large-scale tissue engineering, however, are limited by the cells' secretory capacity of extracellular matrix molecules, high cell density required for seeding, and diffusion of nutrients through a dense matrix with development. Regardless of tissue engineering system, *in vitro* tissue formation and development is governed by signals in the culture environment. *In this dissertation research, I developed a scaffold-free self-organizing tissue engineering system with which to generate large-scale neocartilage tissues with cells derived from adult humans.*

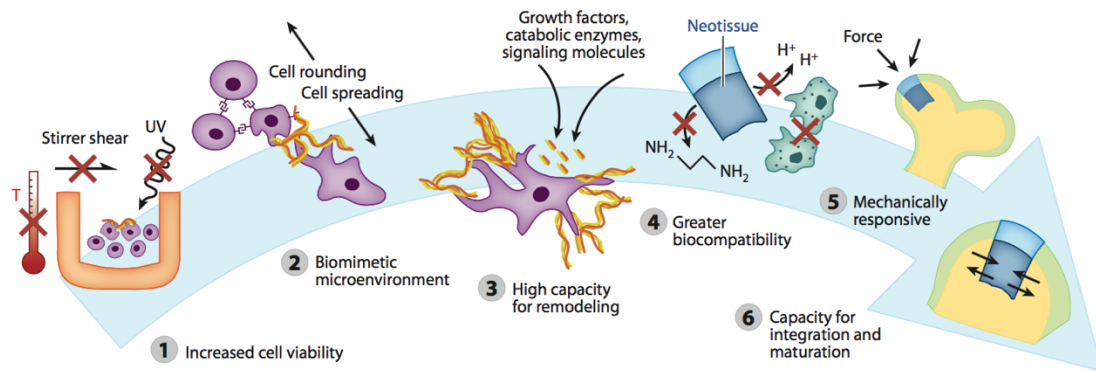


FIGURE 1.11 – ADVANTAGES OF SCAFFOLD-FREE TISSUE ENGINEERING.

Scaffold-free tissue engineering displays significant advantages from construct formation *in vitro* to implantation of tissue *in vivo*. Reproduced with permission from Athanasiou et al. © 2013, Annual Reviews (142).

1.4.3 SIGNALS

As the third element of the tissue engineering triad, signals in the culture environment direct cellular phenotype and tissue organization. Signals include chemical molecules, such as growth factors and nutrients, and physical perturbations, such as mechanical stimuli and perfusion. Growth factors that regulate chondrogenesis, low oxygen level, and dynamic mechanical stimulation are of particular interest toward engineering articular cartilage because these conditions, in part, regulate tissue development and extracellular matrix metabolism *in vivo*. Similar to the native joint environment, the temporospatial sequence of each of these factors in a tissue engineering system influence cartilage tissue formation and maturation. Moreover, many stimulating factors share common pathways through which they modulate cell differentiation and metabolism, and the ideal tissue engineering system is likely one that utilizes a variety of signals that work in synergy.

1.4.3.1 GROWTH FACTORS

A number of growth factors are known to influence *in vitro* chondrogenesis. Members of the TGF- β family have been identified as key regulators of both *in vitro* and *in vivo* chondrogenesis from cell condensation through terminal differentiation. During condensation, TGF- β s promote synthesis of N-cadherin for cell-cell interactions and fibronectin and tenascin for cell-matrix interactions (163,164). TGF- β s subsequently regulate cell proliferation, strongly promote extracellular matrix anabolism, and stimulate Sox9 transcription during chondrogenic differentiation. In late stages of chondrogenesis, TGF- β s have been shown to inhibit chondrocyte hypertrophy and terminal differentiation (24,164). Bone morphogenetic proteins (BMPs), which are also members of the TGF- β superfamily, and insulin-like growth factors (IGFs) have many overlapping functions to TGF- β s during chondrogenic differentiation from control of *SOX* genes to stimulation of proteoglycan and collagen synthesis and regulation of chondrocyte hypertrophy (24,164). Fibroblast growth factors (FGFs) are essential mediators of skeletogenesis, endochondral ossification, and articular cartilage homeostasis (165). When added to progenitor cells in monolayer, FGF2 has been shown to induce mitotic activity and enhance subsequent *in vitro* chondrogenesis (126,128,166). At the tissue level, FGF2 is known to regulate the expression of catabolic and anti-catabolic mediators of tissue remodeling (167-170). While the independent roles of dozens of soluble growth factors have been defined in the context of *in vitro* chondrogenesis, many of these molecules share common signaling pathways and may act synergistically or antagonistically. Ultimately, when applied in tissue engineering systems, growth factors facilitate control over cellular processes that mediate chondrogenic differentiation and tissue development. Soluble growth factors and chemical

signals can be efficiently delivered to cells *in vitro* by inclusion in culture media; however, maintenance of these signals following cell or tissue implantation is a major challenge. Strategies for temporal control of growth factor release *in vivo* include: gene transfer to induce stable or transient cellular expression of the signals and bioactive scaffolds that are tagged with and release signals on demand (92,171).

1.4.3.2 OXYGEN TENSION

Oxygen is a vital metabolite for mammalian cell homeostasis, and each tissue has unique oxygen requirements based on metabolic activity. The physiologic partial pressure of oxygen (physioxia) for any given tissue, however, is well below the relatively hyperoxic atmospheric level (160mmHg, 21.1%) in which the organism resides. By the time air travels through the respiratory tract, fills the alveoli, and diffuses into arterial blood, the partial pressure drops to 100mmHg or 13.2% (172). The partial pressure continues to lower as arterial blood travels to distal organs (Table 1.1). Even highly vascularized bone marrow operates at roughly 5% (~40mmHg) oxygen, which falls as low as 1.3% (10mmHg) in deep peri-sinusoidal regions (173). Oxygen delivery to avascular tissues, including articular cartilage and the growth plate, occurs through diffusion from neighboring compartments such as synovial fluid or bone. Oxygen content in cartilage is estimated between <1 and 5% (7-40mmHg) based on distance from the oxygen source (174,175). During physiologic function, tissues are adapted for the appropriate relative oxygen content. Perturbations from physioxia in both pathologic conditions and *in vitro* culture influence cell and tissue homeostasis through molecular mechanisms. Specifically, in the presence of molecular oxygen, hypoxia-inducible factor (HIF) alpha subunits are targeted for proteosomal

degradation by hydroxylation of proline residues; conversely, hydroxylases are inhibited in the absence of oxygen, and HIF- α heterodimerizes with a HIF- β partner (Figure 1.12). HIF complexes, in turn, exert transcriptional control by transactivation of genes with hypoxia-responsive elements (HRE), including Sox9, the master transcriptional regulator of chondrogenesis (176,177). Consequently, HIFs, within the physiologic low oxygen environment, influence chondrocyte differentiation and subsequent cartilage tissue formation, maturation, and homeostasis. Through our laboratory's previous work, along with results from other groups, we have consistently found that culture in lowered oxygen tension from hyperoxia at 20% oxygen to physioxia at 2% promotes chondrogenic differentiation and biochemical anabolism while suppressing markers of hypertrophy (117,178). Thus, oxygen tension within an *in vitro* tissue engineering system represents a tunable variable with potential to influence cell and tissue phenotype. *This is the basis for the hypotheses that I tested in the work presented in Chapters 3 & 4 of this dissertation.*

	pO ₂	
	mmHg	%
Air	160	21.1
Inspired air (in the tracheus)	150	19.7
Air in the alveoli	110	14.5
Arterial blood	100	13.2
Venous blood	40	5.3
Cell	9.9–19	1.3–2.5
Mitochondria	<9.9	<1.3
Brain	33.8 ± 2.6	4.4 ± 0.3
Lung	42.8	5.6
Skin (sub-papillary plexus)	35.2 ± 8	4.6 ± 1.1
Skin (dermal papillae)	24 ± 6.4	3.2 ± 0.8
Skin (superficial region)	8 ± 3.2	1.1 ± 0.4
Intestinal tissue	57.6 ± 2.3	7.6 ± 0.3
Liver	40.6 ± 5.4	5.4 ± 0.7
Kidney	72 ± 20	9.5 ± 2.6
Muscle	29.2 ± 1.8	3.8 ± 0.2
Bone marrow	48.9 ± 4.5	6.4 ± 0.6

TABLE 1.1 – OXYGEN TENSION WITHIN HUMAN TISSUES. Normal values of partial pressure of oxygen (pO₂) in various human tissues, expressed in mmHg and in percentage of oxygen in the microenvironment. Adapted with permission from Carreau et al. © 2011, John Wiley & Sons (172).

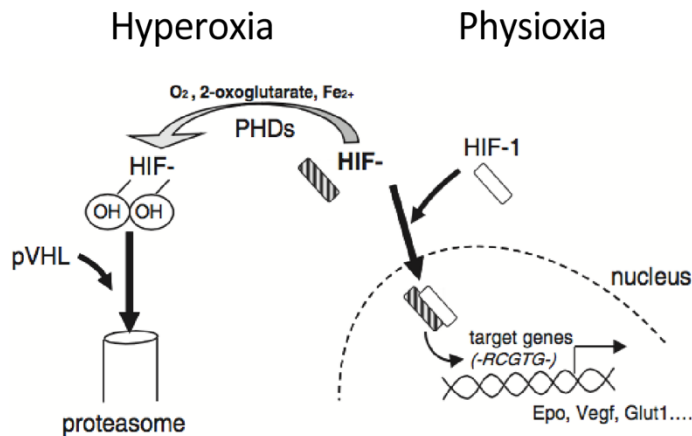


FIGURE 1.12 – HIF REGULATION AND SIGNALING.

Hydroxylation of hypoxia inducible factor- α (HIF- α) is inhibited in low oxygen environment (around 5%) because prolylhydroxylases (PHDs) activity is dependent on molecular oxygen. Then non-hydroxylated HIF- α can heterodimerize with HIF1- β , and translocate into the nucleus, where it binds to consensus sequences. Adapted with permission from Lafont et al. © 2010, John Wiley & Sons (176).

1.4.3.3 MECHANICAL STIMULATION

Articular cartilage develops, matures, and resides in a complex biomechanical environment with contributions from compressive and shear strains and from hydrostatic and osmotic pressures (25). It is well known that the mechanical environment is necessary to drive joint development and native tissue maturation toward anisotropy (23,38,39); although, the exact mechanisms remain unclear. The *in situ* mechanical environment is most suited for optimized tissue function, but *in vitro* mechanical bioreactors have been extensively applied in tissue engineering systems to create loading regimes inspired by the native joint milieu. The diversity of bioreactors employed in cartilage tissue engineering applications is roughly proportional to the number of research groups studying the influence of mechanical stimuli in a tissue engineering system; there is little standardization of bioreactor design across laboratories (Figure 1.13). Further, both cell-

and tissue-level responses to mechanical conditioning are highly dependent on the material and biomechanical properties of the scaffold. In general, loading within physiological parameters enhances chondrocyte- and progenitor cell-mediated extracellular matrix anabolism and tissue formation, while supra-physiologic loading regimes are detrimental to those outcomes. For either chondrocytes or MSCs seeded into a variety of scaffolds, static and dynamic hydrostatic pressures up to 10MPa have been shown to increase type II collagen and aggrecan at the gene and protein levels, reduce GAG loss from the extracellular matrix, and increase tissue stiffness (92,179,180). Long-term static compression, either confined or unconfined, of chondrocyte or MSC-loaded hydrogels is detrimental to cell-mediated anabolism; however, dynamic compression promotes ECM synthesis and enhances tissue compressive stiffness (181-183). In comparison with static loading, dynamic loading regimes drive mass transport of nutrients through the bulk of the tissue which likely enhances synthetic activity (28). Dynamic shear bioreactors that impart translational or rotational strains at a tissue surface have been shown to enhance tissue tensile strength and promote lubricin production at the bearing surface (184,185). The majority of bioreactors employed in articular cartilage tissue engineering applications to date represent a single-axis or mode loading regime; however, the development of multi-axis bioreactors may be necessary to recreate the complex tissue structure and anisotropy required for function in the native environment (185). *In the work presented in Chapter 5 of this dissertation, I designed and built a dynamic compressive bioreactor to study the effect of mechanical stimulation on the maturation of scaffold-free neocartilage tissues.*

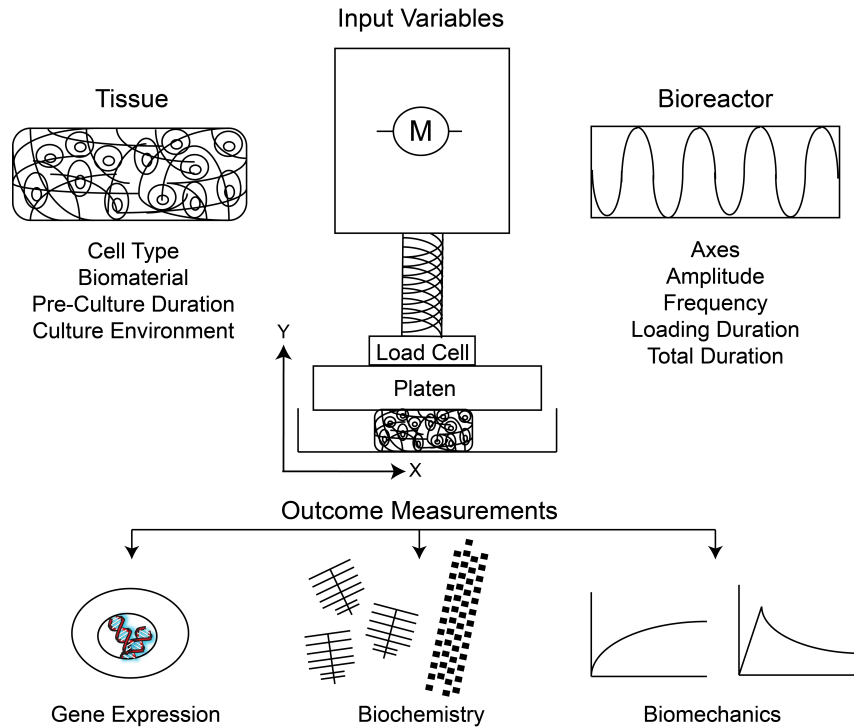


FIGURE 1.13 – BIOREACTORS IN ARTICULAR CARTILAGE TISSUE ENGINEERING. Schematic representing the diversity of both input variables and output measurements for use of a bioreactor in tissue engineering systems.

1.5 DISSERTATION OBJECTIVE & AIMS

The overall objective of my dissertation research has been to develop a novel scaffold-free tissue engineering system through which to grow structurally mature articular cartilage from a single progenitor cell. The ability to build autologous tissue that both resembles the native structure and that can properly function in a mechanical environment would enhance the potential for personalized therapies to repair focal articular cartilage defects before inevitable progression to degeneration and further disability. To develop strategies to grow mature scaffold-free neocartilage through a tissue engineering approach, I integrated experimental investigation of cells, the extracellular matrix scaffold, and environmental signals in the following aims:

Aim 1. Define the extent to which intrinsic chondrogenic differentiation capacity of a cell population influences neocartilage tissue formation in physioxia. The avascular nature of native articular cartilage creates a physiologically low oxygen (physioxia) environment in which the tissue develops, matures, and functions. Further, oxygen is a known mediator of chondrogenic differentiation and extracellular matrix anabolism; however, the role of physioxia in tissue engineering from human-derived stem and progenitor cells remains unclear. Utilizing adult human-derived cells in musculoskeletal tissue engineering facilitates development of translatable therapies; however, there exists immense variation in the phenotype of cells derived from a diverse and aged human population. In order to interpret results from experiments utilizing adult human-derived cells, we must first understand the intrinsic chondrogenicity of a given population of cells prior to experimental perturbation, such as culture in physioxia.

Hypothesis: *The variation in chondrogenic differentiation potential for cells derived from different biologic donors, as well as for cells derived from clonal populations from a single donor, will dictate the response of stem cell populations to culture in physioxia and is the basis for varied results in the literature.*

Aim 2. Establish the role of physioxia in promoting the biochemical anabolism of the extracellular matrix within a novel scaffold-free tissue engineering system. Historically, generating large-scale cartilaginous tissues in a low oxygen environment has proven challenging due to nutrient restriction. We sought to optimize a robust scaffold-free tissue engineering system to generate large-scale tissues from a variety of human-derived cells for the first time. This system allowed us to characterize not only temporospatial tissue development but also cellular responses to environmental signals, including physioxia.

Hypothesis: *Physioxia promotes chondrogenic differentiation and extracellular matrix anabolism in scaffold-free neocartilage tissues. ACPs generate articular cartilage, while ACs generate fibrocartilage, in a scaffold-free tissue engineering system.*

Aim 3. Define the role of dynamic mechanical stimulation in the creation of articular cartilage anisotropy. Evidence from native mammalian articular cartilage suggests that neonatal tissue is relatively isotropic in comparison with adult tissue. Mechanical stimulation during the postnatal period is hypothesized to drive both the depth-dependent zonal organization and pericellular matrix elaboration; although, the mechanisms of tissue reorganization are unknown. The development tissue anisotropy in scaffold-free neocartilage remains unexplored, and our scaffold-free system provided a platform to study tissue maturation in the dynamic compressive mechanical environment.

Hypothesis 1: *A dynamic compressive mechanical environment drives tissue maturation through active cellular responses to reorganize the extracellular matrix.*

Hypothesis 2: *Endogenous FGF2 bound to perlecan in the pericellular matrix mediates tissue reorganization through control of catabolic and anti-catabolic mechanisms following growth factor mobilization in the mechanical environment.*

CHAPTER 2: MATERIALS & METHODS

2.1 CELL & TISSUE CULTURE

2.1.1 CELL HARVEST & ISOLATION:

Human mesenchymal stem cells were isolated from iliac crest bone marrow aspirates and expanded in monolayer culture as described previously (129,186). Briefly, bone marrow aspirates were obtained, with approval from the Institutional Review Board at Oregon Health & Science University, Portland, OR, USA (IRB00000605) and fractionated on a Percoll density gradient. Cells were plated at 160,000 cells/cm² in Dulbecco's Modified Eagle Medium (DMEM; Life Technologies, Grand Island, NY) with 1 mg/ml L-glucose, 10% (v/v) fetal bovine serum (FBS) and 1% (v/v) penicillin-streptomycin (P/S). Adherent cells were cultured at 37 °C, 5% CO₂ and atmospheric oxygen with medium changes every 3 to 4 days until confluent, at which point expansion medium was supplemented with 10 ng/ml basic fibroblast growth factor (FGF-2; PeproTech, Rocky Hill, NJ).

Human articular chondrocytes and articular cartilage progenitors were harvested from the femoral condyles of healthy human donors. Human tissue was obtained without patient identifiers and with relevant ethical approval from the Institutional Review Board at Oregon Health & Science University (IRB exempt, Portland, OR, USA) and the NHS Blood and Tissue bank, Liverpool, UK (NRES number: 09/WSE04/35). Cartilage was removed from the condyles and finely minced before enzymatic digestion. ACs were digested from tissue with 1% pronase (w/v) from *Streptomyces griseus* for 1 hr at 37°C followed by 1,300 U/ml collagenase II (Worthington Biochemical, Lakewood, NJ, USA)

for 3 hr at 37°C, both in DMEM supplemented with 1 mg/ml L-glucose, 1% P/S. Following digestion, ACs were plated at 7,000/cm² and expanded in monolayer in DMEM supplemented with 1 mg/ml L-glucose, 10% (v/v) FBS, and 1% (v/v) P/S.

ACPs were isolated from separate donors to ACs through sequential pronase (70 U/ml for 20 min at 37°C) and type I collagenase (300 U/ml for 4 hr at 37°C) digestion. ACPs were selected from a total chondrocyte population through differential adhesion to fibronectin as previously described (19), and clonal populations of colony forming cells were expanded in monolayer in DMEM/F12 (1:1) medium containing 1 mg/ml L-glucose, 10mM HEPES, 10% (v/v) FBS, 1% (v/v) P/S, 0.1 mM ascorbic acid 2-phosphate (Wako, Cape Charles, VA), 1 ng/ml transforming growth factor β 1 (TGF- β 1, PeproTech) and 5 ng/ml FGF-2. ACs and ACPs were expanded in a standard tissue culture incubator with atmospheric oxygen and 5% CO₂.

2.1.2 PELLET CULTURE:

Chondrogenic differentiation was induced in serum-free DMEM containing 4.5 mg/ml L-glucose, 10 ng/ml TGF- β 1, 10⁻⁷M dexamethasone (Sigma-Aldrich, St. Louis, MO, USA), 37.5 μ g/ml ascorbic acid 2-phosphate, 1 mM sodium pyruvate, 40 μ g/ml L-proline, 1% (v/v) ITS+ Universal Culture Supplement Premix (BD Biosciences, San Jose, CA, USA) and 1% (v/v) P/S (129). Pellet cultures were formed by centrifuging 5 \times 10⁴ (MSCs) or 1 \times 10⁵ cells (ACPs) at 500 \times g for 5 minutes in 240 μ l of medium in Nunc polypro- pylene V-bottom 96-well plates (Thermo Fisher Scientific, Waltham, MA, USA). The ratio of cell density to medium volume was optimized in another study utilizing articular chondrocytes, results for which are presented in Appendix C. Cultures were

maintained in a low oxygen incubator (Thermo Fisher Scientific) set at 2% oxygen and 5% CO₂ (physioxia), or in a standard tissue culture incubator at 20% oxygen and 5% CO₂ (hyperoxia). By convention, we refer to the atmospheric, thus hyperoxic, condition as 20% oxygen. Medium was changed every 2 to 3 days, with that of the physioxic cultures being done at 2% oxygen in a low oxygen chamber (BioSpherix, Lacona, NY, USA) using medium pre-gassed to 2% oxygen, ensuring cells consistently saw that level of oxygen for the entire experimental period.

2.1.3 TISSUE CULTURE:

Cells were passaged with TrypLE reagent (Life Technologies), rinsed in serum-free DMEM with 1 mg/ml L-glucose, 1% (v/v) P/S, and resuspended at the defined seeding density in 200 µl in serum-free chondrogenic differentiation medium defined above (129). A cell suspension of 2×10^6 was pipetted drop-wise into a Transwell insert (Corning, Inc., Corning, NY, USA) containing a 6.5 mm diameter, 0.4 µm pore size, polyester membrane, which was either uncoated, coated with 2% agarose (w/v) (Sigma-Aldrich), or coated with 50 µg/ml bovine plasma fibronectin in DMEM (CalBioChem, Merck, Darmstadt, Germany) for 1 hr at room temperature. The cell-laden inserts were centrifuged at $200 \times g$ for 5 min in 24-well plates with 1 ml medium below the membrane. On the second day, the insert was transferred to a custom 12-well plate configuration containing 4.8 ml medium to create open medium flow between the top and bottom of the membrane. Tissues were cultured on an orbital shaker at 1 Hz frequency and maintained in a low oxygen incubator (Thermo Fisher Scientific) set at 5% oxygen and 5% CO₂ (physioxia) or in a standard tissue culture incubator at 20% oxygen and 5% CO₂ (hyperoxia). Medium was

changed 2 times weekly, with physioxic cultures being done at 5% oxygen in a low oxygen chamber (BioSpherix) with medium pre-gassed to ensure consistent oxygen levels throughout the experimental period. On the tenth day of culture, tissues were released from the membrane into free swelling culture in 0.9% w/v poly-2-hydroxyethylmethacrylate (poly-HEMA) (Sigma-Aldrich) coated 12-well plates containing 3 ml differentiation medium, a minimum volume optimized for high cell densities based on our prior work (Appendix C). Cultures were maintained to day 28 ensuring that the original membrane-oriented side was facing upward.

2.2 TISSUE ANALYSIS

2.2.1 BIOCHEMICAL ANALYSIS:

Triplicate pellets from each condition were rinsed with phosphate-buffered saline (PBS) and digested overnight at 60°C in 4 U/ml papain (Sigma-Aldrich) in PBS containing 6 mM Na₂-ethylenediaminetetraacetic acid and 6 mM L-cysteine (papain buffer, pH 6.0). Neocartilage discs were sectioned into quarters, and triplicate sample replicates from each condition were weighed, rinsed, and digested in the same solution.

Total DNA and sulfated glycosaminoglycan (GAG) content were quantified using Hoechst and 1,9-dimethylmethylene blue (DMMB) assays, respectively (178). DNA content of pellet and disc digests was quantified using calf thymus DNA diluted in papain buffer as a standard in serial dilution. Diluted samples, standards, and blanks were added to Hoechst dye (2 µg/ml), and fluorescence emission was measured with a multi-well plate reader (excitation 355 nm, emission 455 nm).

Supernatant was collected at each medium change to quantify the total amount of

GAGs produced and lost into the medium. GAG content of pellet and disc digests and supernatant was quantified using shark chondroitin sulfate (Sigma-Aldrich) diluted in either DMEM or papain buffer as a standard in serial dilution. DMMB dye (18 µg/ml in 0.5% ethanol, 0.2% formic acid, 30 mM sodium formate; pH 3.0) was added to samples, standards, and blanks, and absorbance was measured (575 nm).

Hydroxyproline content was quantified using an adaptation of the chloramine-T hydrate oxidation/p-dimethylaminobenzaldehyde development method with solid-phase hydrolysis on Dowex 50WX8-400 ion exchange resin (Thermo Fisher Scientific) (178). Trans-4-hydroxy-L-proline in papain buffer was used to generate a standard curve, and absorbance was measured at 560 nm.

2.2.2 BIOMECHANICAL ANALYSIS:

Mechanical properties of three full size disc replicates from each condition were tested in unconfined compression using a custom apparatus (187). Briefly, sample dimensions were measured with a digital micrometer, and the tissue was subjected to a creep test under 0.02 N load until equilibrium was reached at ~300 s. Upon equilibrium, iterative stress relaxation tests were performed at 1 mm/s to 10, 20, 30, and 40% compressive strain to derive the peak stress and equilibrium compressive Young's modulus at each ramp. Between each stress relaxation ramp, a dynamic test was carried out by applying 1% oscillatory strain at 1 Hz frequency to derive the dynamic compressive modulus.

2.2.3 GENE EXPRESSION ANALYSIS:

RNA was isolated from 6 pellets or 3 quarter discs of each biologic replicate in each condition. Briefly, tissues were snap frozen directly in liquid nitrogen, crushed with a mini pestle, and lysed with Buffer RLT (QIAGEN, Germantown, MD, USA) containing 40mM dithiothreitol (DTT). RNA isolation was performed with the RNeasy Mini Kit (QIAGEN) according to manufacturer's instructions. Total RNA was quantified on a NanoDrop Spectrophotometer (NanoDrop, Wilmington, DE, USA) and 250 to 500 ng were reverse-transcribed using qScript cDNA SuperMix (Quanta BioSciences, Gaithersburg, MD, USA). Quantitative polymerase chain reaction (qPCR) was performed with a dilution of cDNA using a StepOnePlus thermal cycler (Life Technologies) with TaqMan Fast Advanced Master Mix and TaqMan assay primers (Life Technologies) listed in Table 2.1. Cycling parameters were 50°C for 2 minutes, 95°C for 20 seconds, then 95°C for 1 seconds and 60°C for 20 seconds for a total of 40 cycles. Results were analyzed using the $2^{-\Delta C_t}$ method relative to the most stably expressed housekeeping gene across all experimental replicates and between groups. Gene expression was normalized to either the paired condition or the baseline condition.

Table 2.1 TaqMan Primers	
Gene	TaqMan Primer
<i>18S</i>	Hs99999907_m1
<i>ACAN</i>	Hs00153936_m1
<i>B2M</i>	Hs99999907_m1
<i>COL1A1</i>	Hs00164004_m1
<i>COL2A1</i>	Hs00264051_m1
<i>COL6A1</i>	Hs00242448_m1
<i>COL9A1</i>	Hs00932129_m1
<i>COL10A1</i>	Hs00166657_m1
<i>COL11A2</i>	Hs00365416_m1
<i>COMP</i>	Hs00164359_m1
<i>INHBA</i>	Hs01081598_m1
<i>LOX</i>	Hs00942480_m1
<i>MMP1</i>	Hs00899658_m1
<i>MMP13</i>	Hs00233992_m1
<i>MTN3</i>	Hs00159081_m1
<i>PIEZO1</i>	Hs00207230_m1
<i>PRG4</i>	Hs00195140_m1
<i>L-SOX5</i>	Hs00374709_m1
<i>SOX6</i>	Hs00264525_m1
<i>SOX9</i>	Hs01001343_g1
<i>TBP</i>	Hs00427620_m1
<i>TIMP1</i>	Hs00171558_m1
<i>TRPV4</i>	Hs01099348_m1
<i>VCAN</i>	Hs00171642_m1

2.2.4 HISTOLOGY & IMMUNOHISTOCHEMISTRY:

Pellets, discs, or native cartilage were fixed in 10% neutral buffered formalin, embedded in paraffin (formalin-fixed, paraffin embedded, FFPE) and sectioned onto silane-coated slides. Proteoglycan content was visualized by histochemical staining with toluidine blue (0.04% toluidine blue, 0.2M acetate buffer, pH=4.00) after deparaffinization. Tissues destined for immunohistochemistry of frozen sections were flash frozen in cold boiling hexanes for 1 minute, embedded in optimal cutting temperature (OCT) compound (TissueTek, Sakura, Torrance, CA), and cryo-sectioned (Thermo Fisher Scientific) at a 5µm thickness onto BioBond-coated (Electron Microscopy Sciences, Hatfield, PA) plain glass slides or 22mm diameter cover slips.

For immunohistochemistry, FFPE sections were deparaffinized and rehydrated through sequential alcohol baths. FFPE or frozen tissues were pretreated for antigen retrieval according to the parameters identified for each antibody listed in Table 2.2. Sections were blocked with a blocking buffer composed of either 4% normal goat serum (NGS), 1% bovine serum albumin (BSA), and 0.3% Triton X-100 in 1X PBS or 5% BSA in 1X PBS and were subsequently probed with primary antibodies (Table 2.2) overnight at 4°C in a 1% dilution of the respective blocking buffer. Species-matched secondary antibodies (Table 2.3) were diluted in 1% blocking buffer and incubated on slides for 45 min at room temperature. Slides were mounted with ProLong Gold antifade reagent containing 4',6-diamidino-2-phenylindole (DAPI, Life Technologies) and imaged using a Leica DM4000b upright fluorescent microscope (Leica Microsystems, Buffalo Grove, IL, USA).

Antibody	Manufacturer/Gift Source	Product #	Host species	Type	Application	Cryo or FPPE	Pretreatments	Dilution
ERK1/2	Cell Signaling Technology	137F5	Rabbit	mono IgG	WB	NA	Enhanced RIPA + Protease/Phosphatase Inhibitor	1000
FGF2	Millipore	05-118	Mouse	mono IgG	IHC	Cryosection	0.1% hyaluronidase	100
FGF2	Santa Cruz Biotechnology	sc-79	Rabbit	poly IgG	WB	NA	Enhanced RIPA + Protease/Phosphatase Inhibitor	500
Fibronectin	Sigma-Aldrich	IST-4	Mouse	mono IgG	IHC	FPPE	BioWave H1AR, 0.1% hyaluronidase	200
GAPDH	Millipore	MAB374	Mouse	mono IgG	WB	NA	8M Urea + Protease Inhibitor	300
Laminin	Abcam	Ab11575	Rabbit	poly IgG	IHC	Cryosection	BioWave H1AR, 0.1% hyaluronidase	50
Lubricin	Millipore	MABT401	Mouse	mono IgG	IHC	FPPE	BioWave H1AR, 0.1% hyaluronidase	200
Mouse IgG Negative Control	Santa Cruz Biotechnology	sc-2025	Mouse	IgG	IHC	Both	protocol matched	concentration matched
N-Cadherin	Abcam	Ab12221	Rabbit	poly IgG	IHC	FPPE	BioWave H1AR, 0.1% pronase, 0.1% hyaluronidase	200
Perlecan	Millipore	MAB1948P	Rat	mono IgG	IHC	Cryosection	0.1% hyaluronidase	200
phospho-ERK1/2 (p44/42 MAPK)	Cell Signaling Technology	Thr202/Tyr204	Rabbit	mono IgG	WB	NA	Enhanced RIPA + Protease/Phosphatase Inhibitor	1000
Rabbit IgG Negative Control	Santa Cruz Biotechnology	sc-2027	Rabbit	IgG	IHC	Both	protocol matched	concentration matched
Tenascin C	Sigma-Aldrich	T2551	Mouse	mono IgG	IHC	FPPE	BioWave H1AR, 0.1% pronase, 0.1% hyaluronidase	2000
Type I Collagen	Anthony Hollander	NA	Rabbit	poly IgG	IHC	FPPE	0.1% pronase, 0.1% hyaluronidase	200
Type II Collagen	NIH DSHB	II-H16B3	Mouse	mono IgG	IHC	FPPE	0.1% pronase	50
Type VI Collagen	Santa Cruz Biotechnology	sc-20649 (H-200)	Rabbit	poly IgG	IHC	FPPE	BioWave H1AR, 0.1% pronase, 0.1% hyaluronidase	200
Type X Collagen	Gary Gibson	NA	Mouse	poly IgG	IHC	FPPE	0.1% pronase	250
Type X Collagen	Greg Lunstrum	X53-HRP conj.	Mouse	mono IgG	WB	NA	8M Urea + Protease Inhibitor	5000

Secondary Antibody	Manufacturer	Product #	Host species	Type	Application	Dilution
Oregon Green 488	Life Technologies	11038	goat anti-rabbit	poly IgG	IHC	250
AlexaFluor 594	Life Technologies	A-11032	goat anti-mouse	poly IgG	IHC	250
AlexaFluor 488	Life Technologies	A-11006	goat anti-rat	poly IgG	SRM	1000
AlexaFluor 647	Life Technologies	A-21235	goat anti-mouse	poly IgG	SRM	1000
CF680	Biotium	CF680	goat anti-rabbit	poly IgG	SRM	800
CF680	Biotium	CF680	goat anti-rat	poly IgG	SRM	800
Goat anti-rabbit IgG-HRP	Santa Cruz Biotechnology	sc-2004	goat anti-rabbit	poly IgG-HRP	WB	5000
Goat anti-mouse IgG-HRP	Santa Cruz Biotechnology	sc-2005	goat anti-mouse	poly IgG-HRP	WB	5000

2.2.5 WESTERN BLOTTING:

For protein identification from neocartilage pellets or discs, tissues were digested in a lysis buffer (later specified for each experiment) under reducing conditions. Total protein concentration was quantified through a BCA Assay (Thermo Fisher Scientific), equal quantities were loaded onto an 8, 10 or 15% polyacrylamide gel depending on target protein size, and gels were run in electrophoresis. Protein was transferred to polyvinylidene difluoride (PVDF) membrane, blocked with either 2% non-fat milk or 5% BSA, and probed with a primary antibody (Table 2.2) against the target protein of interest. Membranes were subsequently probed with HRP-conjugated secondary antibody (Table 2.3) for 45 min at room temperature. HRP-conjugated antibodies were reacted with Western Lighting Plus ECL (Perkin Elmer, Waltham, MA, USA) chemiluminescence HRP substrate and visualized with a c-Digit blot scanner (LI-COR, Lincoln, NE, USA).

2.3 STATISTICAL ANALYSIS:

All statistical analyses were performed using GraphPad Prism v7.0 (GraphPad, La Jolla, CA, USA). Normality for each condition within a single cell type was assessed using D'Agostino-Pearson omnibus K2 test for Chapter 3 or Shapiro-Wilk test for Chapter 4 & 5 based on sample size. Normally distributed groups did not meet significance of $p < 0.05$ for distribution other than Gaussian. Specific statistical analyses are further described in each subsequent chapter.

CHAPTER 3:

RESPONSES TO ALTERED OXYGEN TENSION ARE DISTINCT BETWEEN HUMAN STEM CELLS OF HIGH AND LOW CHONDROGENIC CAPACITY

Devon E. Anderson,¹ Brandon D. Markway,¹ Derek Bond,¹ Helen E. McCarthy,² and
Brian Johnstone¹

¹Oregon Health & Science University, Department of Orthopaedics & Rehabilitation

²Cardiff University, School of Biosciences

Manuscript submitted to *Stem Cell Research & Therapy*, April 2016. Data has been presented as:

OARSI World Congress 2016 Amsterdam, Netherlands. *Responses to altered oxygen tension are distinct between human stem cells of high and low chondrogenic capacity.* Poster Presentation

Orthopaedic Research Society 2016 Orlando, FL. *Hypoxia promotes stable chondrocyte differentiation of articular cartilage progenitor cells.* Poster & Podium Presentations

Devon executed all aspects of this project from experimental design through data collection and analysis; he was the primary author of the manuscript.

3.1 ABSTRACT:

Introduction: Lowering oxygen from atmospheric (hyperoxia) to the physiological level (physioxia) of articular cartilage promotes mesenchymal stem cell (MSC) chondrogenesis. However, the literature is equivocal regarding the benefits of physioxic culture on preventing hypertrophy of MSC-derived chondrocytes. Relative to MSCs, articular cartilage progenitors (ACPs) undergo chondrogenic differentiation with reduced hypertrophy marker expression in hyperoxia but have not been studied in physioxia. This study sought to delineate the effects of physioxic culture on both cell types undergoing chondrogenesis.

Methods: MSCs were isolated from human bone marrow aspirates and ACP clones were isolated from healthy human cartilage. Cells were differentiated in pellet culture in physioxia (2% O₂) or hyperoxia (20% O₂) over fourteen days. Chondrogenesis was characterized by biochemical assays and gene and protein expression analysis.

Results: MSC preparations and ACP clones of high intrinsic chondrogenicity (termed high-GAG) produced abundant matrix in hyperoxia and physioxia. Poorly chondrogenic cells (low-GAG) demonstrated a significant fold-change matrix increase in physioxia. Both high- and low-GAG groups of MSCs and ACPs significantly upregulated chondrogenic genes; however, only high-GAG groups had a concomitant decrease in hypertrophy-related genes. High-GAG MSCs upregulated many common hypoxia-responsive genes in physioxia while low-GAG cells downregulated most of these genes. In physioxia, high-GAG MSCs and ACPs produced comparable type II but less type I collagen than those in

hyperoxia. Type X collagen was detectable in some ACP pellets in hyperoxia but reduced or absent in physioxia. In contrast, type X collagen was detectable in all MSC preparations in hyperoxia and physioxia.

Conclusions: MSC preparations and ACP clones had a wide range of chondrogenicity between donors. Physioxia significantly enhanced the chondrogenic potential of both ACPs and MSCs compared with hyperoxia, but the magnitude of response was inversely related to intrinsic chondrogenic potential. Discrepancies in the literature regarding MSC hypertrophy in physioxia can be explained by the use of low numbers of preparations of variable chondrogenicity. Physioxic differentiation of MSC preparations of high chondrogenicity significantly decreased hypertrophy related genes but still produced type X collagen protein. Highly chondrogenic ACP clones had significantly lower hypertrophic gene levels, and there was little to no type X collagen protein in physioxia, emphasizing the potential advantage of these cells in articular cartilage tissue engineering applications.

3.2 INTRODUCTION:

Articular cartilage demonstrates limited potential to repair or regenerate following acute injury and chronic degeneration due to lack of a blood supply, low cell density, and highly organized extracellular matrix. Tissue engineering strategies to repair articular cartilage remain limited by our inability to differentiate cells *in vitro* toward the stable articular cartilage tissue phenotype, characterized by high type II collagen and aggrecan and low type I and type X collagen in the extracellular matrix. Human bone marrow-derived mesenchymal stem cells (MSCs) are an attractive candidate as an autologous cell

source for tissue engineering application because they are easily harvested through bone marrow aspiration from adults; however, MSCs invariably progress toward the hypertrophic phenotype during *in vitro* chondrogenesis (129,171).

One of the variables to be considered during *in vitro* chondrogenesis is the oxygen level in which cells are differentiated, since the physiologic oxygen tension (physioxia) within tissues in the human body is well below atmospheric (hyperoxia), with the highest in the alveoli (110 mmHg) and arterial blood (100 mmHg) (172). Articular chondrocytes live in a physiologic environment of 1 to 5% (8-40 mmHg) oxygen, and bone marrow resides in approximately 7% oxygen (50 mmHg) (172,174,175). It is well known that oxygen deprivation in tissues stabilizes expression of hypoxia-inducible factors (HIFs), which directly modulate *in vitro* chondrogenesis through transactivation of regulatory transcription factors, including (sex determining region Y)-box 9 (SOX9)—the master regulatory transcription factor for chondrogenesis (176,177). Oxygen-mediated mechanisms drive anabolism of the extracellular matrix molecules toward the articular cartilage phenotype, but the role of physioxia remains equivocal with regard to MSC terminal differentiation toward the hypertrophic phenotype.

We have found that genes of the hypertrophic phenotype, *COL10A1* and *MMP13*, and of the fibrocartilaginous phenotype, *COL1A1*, are significantly lower in both healthy and osteoarthritic adult human chondrocytes during redifferentiation in low oxygen culture, which further increases proteoglycan production and promotes expression of cartilage matrix genes, including *COL2A1* and *ACAN* (178). The effect of lowered oxygen tension on markers of hypertrophy during chondrogenic differentiation of bone marrow-derived MSCs is less clear, with results ranging from downregulation (117,186,188-190)

to no change (191-193) to upregulation (194,195) of *COL10A1* and/or *MMP13*. In our own previous work, we found that while proteoglycan production and *COL2A1* and *ACAN* expression are promoted in MSCs, *COL10A1* expression is enhanced rather than suppressed in low oxygen culture (194). These studies, however, were conducted using MSCs that had been expanded without FGF-2 supplementation, which is known to improve subsequent chondrogenesis (126-128), and the pellets exhibited poor chondrogenesis regardless of oxygen tension. In our more recent studies, using highly chondrogenic preparations, MSCs cultured at low oxygen downregulated hypertrophic genes (186).

Articular cartilage progenitor cells (ACPs) are a cell population that exists in the upper layer of mature articular cartilage. They have generated significant interest with regard to their role in tissue development (16,17,20), *in situ* response to injury (62,134,136,137,196), and tissue engineering (19,138-140). Increasing evidence suggests that ACPs generate stable articular chondrocytes of native tissue through appositional growth of clonal populations (20). *In vitro*, clonal ACPs undergo chondrogenic differentiation with reduced potential for terminal differentiation toward the hypertrophic phenotype, in contrast with MSCs (139). Further, chondrogenic potential is maintained with extended population doublings and reduced telomere shortening in sub-clonal populations (197). Although ACPs reside in a low oxygen environment *in vivo*, where oxygen tension likely influences both differentiation and subsequent tissue homeostasis, the data concerning their differentiation were all generated in a hyperoxic environment of 20% oxygen *in vitro*.

While adult stem cells, including bone marrow-derived MSCs and tissue-derived ACPs, are promising cell candidates for autologous tissue regeneration, there exists

substantial heterogeneity across populations of cells from adult human donors (188,198-201). Generating clonal populations of MSCs is technically very challenging. Among the few successful examples, clonal MSC populations derived from individual human donors demonstrate intra-clonal heterogeneity with respect to proliferative efficiency, differentiation capacity, and phenotype (118,119). In contrast to MSCs, ACPs are clonable, but intra-donor variation has only been defined at the level of colony-forming efficiency (19), and intra-clonal variation remains undefined. Without standardized cell isolation and differentiation protocols in articular cartilage tissue engineering, generalized comparisons across and within cell populations from adult human donors, especially when pooled from multiple donors, may hinder our ability to identify subsets of cells with which to effectively generate autologous tissue applicable to adult patients.

The objective of the current study was to define the influence of oxygen tension on chondrogenic differentiation, specifically gene and protein expression, of adult MSCs and ACPs. In particular, we focused on intra-donor variability of MSCs and both intra-donor and intra-clonal variability of ACPs. We reasoned that not all adult human stem cells are equivalent, and there exists a range of chondrogenic potential for cells derived from different biologic donors as well as for cells derived from clonal populations from a single donor. This may have consequences for understanding the response of stem cell populations to biological stimuli; for example, the discrepancies in reports on the effects of oxygen on MSC hypertrophy. Thus, we investigated whether stem cell responses to changes in oxygen level during differentiation depends on intrinsic chondrogenic capacity.

3.3 MATERIALS & METHODS:

Cell harvest and isolation: Human-derived cells were isolated, expanded, and cultured according to methods in Chapter 2. Briefly, human MSCs were isolated from iliac crest bone marrow aspirates of 14 consenting donors (9 females, 5 males, age 46-74). Articular chondrocytes (ACs) were isolated from full thickness articular cartilage from the femoral condyles of cadaveric specimens through enzymatic digestion. Colony forming articular cartilage progenitor cells (ACPs) were isolated from the chondrocyte population through differential adhesion to fibronectin (19). A total of 18 ACP clones from four biologic donors (all male, age 26-33) were evaluated.

Pellet Culture: Chondrogenic differentiation was induced in serum-free defined chondrogenic medium in pellet culture described in Chapter 2. Cultures were maintained in a low oxygen incubator (Thermo) set at 2% oxygen and 5% CO₂ (physioxia), or in a standard tissue culture incubator at 20% oxygen and 5% CO₂ (hyperoxia).

Biochemical Analysis: Total DNA, sulfated glycosaminoglycan (GAG), and collagen content in each pellet were quantified from triplicate sample replicates after 14 days of pellet culture according to DNA, DMMB, and hydroxyproline biochemical assays, respectively, described in Chapter 2. GAGs that were released into the medium over the duration of pellet were quantified from triplicate sample replicates with a DMMB assay.

Each cell type, MSCs and ACPs, was divided into two groups based on GAG production in hyperoxia relative to human chondrocytes cultured in standard chondrogenic pellet culture conditions (n=4 each of 5×10^4 and 1×10^5). Preparations or clones within

two standard deviations of GAG production for the human chondrocytes were considered ‘high-GAG’, and those below two standard deviations were considered ‘low-GAG.’

Gene Expression Analysis: RNA was isolated from 6 pellets of each replicate in each condition with the RNeasy Mini Kit according to methods in Chapter 2. Quantitative polymerase chain reaction (qPCR) was performed according to methods in Chapter 2 with reverse transcribed cDNA and TaqMan assay primers listed in Table 2.1 for the following gene targets: *COL2A1*, *COL9A1*, *COL11A2*, *COL6A1*, *COL1A1*, *COL10A1*, *SOX9*, *L-SOX5*, *SOX6*, *ACAN*, *PRG4*, *LOX*, *MMP13*. Results were analyzed using the $2^{-\Delta C_t}$ method relative to *18S* housekeeping gene—the most stably expressed of four evaluated housekeeping genes across all experimental replicates and between groups. Gene expression in physioxia was normalized to the paired gene in hyperoxia to calculate relative fold change expression.

To evaluate a panel of oxygen-tension mediated genes, RNA was pooled at equal quantities from each group, and 5ng of cDNA was loaded to each well of a human TaqMan gene array (catalog #4414090, Life Technologies). Results were analyzed using the $2^{-\Delta C_t}$ method relative to *18S* housekeeping gene, consistent with single gene analysis. A cycle threshold of 36 was defined for minimum expression levels across the panel, and undetectable genes above the threshold were not evaluated. Gene expression in physioxia was normalized to the paired gene in hyperoxia to calculate relative fold change expression. Heatmaps were generated in RStudio (Boston, MA): one without scaling to reflect fold change expression and one with a z-score cluster analysis. Gene relationships were defined using the STRING (Search Tool for the Retrieval of Interacting Genes/Proteins) database

v10, and genes were grouped according to common biological processes of gene ontology.

Histology and Immunohistochemistry: Pellets were fixed in 10% neutral buffered formalin, embedded in paraffin and sectioned onto slides. Proteoglycan content was visualized by histochemical staining with toluidine blue. Pellet size was determined by measuring the widest diameter with digital analysis of toluidine blue stained sections taken from the middle of the pellet (ZEN blue, Zeiss, Oberkochen, Germany). For immunohistochemistry, tissue sections were deparaffinized, pretreated for antigen retrieval, and probed for types I, II, and X collagen according to specifications listed for each antibody in Table 2.2.

Western Blotting: To confirm the presence of protein visualized in immunohistochemistry, ten pellets from ACP clones were digested in 8M urea under reducing conditions. Total protein concentration was quantified through a BCA Assay, and equal quantities were loaded onto an 8% polyacrylamide gel. Gels were run in electrophoresis and transferred to a PVDF membrane, which was subsequently blocked with 2% non-fat milk and probed for type X collagen with the X53 antibody according to specifications in Table 2.2 The X53 antibody was prepared and characterized as described by Girkontaite et al. (1996), and full length collagen type X stably expressed in HEK293 cells was affinity purified as outlined in Wagner et al. (2000) (202,203). As a loading control, the membrane was probed with a primary antibody to GAPDH (Table 2.2) for 1 hr at room temperature and subsequently probed with HRP-conjugated goat anti-mouse (Table 2.3) for 45 min at room temperature. HRP-conjugated antibodies were reacted with HRP substrate and visualized with a blot scanner.

Statistical Analysis: All statistical analyses were performed using GraphPad Prism v7.0 (GraphPad, La Jolla, CA, USA). Normality for each condition within a single cell type was assessed according to methods in Chapter 2. Comparison of GAG content and gene expression between physioxia and hyperoxia within a given group was assessed using a paired t-test for normal data and Wilcoxon matched-pairs signed rank test for non-normal data, with significance set at $p < 0.05$. Comparison of GAG content between normally distributed groups was performed with an unpaired t-test, with significance set at $p < 0.05$. Mean and standard deviation for fold change gene expression was calculated as physioxia relative to hyperoxia for each group.

3.4 RESULTS:

Stem cell populations vary in their response to physioxia during chondrogenic differentiation. Quantification of total glycosaminoglycans (GAG) per pellet as a readout for overall chondrogenic differentiation revealed that culture in physioxia significantly favored chondrogenic extracellular matrix anabolism when compared with culture in hyperoxia ($p = 0.0002$ for MSCs, $p = 0.0124$ for ACPs). There existed a wide range of both baseline GAG content in hyperoxia and fold change GAG content from hyperoxia to physioxia across individual populations of cells (Figure 3.1A). Each biologic replicate of MSCs and ACPs was categorized as high- or low-GAG based on a threshold defined by their total GAG production in hyperoxia relative to that of pellet cultures of healthy human articular chondrocytes in the same pellet culture conditions that we previously optimized (Figure 3.2, Appendix C). Specifically, cell populations that produced GAGs within two

standard deviations of human chondrocyte pellets were considered high-GAG cells, and those below the two standard deviation threshold were considered low-GAG cells. While physioxic culture increased GAG production across all MSC preps and the majority of ACP clones, physioxia was of greater benefit to biologic replicates that exhibited very low GAG production at baseline in hyperoxia, driving a greater fold change than for clones that started with high GAG production and chondrogenic capacity in hyperoxia (Figure 3.1B). There were no statistically significant differences in pellet DNA content between oxygen levels, GAG levels, nor cell types, indicating that differences in GAG content were not due to cell proliferation or death (Figure 3.1C). Even with a significantly higher fold-induction, the pellets of low-GAG cell preparations of both cell types were still poorly chondrogenic in comparison with matched high-GAG pellets. This can also be easily discerned in the qualitative analysis of proteoglycan and glycosaminoglycan production through toluidine blue staining and quantitative analysis of pellet size; low-GAG pellets of each cell type were significantly smaller in pellet diameter with much less metachromasia than high-GAG pellets of the same cell type (Figure 3.3).

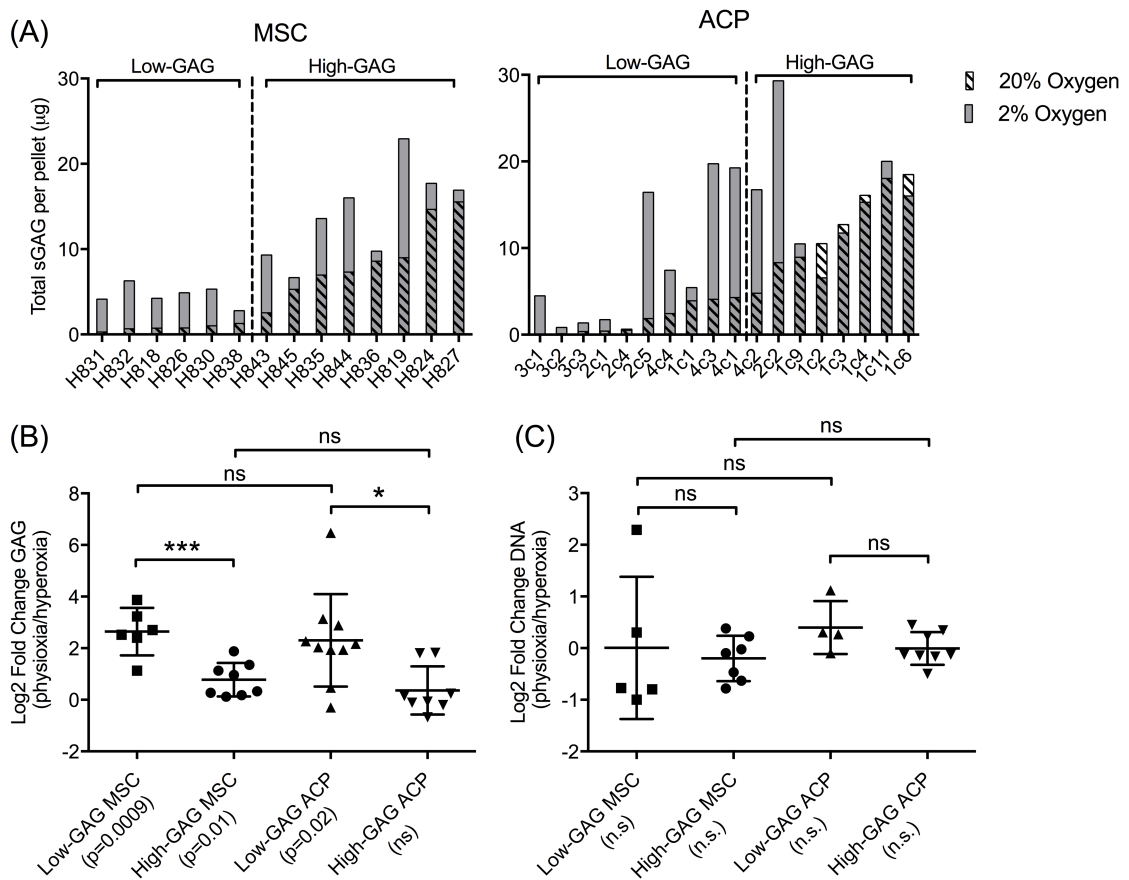


FIGURE 3.1 – BIOCHEMICAL ANALYSIS OF PROGENITOR CELL CHONDROGENESIS. (A) Total glycosaminoglycan (GAG) production per pellet for each MSC preparation and ACP clone indicated variation among human donors. A threshold (--) defined as two standard deviations from the total GAG production during pellet chondrogenesis for healthy human chondrocytes was set for each cell type, and low- and high-GAG producing groups were categorized. (B) Mean (±SD) fold change GAG production in physioxia relative to hyperoxia was significant for all groups other than high-GAG ACPs, and a significant difference existed between the fold-change for low- and high-GAG groups of each cell type. (C) Mean (±SD) fold change DNA content in physioxia relative to hyperoxia was no different between oxygen level, GAG level, nor cell type. Statistical significance defined as * $p < 0.05$, *** $p < 0.001$ by a paired or unpaired t-test where appropriate.

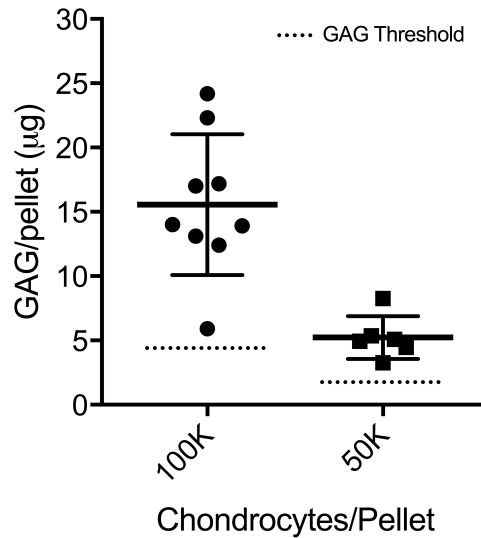


FIGURE 3.2 – THRESHOLD FOR PROTEOGLYCAN PRODUCTION.

Total glycosaminoglycan (GAG) production per pellet (mean \pm SD) for healthy human chondrocytes cultured at densities of 100,000 or 50,000 cells per pellet over 14 days of chondrogenic differentiation. Two standard deviations below the mean of each group was used to define the threshold for grouping MSC and ACP preparations based on proteoglycan production for the matched cell density.

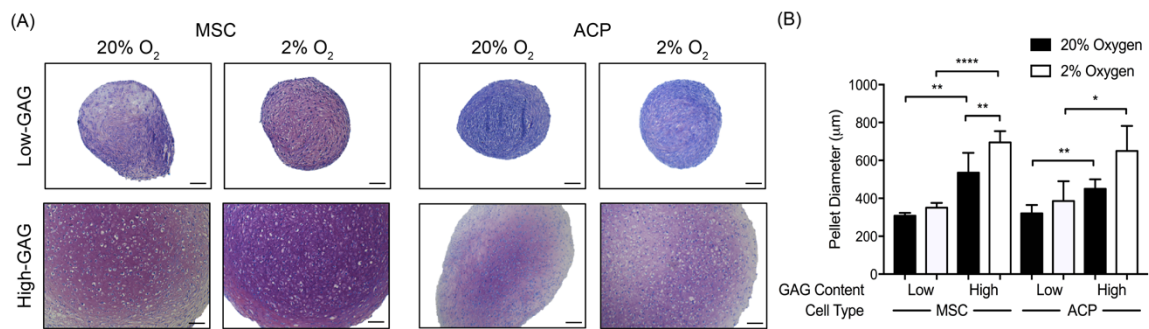


FIGURE 3.3 – QUALITATIVE ANALYSIS OF PROTEOGLYCAN PRODUCTION.

(A) Representative toluidine blue stain for total proteoglycans demonstrates smaller pellets with less metachromasia for low-GAG producing MSC preparations and ACP clones in both hyperoxia and physioxia relative to paired high-GAG MSC preparations and ACP clones at the respective oxygen levels. Images were acquired with bright-field microscopy, scale bars = 100 μ m. (B) Measurement of pellet diameter (mean \pm SD) revealed a statistically significant difference in pellet size between both MSCs and ACPs of high or low chondrogenicity and between high-GAG MSCs at physioxia or hyperoxia. Statistical significance defined as * p <0.05, ** p <0.01, **** p <0.0001 by a paired or unpaired t-test where appropriate.

Effect of physioxia on gene expression corresponds with intrinsic chondrogenic capacity. All cell preparations and clones were evaluated for chondrogenic markers including those of the articular chondrocyte (*COL2A1*, *ACAN*), the fibrochondrocyte (*COL1A1*), and the hypertrophic chondrocyte (*COL10A1*, *MMP13*) phenotypes. Physioxic culture significantly upregulated *COL2A1* and *ACAN* in low-GAG preps from both cell types (Figure 3.4). However, among low-GAG cells, only ACPs demonstrated significant downregulation of *COL10A1* while MSCs did not downregulate either marker of the hypertrophic phenotype, *COL10A1* or *MMP13*. Physioxic culture of the high-GAG cells demonstrated significant upregulation of *COL2A1* and *ACAN* for both ACPs and MSCs, with a corresponding significant downregulation of *COL10A1* and *MMP13* relative to culture in hyperoxia. Only high-GAG MSCs demonstrated a significant downregulation of *COL1A1* gene expression.

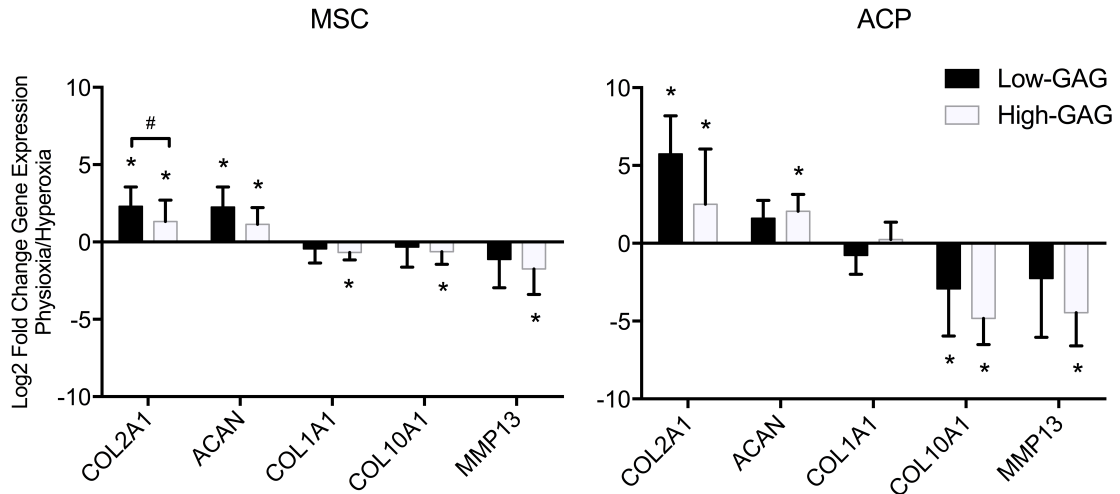


FIGURE 3.4 – DIFFERENTIAL GENE EXPRESSION BASED ON CHONDROGENICITY.

Gene expression analysis for fold-change of chondrogenic markers of the articular cartilage phenotype (*COL2A1*, *ACAN*), the fibrocartilaginous phenotype (*COL1A1*), and the hypertrophic phenotype (*COL10A1*, *MMP13*) demonstrates varied chondrogenic responses by high- and low-GAG groups of each cell type, MSCs and ACPs, during pellet culture in physioxia relative to hyperoxia conditions. Data are mean \pm standard deviation of fold change for each group (n = 6 to 10). Statistical significance defined as #,*p<0.05 by a paired or unpaired t-test where appropriate.

Oxygen-dependent genes are differentially expressed between groups of low and high chondrogenicity. When evaluated with a panel of oxygen-responsive genes, high-GAG MSCs and ACPs displayed a differential expression pattern to the matched low-GAG group for each cell type. Based on cluster analysis, cell groups were more closely related based on GAG production and intrinsic chondrogenicity than on cell type; low-GAG MSCs and ACPs clustered together, which then clustered with high-GAG ACPs and finally with high-GAG MSCs (Figure 3.5A). When evaluated as relative fold change from hyperoxia to physioxia (Figure 3.5B), high-GAG MSCs upregulated a majority (80%) of oxygen-responsive genes, including those of the HIF regulatory and TGF- β signaling pathways, both of which modulate chondrogenic differentiation. These cells also either upregulated

or did not change oxygen-responsive genes that regulate other biological processes, grouped by gene ontology, including cell cycle control, metabolism, and angiogenesis; many genes were involved in two or more processes. In contrast, low-GAG MSCs downregulated 74% of these same genes across all groupings. Both high- and low-GAG ACPs downregulated a majority of these oxygen-dependent genes, and the response between groups was similar in magnitude as well as direction for most genes.

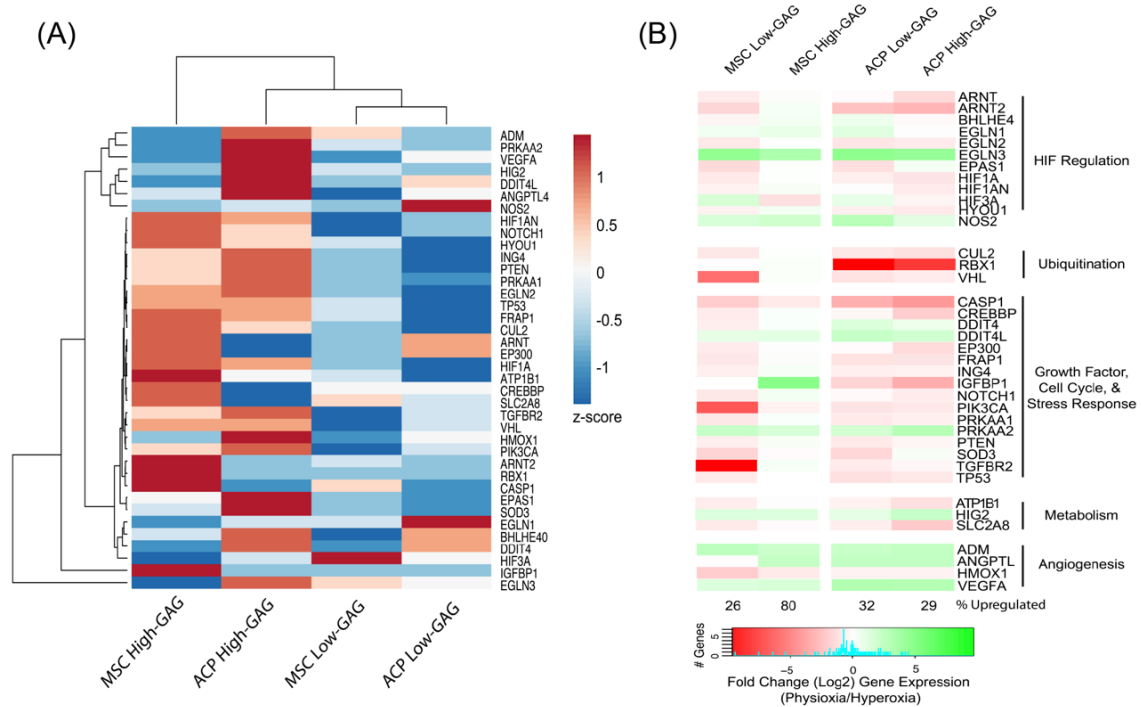


FIGURE 3.5 – OXYGEN-DEPENDENT GENE EXPRESSION.

(A) Clustering of oxygen-dependent gene expression based on z-score demonstrates that groups of MSCs and ACPs are more similar between GAG-level than within cell type in response to culture in physioxia relative to culture in hyperoxia. (B) Fold-change gene expression from hyperoxia to physioxia across an array of oxygen-dependent genes demonstrates differential expression patterns between high- and low-GAG groups of each cell type, MSCs and ACPs. Genes labeled in green were upregulated in physioxia relative to hyperoxia, and genes labeled in red were downregulated in physioxia relative to hyperoxia. Genes were categorized according to associations of gene ontology for biologic processes based on associations and clusters in the STRING database.

Physioxia promotes the articular chondrocyte phenotype in highly chondrogenic cells. High-GAG cells of both MSCs and ACPs demonstrated significant upregulation of *COL2A1*, *COL11A2*, *COL6A1*, *ACAN*, *PRG4*, and *SOX9* and downregulation of *COL10A1* and *MMP13* in physioxia relative to hyperoxia (Figure 3.6). High-GAG MSC preps also demonstrated significant upregulation of *COL9A1*, and *L-SOX5* and downregulation of *COL1A1* in physioxia. High-GAG ACP clones further demonstrated significant upregulation of *SOX6* and *LOX*. *COL9A1* was undetectable in five of eight high-GAG ACP clones cultured in hyperoxia but present at detectable levels in all clones cultured in physioxia.

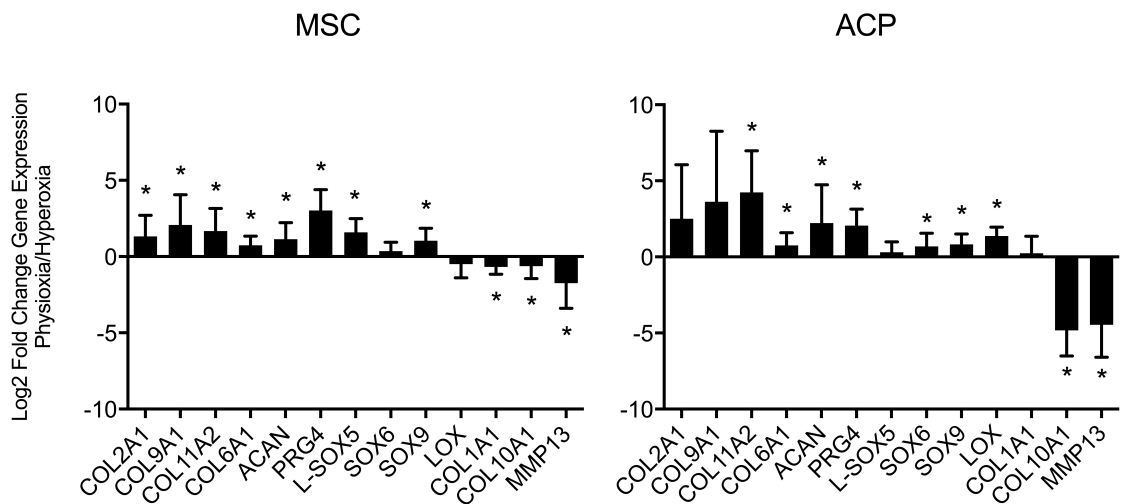


FIGURE 3.6 – GENE EXPRESSION OF HIGHLY CHONDROGENIC PROGENITOR CELLS. Gene expression analysis for fold-change of chondrogenic markers in physioxia relative to hyperoxia demonstrates that high-GAG groups of both MSCs and ACPs are highly responsive to oxygen level and upregulate a majority of genes representative of the articular cartilage phenotype in low oxygen environments. Data are mean \pm standard deviation of fold change in gene expression for each group (n = 8). Statistical significance defined as *p<0.05 by a paired t-test for normal data and a Wilcoxon matched-pairs signed rank test for non-normal data.

Physioxia promotes collagen protein expression representative of articular cartilage. Culture of high-GAG MSCs and ACPs in both physioxic and hyperoxic environments generated cartilage pellets with robust type II collagen expression throughout (Figure 3.7). MSCs cultured in hyperoxia exhibited highest type I collagen expression in the outer region of the pellet, whereas MSCs cultured in physioxia demonstrated less staining of extracellular type I collagen, consistent with significant downregulation of *COL1A1*. Similarly, high-GAG ACPs demonstrated a reduction in extracellular type I collagen in physioxia compared with hyperoxia. Type X collagen remained consistently high in all high-GAG MSC preps evaluated, regardless of oxygen tension. Conversely, high-GAG ACPs cultured in hyperoxia demonstrated variable type X collagen protein between clones, ranging from abundant to absent. Significantly, type X collagen protein expression was undetectable in the extracellular matrix of all clones cultured in physioxia. Western blots of pellet extracts with antibodies to type X collagen generated consistent results with little to no detectable protein in ACP clones at physioxia (Figure 3.8).

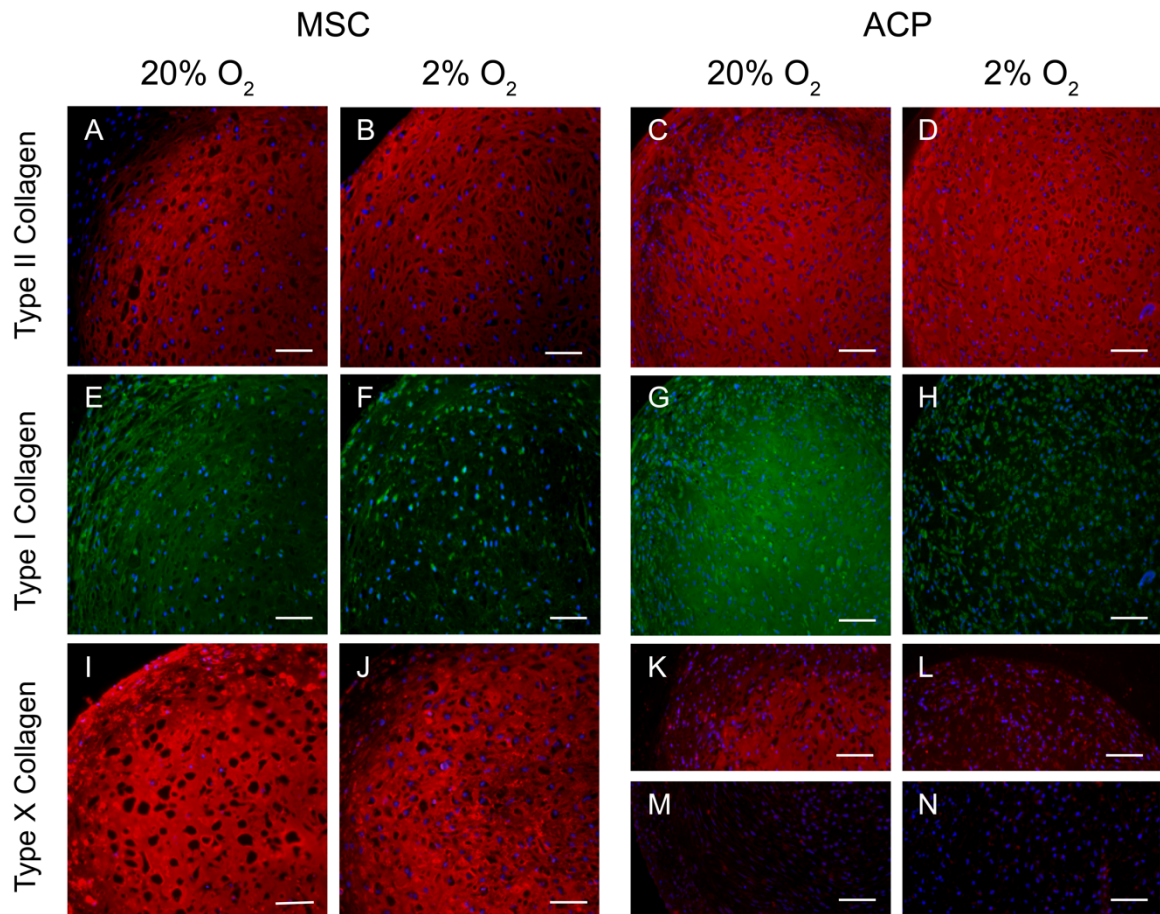


FIGURE 3.7 – QUALITATIVE IMMUNOHISTOCHEMICAL ANALYSIS OF COLLAGENS.

Representative immunohistochemistry demonstrates that cartilage pellets cultured in hyperoxia (20% O₂) and physioxia (2% O₂) exhibit oxygen-dependent expression of extracellular collagen protein, including type II collagen (A-D) of the articular cartilage phenotype, type I collagen (E-H) of the fibrocartilaginous phenotype, and type X collagen (I-N) of the hypertrophic phenotype. Type X collagen expression was variable among ACP clones differentiated in hyperoxia (K, M). Nuclei were counterstained blue with DAPI, and composite images of collagen staining and nuclei were digitally merged using ImageJ software (National Institutes of Health, Bethesda, MD, USA). Negative controls with isotype-matched antibodies were used for background correction (images not shown). Scale bars = 100 μm.

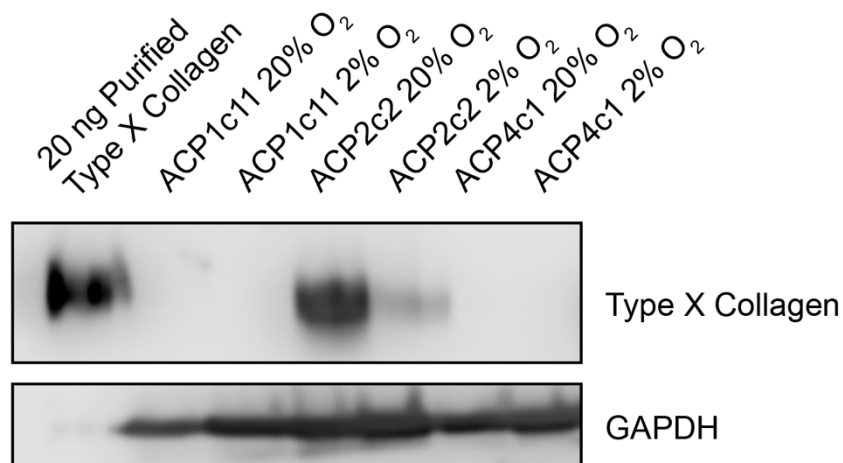


FIGURE 3.8 – TYPE X COLLAGEN WESTERN BLOTS FOR CHONDROPROGENITORS. Western blotting to detect type X collagen in total protein lysates from ACP pellets cultured for 14 days demonstrates that ACPs either lack type X collagen expression in all conditions or reduce expression with culture in physioxia relative to culture in hyperoxia.

3.5 DISCUSSION:

From our results, we can state that physioxia promotes the stable articular cartilage phenotype at both the gene and protein level during chondrogenic differentiation of ACPs in three-dimensional culture. MSCs demonstrated a similar response with respect to gene expression; however, type X collagen expression persisted in the physioxic environment. The magnitude of anabolic response to culture in physioxia was inversely related to the intrinsic chondrogenic potential in hyperoxia for both cell types. To account for differences in the chondrogenic capacity of stem cells at baseline, we divided the cell populations based on total GAG production. Those that produced low quantities of GAGs in a hyperoxic environment gained significant benefit from culture in physioxia but not enough to elaborate matrix to the levels produced by cells with high intrinsic chondrogenic capacity. In contrast, cells that produced high quantities of GAGs in hyperoxia did not respond as

robustly to lowered oxygen; these cells may be closer to reaching their maximum rate of proteoglycan synthesis such that oxygen-related mechanisms are unable to further increase. The differences in GAG production between replicates and clones was due to enhanced anabolism and not cell proliferation or death, as the DNA content was not different between these groups. While we did not directly measure the influence of donor age or gender on variation in chondrogenic capacity, the wide range across ACP clones and replicates, which were all derived from young males, demonstrates the extent of variation in human cells; these cells showed as wide a range in chondrogenicity as MSCs, which were derived from older male and female donors.

For low-GAG MSCs and ACPs, a significant increase in markers of the articular cartilage tissue phenotype, including glycosaminoglycan content and *COL2A1* and *ACAN* gene expression, was not complemented by significantly decreased expression of both hypertrophic genes, *COL10A1* and *MMP13*. Despite a substantial fold change in chondrogenic markers from hyperoxia to physioxia, these cells produced consistently smaller and more fibrous pellets in comparison with the high-GAG producers of the same cell type. In contrast, high-GAG MSC preparations and ACP clones significantly downregulated hypertrophic markers with culture in physioxia, demonstrating a distinct phenotypic difference between groups of cells of varied chondrogenic differentiation potential at baseline. Differences in gene expression between high- and low-GAG preparations were not limited to genes of chondrogenic differentiation; at low oxygen tension, high-GAG MSCs upregulated canonical hypoxia-responsive genes—including those of HIF regulation, constituents of TGF- β and IGF signaling, and cell cycle regulators—relative to hyperoxic culture. In contrast, low-GAG MSCs were most similar

to ACPs of low chondrogenicity, for both downregulated or did not change a majority of these oxygen-responsive genes in response to culture in physioxia. Expression of oxygen-responsive genes for high-GAG ACPs clustered with high-GAG MSCs and the grouping of low-GAG cell populations, indicating a mid-range response to physioxia in comparison to high-GAG MSCs, which were most responsive to physioxia. The differences between MSCs of high and low chondrogenicity in both direction and magnitude may be due to the cellular heterogeneity within a given preparation, which represents the total population of plastic adherent mononuclear cells from a bone marrow aspirate. Poorly chondrogenic cells expanded from this material may originate from a different population of cells than highly chondrogenic cells, and their dramatically different response across oxygen-dependent genes indicates they are indeed very different cells, not simply different in their ability to express cartilage genes and elaborate matrix. ACPs, on the other hand, are selected based on expression of specific integrins from a comparatively homogeneous initial pool of cells. These cells correspondingly are overall much more similar in their response to changes in oxygen, regardless of their ability to produce matrix-rich tissue. Taken together, our findings regarding both chondrogenic and oxygen-dependent gene expression indicate that low-GAG MSCs may be intrinsically limited in their overall response to altered oxygen levels.

Discrepancies in the literature regarding MSC hypertrophy during chondrogenic differentiation in lower oxygen may be due to inclusion of preparations of low chondrogenic capacity, and the present results demonstrate wide variation not previously taken into consideration for either cell type when examining their responses to alterations in oxygen level. An earlier study of MSC chondrogenesis in lowered oxygen tension

reported a significant upregulation of *COL10A1* for cells expanded without FGF-2 (194), which is known to aid retention of chondrogenic capacity in these cells (126-128). Our later studies demonstrated a significant downregulation of hypertrophic genes when differentiating MSCs of previously defined high chondrogenic capacity in lowered oxygen (186). Other recent studies have also reported downregulation of hypertrophic genes during MSC differentiation in lowered oxygen tension (117,188-190). Adesida et al. (2012) reported that MSCs expanded and differentiated in pellet culture at low oxygen tension significantly downregulate *COL10A1* in comparison with hyperoxic cultured MSCs (117); however, Bornes et al. (2015) from the same laboratory found no change in *COL10A1* expression for ovine MSCs cultured at low and high oxygen in a scaffold-based culture system (193). Studies of a larger set of human MSC preparations found no change in *COL10A1* expression with culture in physioxia when compared with hyperoxia, but these studies did not characterize individual preparations for baseline chondrogenicity (191,192). Finally, Duval et al. (2012) showed that *COL10A1* expression is downregulated in the presence of HIF-1 α and upregulated with blockade of this protein (189); however, mechanisms underlying HIF activity and *COL10A1* expression remain unclear (186,204-206). Based on our investigation, we suggest that the variation in the reported results for the hypertrophic response of MSCs in lowered oxygen tension may be due to the disparity of the intrinsic chondrogenic capacity of these cells at baseline: highly chondrogenic cells significantly downregulate genes of hypertrophy, and cells of lower chondrogenic potential are much less responsive.

We reasoned that that cells of low chondrogenic capacity, such as the low-GAG MSC preparations and ACP clones, are unsuitable candidates for articular cartilage tissue

engineering application and focused on the responses of high-GAG cells to culture in physioxia to further characterize the effects of oxygen on the articular chondrocyte phenotype. In low oxygen conditions, HIF-1 α and HIF-2 α are considered pro-chondrogenic through induction of *SOX9*, the gene coding for the master transcriptional regulator of chondrogenesis, *SOX9*, that in turn promotes *COL2A1* and *ACAN* gene expression to drive extracellular matrix anabolism of type II collagen and aggrecan, respectively (207,208). As expected, both MSCs and ACPs significantly upregulated *SOX9* in response to lowered oxygen, and MSCs significantly upregulated *L-SOX5*, the gene for a complementary chondrogenic transcription factor, while ACPs significantly upregulated *SOX6*. HIF-1 α has also been reported to activate transcription of *LOX*: the gene coding for lysyl oxidase, which is an enzyme that catalyzes collagen crosslinking in articular cartilage through a hypoxia-responsive element (HRE) (209), but only ACPs demonstrated a significant upregulation of *LOX*. Conclusions regarding the regulation of *PRG4*—the gene for lubricin—in response to alterations in oxygen vary in the literature, even though *PRG4* also contains an HRE in the promoter region (206,210,211). We have shown here that highly chondrogenic cells upregulated *PRG4* gene expression in physioxia. *COL9A1*, *COL11A1*, and *COL6A1*, the genes for type IX, XI, and VI collagen respectively, were upregulated in both cell types, indicating that the collagen network is extensively influenced by lowered oxygen tension toward the articular phenotype. Only MSCs demonstrated a significant downregulation of *COL1A1*; however, both MSCs and ACPs demonstrated a reduction of extracellular type I collagen protein with culture in physioxia, indicating the influence of oxygen on posttranslational modifications of the collagen network formed by these cells. Specifically, proline hydroxylation is a necessary step for

successful collagen secretion, and this oxygen-dependent enzymatic reaction may be attenuated in low oxygen environments (212). When oxygen is limited, chondrogenic cells may preferentially secrete type II over type I collagen, as *COL2A1* is upregulated in an oxygen-dependent manner through HIF regulation (208). Consistent with this hypothesis, our group has shown that articular chondrocytes also downregulate type I collagen at both the gene and protein level in response to lowered oxygen tension (178). These findings indicate that culture in low oxygen favors the articular chondrocyte phenotype over the fibrocartilage phenotype for multiple cell types.

The findings in this study are in agreement with recent reports on the beneficial effect of low oxygen in reducing markers of hypertrophy at the gene level in MSCs (117,186,190), at least for our preparations of high chondrogenic capacity. Although highly chondrogenic MSC preparations significantly downregulated hypertrophic genes in physioxia, these cells still produced a matrix rich in type X collagen protein. Prior studies that reported a decrease in *COL10A1* for MSCs differentiated in low oxygen did not evaluate type X collagen protein expression (117,186,190). Leijten et al. (2014) recently reported that low oxygen culture of MSCs abrogated expression of typical hypertrophic markers at the mRNA level and diminished subsequent vascular invasion and ossification of implanted constructs (190). While this may indeed be a benefit of low oxygen culture, we show that such preconditioning still likely results in tissue rich in type X collagen protein and this may have consequences unrelated to endochondral ossification. Ultimately, type X collagen establishes a tissue phenotype with increased stiffness that is not suited for articular cartilage repair (213). Culture of MSC-derived cartilage at physioxia

does not overcome the long noted challenge of controlling MSC differentiation to avoid creating the hypertrophic phenotype.

In the initial characterization of chondrogenic differentiation of ACPs in hyperoxia, Williams et al. (2010) did not find clones that produced detectable type X collagen at the protein level (19). In contrast, we found that some ACP clones produced abundant type X collagen in the hyperoxic environment. This notwithstanding, no clone produced detectable type X collagen in the physioxic environment. While both MSCs and ACPs of high chondrogenicity express *COL10A1*, differences in protein expression between physioxia and hyperoxia indicate that these two stem cell populations may have different translational control over this gene. This will be a subject of future studies. Regardless of the mechanism, ACP culture in physioxia consistently promotes a favorable tissue phenotype when compared with MSC-derived tissue.

3.6 CONCLUSIONS:

The variation in chondrogenic capacity among stem/progenitor cell populations from adult human tissues is an important consideration in tissue engineering. Our work suggests that laboratories ought to perform initial assays to characterize individual populations of human-derived stem cells, for variation in intrinsic chondrogenicity will influence experimental results, especially for studies with a small sample size. Though the impact of intrinsic chondrogenicity was not evaluated *in vivo*, we further reason that individual stem cell populations intended for allogeneic or autologous tissue repair should be characterized *in vitro* to identify highly chondrogenic cells prior to application in tissue-engineered therapies. We have shown that the chondrogenic capacity of stem cells

influences the cell's response to culture in a physiologic low oxygen environment: in physioxia, both MSCs and ACPs of high chondrogenicity demonstrate upregulation of the articular chondrocyte phenotype and downregulation of the hypertrophic phenotype. Only ACPs, however, demonstrate a consistent attenuation of type X collagen in the physioxic environment, and these cells may overcome historical challenges of MSC hypertrophy in tissue engineering applications.

CHAPTER 4:

PHYSIOXIA PROMOTES THE STABLE ARTICULAR CARTILAGE TISSUE PHENOTYPE IN HUMAN CELL-DERIVED SELF-ORGANIZED TISSUE

Devon E. Anderson,¹ Brandon D. Markway,¹ Kenneth J. Weekes,¹ Helen E. McCarthy,²
and Brian Johnstone¹

¹Oregon Health & Science University, Department of Orthopaedics & Rehabilitation

²Cardiff University, School of Biosciences

Manuscript in submission to *Tissue Engineering, Part A*, August 2016. Data has been presented as:

International Combined Meeting of Orthopaedic Research Societies 2016 Xi'an, China.
Physioxia promotes the stable articular cartilage tissue phenotype in self-organized tissue. Poster Presentation

Devon executed all aspects of this project from experimental design through data collection and analysis; he was the primary author of the manuscript.

4.1 ABSTRACT:

Introduction: The avascular nature and highly organized structure of articular cartilage limit the tissue's intrinsic ability to repair after injury. Biomaterial-based tissue engineering has not successfully reproduced the structural architecture or functional mechanical properties of native tissue. In scaffold-free tissue engineering systems, cells secrete and organize the entire extracellular matrix over time in response to environmental signals, such as oxygen level. In this study, we investigated the effect of oxygen on the formation of neocartilage from human-derived chondrogenic cells.

Methods: Articular chondrocytes (ACs) and articular cartilage progenitor cells (ACPs) derived from healthy human adults were guided toward self-organization and cell condensation by centrifugation onto polyester Transwell inserts that were uncoated or coated with agarose or fibronectin. Discoid tissue was produced over 28 days from both cell sources only when incubated in chondrogenic medium on fibronectin-coated Transwell inserts. To evaluate the influence of oxygen tension, neocartilage was cultured at hyperoxic (20%) or physioxic (5%) oxygen levels. Biochemical, biomechanical and molecular analyses were used to compare cartilage produced by ACs and ACPs.

Results: Fibronectin-coated Transwell inserts proved optimal for growing cartilaginous discs from both cell types after 28 days. In comparison with culture in hyperoxia, AC-derived neocartilage cultured at physioxia exhibited a significant increase in chondrogenic gene expression, proteoglycan production, and mechanical properties with a concomitant decrease in collagen content. At both oxygen levels, ACP-derived neocartilage produced

tissue with significantly enhanced mechanical properties and collagen content relative to AC-derived neocartilage but had much lower differential responses between physioxia and hyperoxia. Both ACs and ACPs produced substantial type II collagen and reduced levels of types I and X collagen in physioxia relative to hyperoxia. Neocartilage from ACPs exhibited anisotropic organization characteristic of native cartilage with respect to type VI collagen of the pericellular matrix when compared with AC-derived neocartilage; however, only ACs produced abundant surface-localized lubricin.

Conclusions: While scaffold-free tissue engineering methods have been well defined for non-human-derived cells, few methods utilizing adult human cells have been reported. Guiding human-derived cells toward condensation and subsequent culture in physioxia promoted the articular cartilage tissue phenotype for ACs and ACPs. Unlike ACs, ACPs are clonable and highly expandable while retaining chondrogenicity; however, ACP-derived tissues may be limited by a lack of lubricin expression in contrast to AC-derived tissues. The ability to generate large tissues utilizing a scaffold-free approach from a single autologous progenitor cell may represent a promising source of neocartilage destined for cartilage repair.

4.2 INTRODUCTION:

Articular cartilage exhibits complex organization including depth-dependent and cell-outward anisotropy. The tissue's structural heterogeneity and avascular nature facilitate its mechanical function but limit its regenerative capacity in pathologic conditions. While cartilage pathologies are the most common cause of chronic disability

among adults in the United States, early surgical intervention to repair focal defects is key to restoring tissue integrity before chronic degeneration (57,64,65). Unfortunately, successful arthroscopic repair remains a challenge as the resultant tissues lack organization, are fibrocartilaginous, and cannot meet the functional demands of the joint (86). The limited long-term success of current focal repair strategies demands a tissue engineering approach to recapitulate the structural and biomechanical properties of articular cartilage in a biologic therapeutic.

In cartilage tissue engineering, scaffold- or matrix-based biomaterials are often used to guide cell differentiation and provide initial tissue structure; however, the resultant tissue phenotype is constrained by biomaterial influences (142). In contrast, three-dimensional scaffold-free tissue engineering relies on cells to secrete an extracellular matrix scaffold. Over the past decade, a number of scaffold-free methods have emerged for cartilage tissue engineering. Self-assembled tissues, which form through cell interaction and condensation in free-swelling culture in the absence of external stimuli (148,149,152-155). Self-organizing models rely on external cues to guide the cells toward condensation; articular chondrocytes (ACs) and mesenchymal stem cells (MSCs) are typically centrifuged and/or cultured on a substrate including porous polymer membranes (157,162,214-217) and collagen (I, II, or IV)-coated membranes (31,158-160) to define tissue dimensions. Fibronectin is the earliest extracellular matrix protein produced following cell condensation (151,218); however, exogenous fibronectin has not been used in a scaffold-free approach to direct or facilitate cell condensation. To date, self-assembling and self-organizing models have produced three-dimensional cartilaginous tissues, of which the phenotype is dependent on cell source and culture conditions.

Cells drive both tissue formation and maturation in the scaffold-free environment. Thus, selection of a cell with high chondrogenic differentiation and anabolic capacity is essential to generate articular cartilage. Stem and progenitor cell populations overcome challenges of cell availability of primary chondrocytes and phenotypic modulation of expanded chondrocytes. Articular cartilage progenitor cells (ACPs) are postulated to reside in the upper zone of adult cartilage after forming the tissue through appositional growth of clonal populations (16,17,19,20). They can be clonally expanded *in vitro* after harvest of a small amount of tissue from a donor site. *In vitro*, clonal ACPs maintain chondrogenic differentiation potential following extended population doublings, and they demonstrate much-reduced terminal differentiation toward hypertrophic chondrocytes compared with MSCs (139,197). Although they differentiate toward the stable articular chondrocyte phenotype *in vitro*, ACPs generated a fibrocartilaginous repair tissue *in vivo* in an equine autologous or allogeneic implantation model (140). To date, tissue engineering utilizing human ACPs is limited to scaffold-based systems (140,219); ACPs have not been studied in the context of scaffold-free tissue engineering to evaluate *in vitro* tissue development.

While cells within a scaffold-free tissue will determine tissue phenotype, the culture environment will guide tissue development. Without a blood supply, native articular cartilage resides at physiologically low oxygen levels (physioxia), ranging from 1 to 5% oxygen (8-40 mmHg) (172,174). We have previously shown that lowering oxygen from hyperoxia (20% O₂) to physioxia significantly enhances chondrogenesis of expanded human chondrocytes derived from healthy and osteoarthritic tissue (178). We have more recently discovered that the responses to altered oxygen tension for both MSCs and ACPs are dependent on the intrinsic chondrogenicity of the cells in the context of wide inter-

donor and intra-donor clonal variability, but physioxia drives differentiation toward the stable chondrocyte phenotype for highly chondrogenic cells (Chapter 3). Previous studies have found lowered oxygen to be detrimental to scaffold-free tissue development (159,220,221); although, these tissues likely failed due to tissue necrosis under overall nutrient restriction with high cell density in low media volume. While native tissue develops and functions at low oxygen, we sought to evaluate development of scaffold-free neocartilage derived from adult human cells in physioxia with optimization of media volume and cell density to maintain tissue viability.

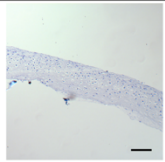
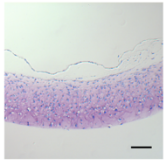
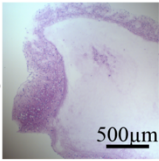
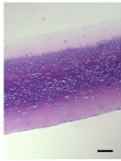
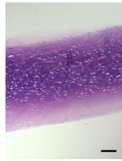
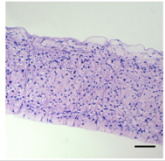
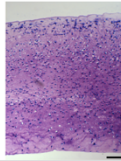
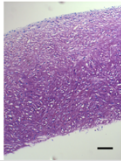
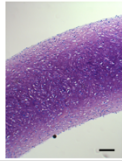
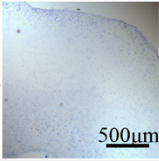
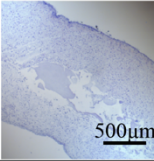
The objective of the current study was to define tissue development of adult human-derived cells in an optimized scaffold-free tissue engineering model that incorporates cues from the condensation phase through tissue development and maturation. We hypothesized that in comparison with fibrocartilaginous redifferentiation of expanded and heterogeneous ACs derived from adult humans, clonal ACPs will retain chondrogenic differentiation potential following extensive expansion to generate tissues of the articular cartilage phenotype, and that lowered oxygen tension would facilitate cell differentiation and extracellular matrix maturation in scaffold-free neocartilage.

4.3 MATERIALS & METHODS:

Cell Isolation: Human articular chondrocytes (ACs) and articular cartilage progenitors (ACPs) were harvested from the femoral condyles of healthy human donors (n = 5 for AC, n = 3 for ACP, all male age 21-33) and isolated according to methods in Chapter 2.

Tissue Culture: Cells were seeded into neocartilage tissue discs according to general methods in Chapter 2. Experiments were conducted to optimize parameters for scaffold-free tissue culture (Table 4.1). Cell density per tissue was selected based on initial experiments with 1, 1.5, 2, 3, or 4 x 10⁶ cells per tissue; whereby, 2 x 10⁶ of each cell type reliably produced a tissue of maximum thickness before void tissue cores developed at higher cell seeding densities (Table 4.2). Tissues were cultured on an orbital shaker at 1 Hz frequency and maintained in a low oxygen incubator (Thermo) set at 5% oxygen and 5% CO₂ (physioxia) or in a standard tissue culture incubator at 20% oxygen and 5% CO₂ (hyperoxia). Cultures were maintained in free-swelling culture from day 10 until harvest at day 28 according to general methods of Chapter 2. Tissues were also harvested at days 1, 4, 7, and 10 to characterize protein expression throughout the culture duration.

TABLE 4.1 PARAMETERS FOR OPTIMIZATION OF THE SCAFFOLD-FREE SYSTEM		
Parameter	Variables	Selection
Cell Density	1M 1.5M 2M 3M 4M	2M cells
Nutrient Considerations	1.2ml medium 4.8ml medium +/- orbital shaker +/- HEPES buffer	4.8 ml medium + orbital shaker
Oxygen Tension	2% 5% 20%	5% vs. 20%
Membrane Coating	Fibronectin Polyester – no coating Polycarbonate – no coating 2% Agarose 0.9% Poly-HEMA	Fibronectin
Confinement	28 day Transwell culture 10 day TW → Free-swelling	Free-swelling at day 10

TABLE 4.3 CELL SEEDING DENSITY				
Cell Density	AC Hyperoxia (20% O ₂)	AC Physioxia (2 or 5% O ₂)	ACP Hyperoxia (20% O ₂)	ACP Physioxia (5% O ₂)
1e6				
1.5e6		2%  500µm		
2e6		5% 		
3e6		5%  500µm		
4e6				 500µm
All scale bars = 100µm, unless otherwise noted. Experiments not performed for blank squares.				

Biochemical and Biomechanical Analysis: Neocartilage discs were sectioned into quarters, and triplicate sample replicates from each condition were analyzed for total DNA, GAG, and hydroxyproline content according to methods of Chapter 2. Mechanical properties of three full size sample replicates from each condition were tested in unconfined compression using a custom apparatus (187) and methods described in Chapter 2 to derive the equilibrium compressive modulus in stress relaxation tests of increasing percent strain

and to derive the dynamic modulus for a dynamic testing regime of 1 Hz and 1% strain on top of 10% static strain.

Gene Expression Analysis: RNA was isolated from one quarter of three pooled sample replicates in each condition with the RNeasy Mini Kit according to manufacturer's instructions and methods of Chapter 2. Quantitative polymerase chain reaction (qPCR) was performed using reverse transcribed cDNA and TaqMan assay primers (Table 2.1) to the following gene targets: *COL2A1*, *COL9A1*, *COL11A2*, *COL6A1*, *COL1A1*, *COL10A1*, *SOX9*, *L-SOX5*, *ACAN*, *VCAN*, *COMP*, *MTN3*, *PRG4*, *LOX*, and *MMP13*. Results were analyzed using the $2^{-\Delta Ct}$ method relative to *TBP* housekeeping gene, which was the most stably expressed of three evaluated housekeeping genes across replicates, between groups, and between cell types. Gene expression in physioxia was normalized to the paired gene in hyperoxia to calculate relative fold change expression.

Live/Dead Assay: A commercial live/dead assay (Life Technologies) was performed to characterize cell viability following 28 days of culture in scaffold-free neocartilage discs. Discs were cut in half with a straight razor and immediately incubated in 500 μ l DMEM supplemented with 8 μ M ethidium homodimer and 8 μ M calcein AM for 30 minutes at 37°C in a tissue culture incubator. Tissues were placed in a glass-bottom petri for imaging in cross-section under fluorescence on a Nikon Eclipse Ti confocal microscope with automatic stitching.

Histology and Immunohistochemistry: Qualitative toluidine blue histology and immunohistochemistry was performed on cross-sectional thin sections of neocartilage tissues from each condition and each cell type according to the methods and antibody parameters described in Chapter 2. Specifically, tissues were probed for n-cadherin, tenascin C, fibronectin, types I, II, VI, and X collagen, perlecan, and lubricin according to the antibody specifications in Tables 2.2 and 2.3.

Collagen Analysis: Commercial sandwich enzyme-linked immunosorbent assays (ELISA) were used to quantify types I and II collagen in neocartilage discs (Chondrex, Redmond, WA). Briefly, tissues were flash frozen in liquid nitrogen, pulverized in a custom mortar and pestle apparatus, and lyophilized. Weighed tissues were rehydrated before sequential digestions in 3M guanidine (Thermo) in 0.05M Tris-HCL buffer, pH 7.5, for 24 hr at 4°C, 1.33 mg/ml pepsin (Sigma-Aldrich) in 0.2M acetic acid, pH 2, for 6 days at 4°C, and 0.1 mg/ml pancreatic elastase (Chondrex) in 1X Tris buffered saline for 24 hr at 4°C, all with constant agitation. Sandwich ELISAs were carried out according to manufacturer instructions (Chondrex catalog #6018, #6021) with dual monoclonal antibodies for respective collagen capture and detection. Type I and type II collagen were quantified relative to a standard curve derived from purified protein.

Total amount of mature collagen crosslinks, hydroxylysyl-pyridinoline (HP) and lysyl -pyridinoline (LP), were quantified relative to purified residue standards through high performance liquid chromatography (HPLC) according to Avery et al. (2009) with modifications (222). Briefly, pooled triplicate discs were flash frozen in liquid nitrogen and pulverized with a custom high-throughput mortar and pestle. Pulverized specimens

were dissolved in 1 mL 150mM NaCl, 50mM NaPO₄, pH 7.5. Sodium borohydride equal to 1% the mass of the ground samples was added to 0.1mL 10mM NaOH and the resultant solution was added to the sample immediately. The solution was placed in a hood for 1 hour, and 100μL of 1M Acetic Acid was added to acidify the solution. Samples were lyophilized and the dried material was hydrolyzed in 6M HCl under argon at 105°C for 24 hours. Hydrolyzed samples were reconstituted in 200μL of 5% HFBA (heptafluorobutyric acid) in water. Analysis was performed on a Waters 2695 HPLC with a Phenomenex 5μm 250 x 4mm C 18 column with 5% HFBA in water as the aqueous buffer and 5% HFBA in acetonitrile as the organic buffer. Sample peaks were detected with a Gilson Model 121 Fluorometer set to 330nm for excitation and 390nm for emission. Data were analyzed using the Waters MassLynx software.

Statistical Analysis: Statistical analyses were performed using GraphPad Prism v7.0, and normality was assessed according to methods in Chapter 2. Comparison of biochemical parameters and gene expression between physioxia and hyperoxia within a given group was assessed using a paired t-test for normal data and Wilcoxon matched-pairs signed rank test for non-normal data, with significance set at $p < 0.05$. Comparison between normally distributed data of each cell type was performed with an unpaired t-test, with significance set at $p < 0.05$. Mean and standard deviation for fold change gene expression was calculated as physioxia relative to hyperoxia for each group.

4.4 RESULTS:

Fibronectin directs tissue geometry in scaffold-free tissue engineered constructs.

Both ACs and ACPs formed flattened discs of a defined geometry over 28 days of culture in a self-organization system that consisted of cell seeding through centrifugation, directed cell condensation on a fibronectin-coated membrane, and extracellular matrix elaboration (Figure 4.1). In contrast to this system, both cell types contracted from a flattened disc morphology into a large pellet within 24 hours of culture in Transwell inserts coated with 2% agarose (Figure 4.2). In agreement with prior work, ACs retained a flattened disc morphology on the uncoated porous polyester membrane of Transwell inserts (31); however, ACPs again contracted into a large pellet within 24 hours. When cultured on a fibronectin-coated porous polyester membrane, both cell types formed a flat disc with proteoglycans distributed throughout the depth (Figure 4.2). Mesenchymal stem cells were also cultured in this system, but the resultant tissues underwent hypertrophy and were excluded from further experimentation (Appendix D).

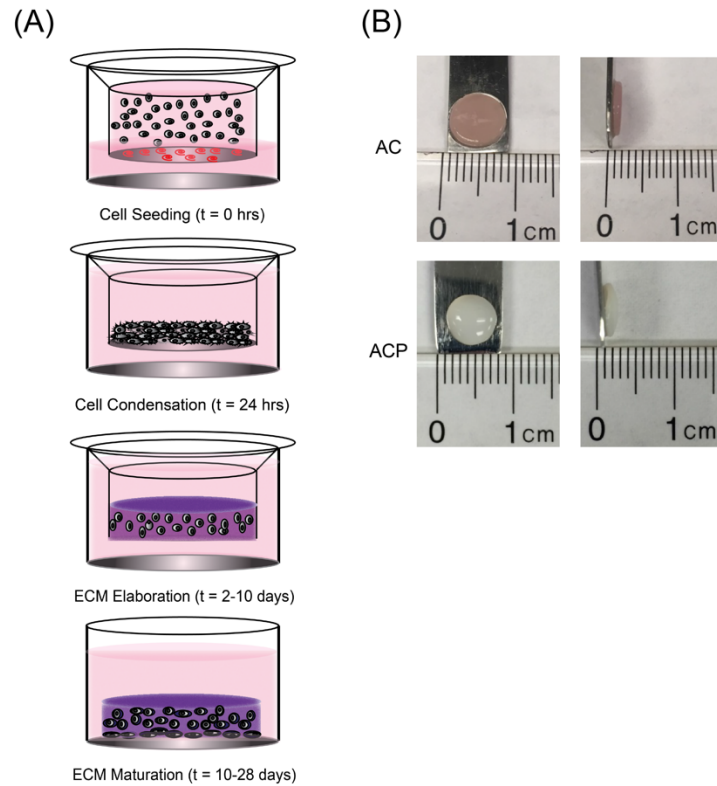


FIGURE 4.1 – SCHEMATIC OF NEOCARTILAGE SELF-ORGANIZATION.

(A) Schematic representing stages of self-organization of scaffold-free neocartilage beginning with cell seeding via centrifugation onto a protein-coated membrane (red spiral) to direct cell condensation into a restricted geometry. Over the course of culture, cells produce an extracellular matrix that starts as an immature homogenous matrix and matures over time with signals from the culture environment. (B) Gross images of AC and ACP-derived neocartilage show that each cell type produced a disc of uniform dimensions after 28 days of culture.

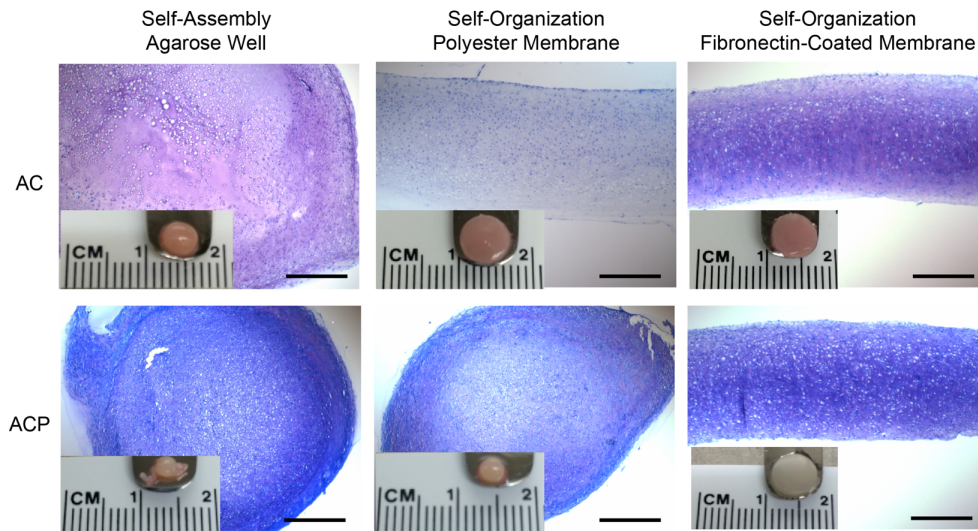


FIGURE 4.2 – COMPARISON OF SCAFFOLD-FREE SYSTEMS.

Toluidine blue histology and gross images demonstrate that human-derived ACs and ACPs formed a large pellet when cultured in non-adherent agarose wells after seeding into a flattened disc. Only ACs retained a disc morphology when cultured on porous polyester membranes, but both cell types retained a disc morphology when cultured on a polyester membrane coated with fibronectin. Scale bars = 500 μm .

Scaffold-free neocartilage develops and survives over time following initial cell condensation. Identified by markers of tissue maturation at various stages of *in vitro* tissue development (Table 4.3), neocartilage undergoes cell condensation (n-cadherin), followed by elaboration of an early cartilaginous extracellular matrix, marked by tenascin C and fibronectin (Figure 4.3). After 28 days in culture, the extracellular matrix is still immature as evidenced by persistence of ECM molecules, and cells survive throughout the depth of the tissue (Figure 4.4). There exists a layer of dead cells at the apical surface of the tissue, a result that was consistent among all samples subjected to a live/dead assay.

TABLE 4.3 MARKERS OF SCAFFOLD-FREE TISSUE MATURATION				
Stage	Seeding	Condensation	Early Matrix	Maturation
Day	0	1	2-10	10-28
Protein	X	Fibronectin Cadherins Tenascin C	Type I, II, X collagen Aggrecan CS6	Type VI Collagen COMP Other PCM CS4 Lubricin
Genes	?	Same as protein	SOX9 COL2A1 COL10A1 ACAN	LOX PRG4
Growth	DNA assay	Live/Dead assay DNA quant Proliferation	DNA Proliferation	Live/Dead Assay DNA quant Proliferation

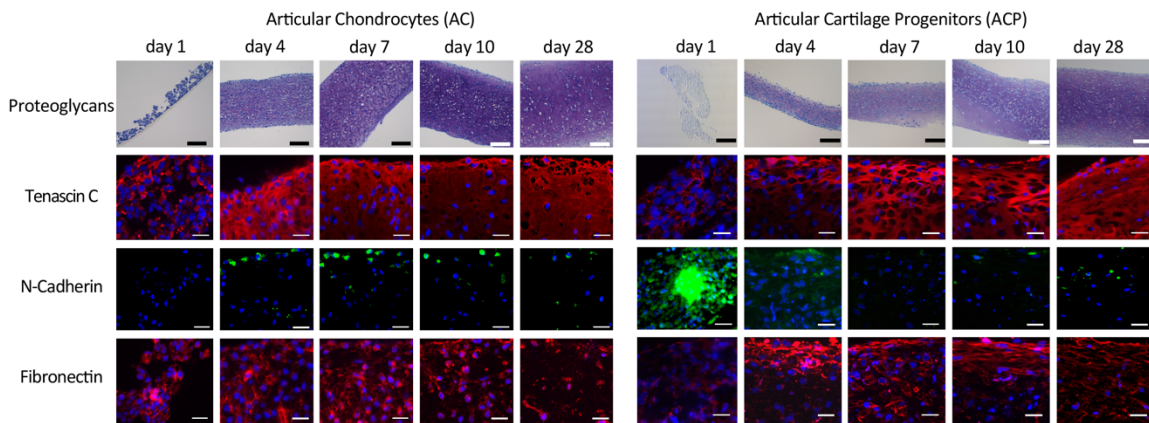


FIGURE 4.3 – DEVELOPMENT OF SCAFFOLD-FREE NEOCARTILAGE OVER TIME.

Over 28 days of culture, both AC- and ACP-derived neocartilage discs grow in thickness with proteoglycans distributed throughout the depth. The day 1 ACP sample curled off of the membrane during tissue processing. When probed for markers of mesenchymal condensation, both AC- and ACP-derived neocartilage displayed a progressive increase in tenascin C and fibronectin with increased time in culture. N-cadherin, a marker of cell-cell interaction, was highly expressed in day 1 ACP-derived neocartilage and minimally expressed between interacting cells in the apical surface at other time points. We were limited by the inability to repeat staining for n-cadherin on the day 1 AC sample based on the minimal amount of tissue, but we reason that it is likely present based on persistence at later time-points. Nuclei counterstained blue with DAPI. Scale = 100 μ m for proteoglycan histology, and 10 μ m for all immunohistochemistry.

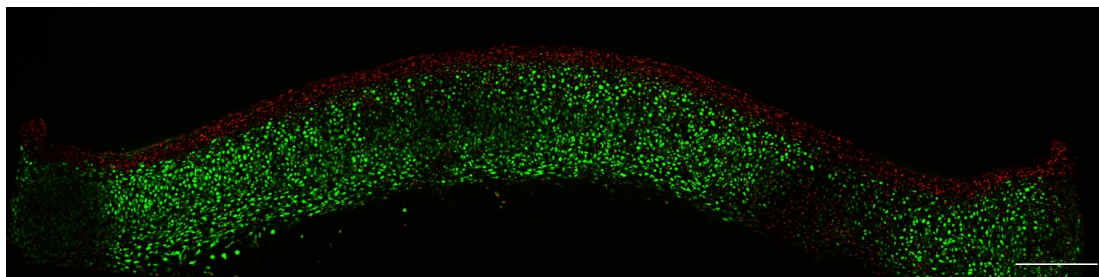


FIGURE 4.4 – CELL VIABILITY WITHIN SCAFFOLD-FREE NEOCARTILAGE.

A live/dead assay of a neocartilaginous disc in cross-section after 28 days in culture reveals that cells remain alive throughout the depth of the tissue; however, there is a region of dead cells at the apical surface. Scale = 500 μ m.

Physioxia promotes biochemical anabolism of ACs toward that of ACPs. Compared with culture in hyperoxia, culture in physioxia significantly increased the total amount of glycosaminoglycans (GAGs) produced by ACs; however, this increase was not significant when normalized to DNA content (Figure 4.5). In contrast, ACPs did not produce significantly more GAGs in physioxia versus hyperoxia. ACPs, however, did produce significantly more GAGs than ACs in hyperoxia, a difference retained with normalization to DNA. DNA content was not different among cell types at varied oxygen tension or between cell types at a given oxygen tension. There was not a statistically significant difference in total collagen content for either cell type between oxygen levels, but ACP-derived neocartilage contained significantly more collagen in physioxia in comparison with AC-derived neocartilage. There were no differences in tissue wet weight or thickness between cell types or oxygen levels.

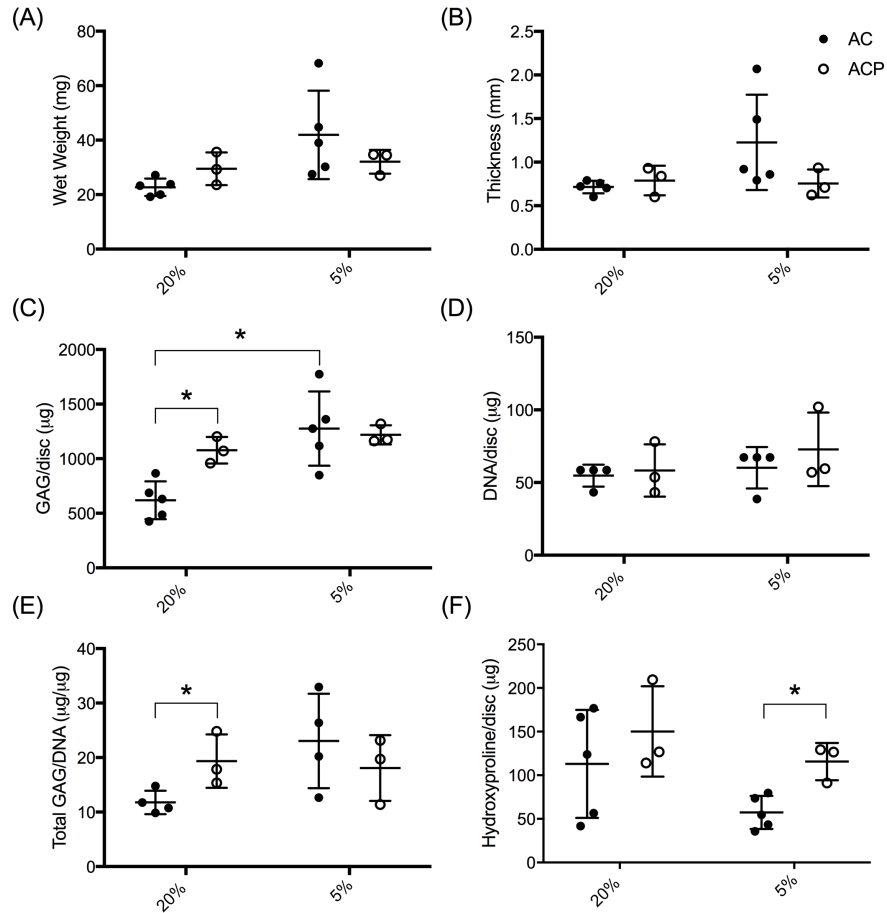


FIGURE 4.5 – BIOCHEMICAL ANALYSIS OF SCAFFOLD-FREE NEOCARTILAGE.

(A) Tissue wet weight and (B) thickness were not different between cell type or oxygen level. Quantitative measurements for biochemical constituents of the neocartilage discs including (C, E) glycosaminoglycans (GAGs) as a readout for total proteoglycan content, (D) DNA for relative cell count, and (F) hydroxyproline for total collagen content indicate that relative to hyperoxia, culture in physioxia significantly increased total GAG content for only ACs. ACPs, however, had a significantly higher total collagen content in than ACs culture in physioxia. Results reported as mean + SD, and statistical significance was determined as * $p < 0.05$ by a paired or unpaired t-test where appropriate.

Physioxia enhances the bulk mechanical properties of AC neocartilage, and ACP neocartilage is mechanically superior. AC-derived neocartilage cultured at physioxia demonstrated significantly increased compressive equilibrium modulus for stress relaxation tests at 10 and 20% strain than those cultured in hyperoxia (Figure 4.6). Further, AC-derived neocartilage exhibited strain stiffening behavior—increasing in stiffness with

increasing deformational compressive strain. The compressive equilibrium modulus for ACP-derived neocartilage was unresponsive to changes in oxygen but was significantly higher than that for AC-derived neocartilage at matched oxygen level for each strain ramp; though, ACP-derived neocartilage also demonstrated strain stiffening behavior in physioxia. The dynamic modulus for 1% dynamic strain at 1Hz frequency was not different between cell types at a given oxygen level or between oxygen levels for a given cell type.

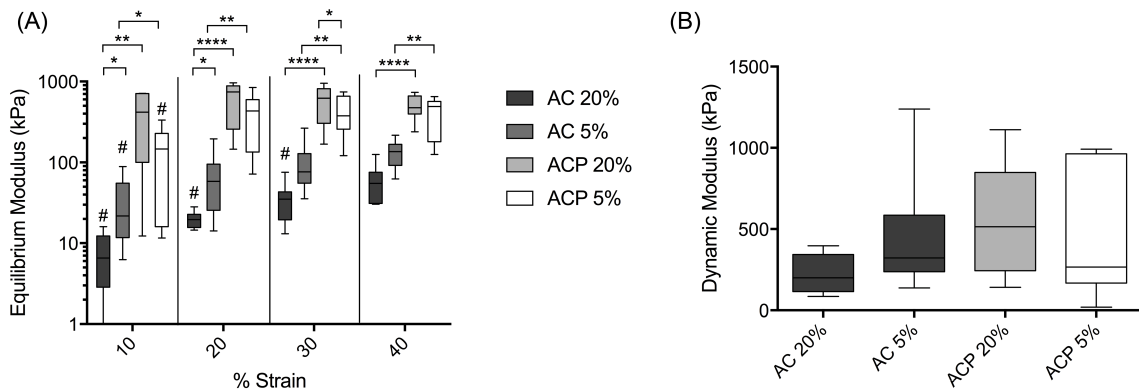


FIGURE 4.6 – BIOMECHANICAL ANALYSIS OF SCAFFOLD-FREE NEOCARTILAGE.

Quantitative analysis of (A) equilibrium compressive modulus reveals that scaffold-free neocartilage demonstrated strain stiffening behavior, physioxia significantly increased the bulk compressive equilibrium modulus for AC neocartilage, and ACP neocartilage was significantly more stiff than AC neocartilage. There were no differences in (B) dynamic compressive modulus between cell types or oxygen levels. Results reported as a box plot representing mean, the 1st and 3rd quartiles, and SD. Statistical significance was determined as * $p < 0.05$, ** $p < 0.01$, **** $p < 0.0001$ by a paired t-test within a cell type between oxygen levels, an unpaired t-test between cell types within a given oxygen level. Statistical significance between consecutive strain ramps for a given group was determined as # $p < 0.05$ to characterize strain stiffening.

Physioxia promotes the stable articular chondrocyte phenotype. Relative to culture in hyperoxia, culture of ACs in physioxia drove a significant fold-change increase in expression of many genes associated with the articular chondrocyte phenotype (*COL2A1*, *COL11A2*, *COL9A1*, *ACAN*, *SOX9*, *PRG4*) and a significant decrease in genes for the

fibrocartilagenous (*COL1A1*) and hypertrophic (*MMP13*) chondrocyte phenotypes (Figure 4.7). *COL10A1* was also consistently decreased among replicates, but not to a significant level. Due to wider intra-donor variation for ACPs than for ACs, there was no difference between the gene expression profile for ACPs cultured in hyperoxic or physioxic oxygen environments, though *COL2A1*, *COL1A1*, and *COL10A1* were each changed in the same direction but to a smaller magnitude as ACs for all ACP biologic replicates. Genes coding for the SOX transcription factors—*SOX9* and *L-SOX5*—were decreased in ACPs. Regardless of oxygen tension, *COL2A1*, *ACAN* and *COL1A1* were highly expressed for both ACs and ACPs relative to the housekeeping gene; *PRG4* was highly expressed for ACs, but very low for ACPs.

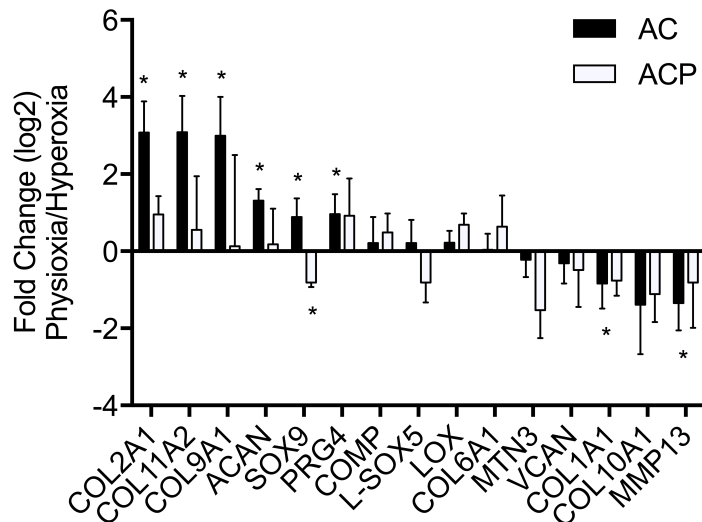


FIGURE 4.7 – CHONDROGENIC GENE EXPRESSION OF SCAFFOLD-FREE NEOCARTILAGE. Fold change in chondrogenic gene expression for culture in physioxia relative to hyperoxia demonstrates that ACs, but not ACPs, were highly responsive to oxygen level and upregulated genes representative of the articular cartilage phenotype in physioxia. Results reported as mean \pm SD of log2 fold change, and statistical significance was determined as * $p < 0.05$ by a paired or unpaired t-test where appropriate.

Physioxia promotes production toward the articular cartilage tissue phenotype.

With culture at hyperoxia or physioxia, AC-derived neocartilage exhibited abundant type II collagen throughout the tissue depth (Figure 4.8). ACP-derived neocartilage had a similar proteoglycan distribution to AC-derived neocartilage, but type II collagen was absent at both edges of each ACP disc in cross-section. Type I collagen was present throughout the matrix after 28 days of culture in hyperoxia but localized to the outer edges of the disc in physioxia for both cell types. Type X collagen was detectable at low levels for AC-derived neocartilage cultured in hyperoxia but undetectable at physioxia. In contrast, type X collagen was undetectable for all ACP-derived neocartilage regardless of oxygen tension. Quantification of types I and II collagen revealed that ACPs expressed more type II than type I collagen and expressed significantly less type I collagen than ACs. ACs, however, reduced the amount of type I collagen in physioxia to improve the ratio of type II/I toward that of ACPs. AC-derived neocartilage produced lubricin that was primarily localized to the side contacting the well in free-swelling culture, and this expression was independent of oxygen tension (Figure 4.9). In contrast, lubricin was not detectable in any of the ACP-derived neocartilage discs. Investigation of pericellular proteins from the native tissue—perlecan and type VI collagen—revealed that perlecan was distributed throughout the bulk of extracellular matrix for both cell types while type VI collagen was more pericellular in distribution for only ACPs; both protein distributions were independent of oxygen level.

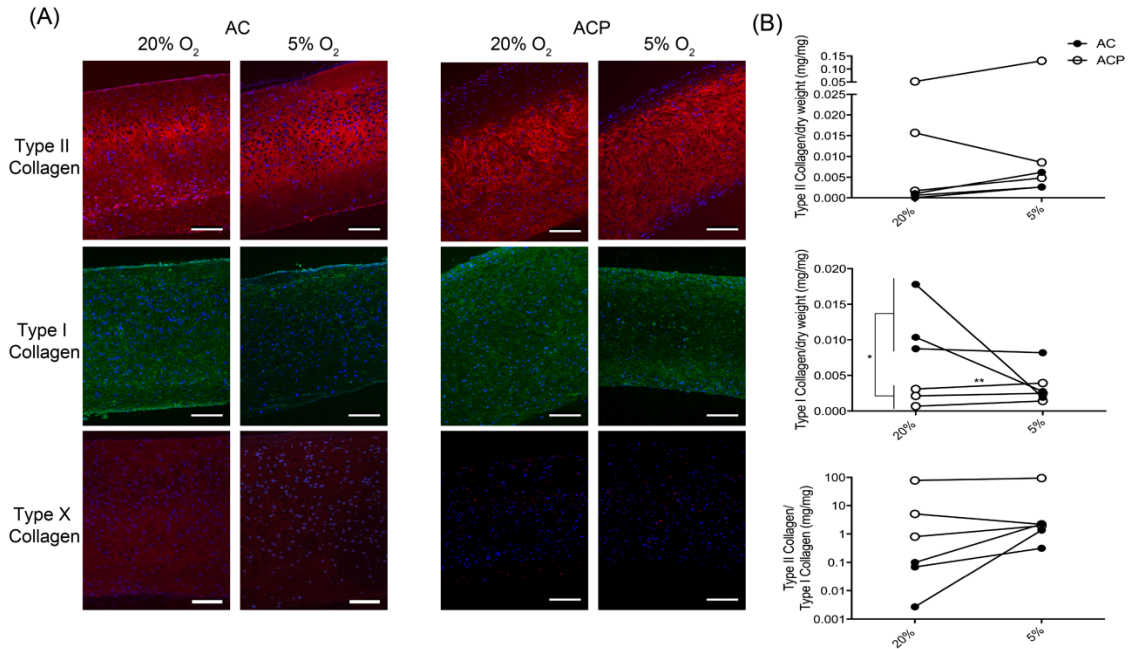


FIGURE 4.8 – COLLAGEN ANALYSIS OF SCAFFOLD-FREE NEOCARTILAGE.

(A) Collagen immunohistochemistry demonstrates consistently high type II collagen expression in tissues derived from both ACs and ACPs in hyperoxia and physioxia but reduced type I collagen for both AC- and ACP-derived tissues in physioxia relative to hyperoxia. AC-derived neocartilage had low type X collagen expression in hyperoxia that was undetectable in physioxia, but ACP-derived neocartilage lacked type X collagen at both oxygen levels. Nuclei counterstained blue with DAPI. Scale bars = 100 μ m. (B) Quantification of collagen by ELISA indicates that ACP-derived neocartilage contained more type II than type I collagen regardless of oxygen level, but AC-derived neocartilage increases the ratio of type II to I collagen with culture in physioxia relative to hyperoxia. Statistical significance was determined as * $p < 0.05$, ** $p < 0.01$ by a paired or unpaired t-test where appropriate.

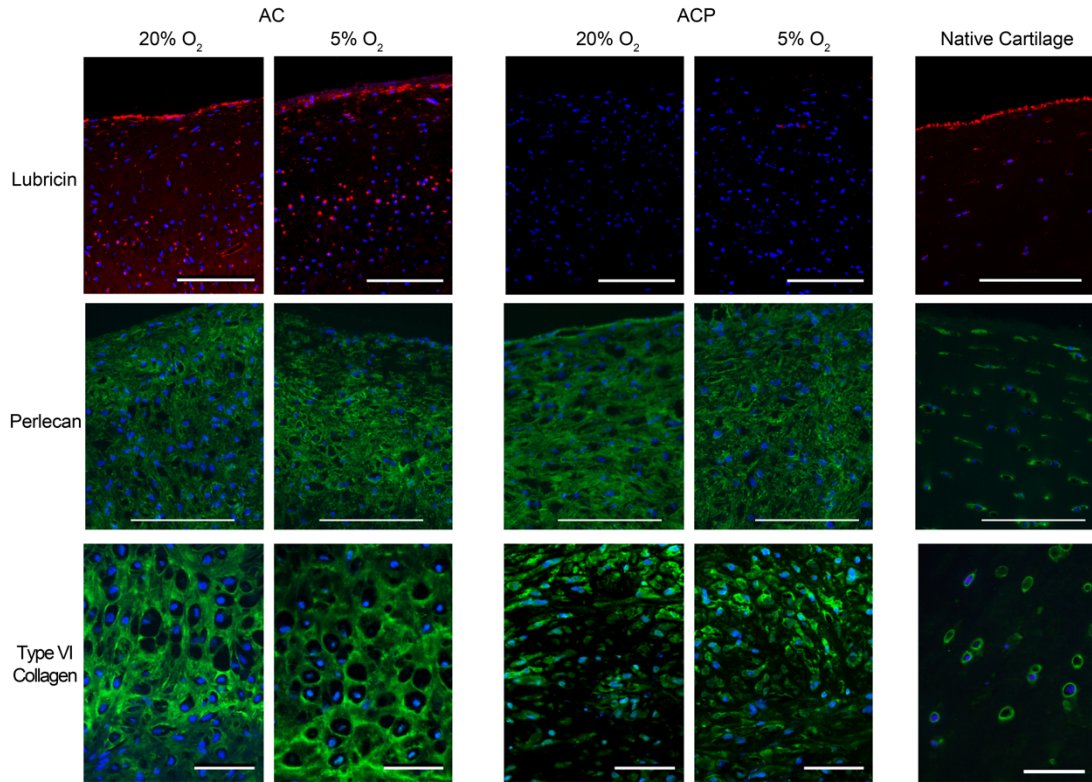


FIGURE 4.9 – LOCALIZED MOLECULES OF SCAFFOLD-FREE NEOCARTILAGE.

Immunohistochemistry of lubricin, perlecan, and type VI collagen revealed that only AC-derived neocartilage produced lubricin that was localized to the surface regardless of oxygen level. Also independent of oxygen level, neocartilage from both cell types produced perlecan that was distributed throughout the extracellular matrix, and ACP-derived neocartilage had type VI collagen localized to the pericellular matrix while type VI collagen was distributed throughout the entire extracellular matrix for AC-derived neocartilage. Nuclei counterstained blue with DAPI. Scale bars = 100 μm for lubricin and perlecan, 20 μm for type VI collagen.

Mature collagen crosslinks were undetectable in scaffold-free neocartilage. In collaboration with the Bächinger Laboratory at the Shriners Hospital for Children, we developed methods to quantify both immature and mature collagen crosslinks to characterize the maturity of the collagen network in scaffold-free tissues cultured for 28 days. We were unable to attempt to quantify immature crosslinks because we could not purchase or generate standards for comparison with neocartilage in HPLC due to cost limitations. We were able to detect mature collagen crosslinks, including hydroxylysyl-

pyridinoline (HP) and lysyl-pyridinoline (LP), in native articular cartilage; however, HP and LP were below the limit of detection in scaffold-free tissues derived from ACs and ACPs. We do not know if the crosslinks were undetectable because of the relatively scarce amount of tissue used for the assay in comparison with native tissue, or if they were undetectable because of tissue immaturity.

4.5 DISCUSSION:

We have developed a reliable method for producing scaffold-free neocartilage discs from adult human-derived stem cells toward the eventual goal of focal articular cartilage repair. Few studies have extensively investigated scaffold-free tissue engineering from adult human-derived cells; the only study to directly compare scaffold-free tissues generated from adult human chondrocytes and MSCs used a single biologic donor for each (156). In the current study, we obtained all results with a minimum of three biological replicates of each cell type. Historically, scaffold-free cartilage tissue engineering emerged in the context of coalescing limb bud mesenchymal cells (145), which subsequently inspired three-dimensional pellet culture to study *in vitro* differentiation of human stem cells (129,147). Studies of scalable scaffold-free techniques independently by Hu et al. (2006), Novotny et al. (2006) and Hayes et al. (2007) showed that neonatal mammalian primary chondrocytes build tissues with characteristics of articular cartilage following self-assembly or self-organization (31,148,149). The scaffold-free systems developed for neonatal primary cells in these initial studies, however, are unlikely to be viable strategies to generate tissues using adult human-derived chondrocytes, which are limited in

metabolism and expansion potential in comparison with neonatal or juvenile mammalian cells (103,223).

We found that expanded adult human chondrocytes maintained a disc-like tissue morphology when cultured on a polymer substrate—results consistent with a previous report of scaffold-free human cell-based tissue generation (160)—but contracted into macro-pellets in non-adherent culture. Unlike ACs, we found that chondroprogenitors needed a protein substrate to retain tissue geometry. This is the first report of scaffold-free tissue engineering utilizing ACPs. The high binding affinity between fibronectin and abundant cell surface integrins on these cells informed our decision to employ fibronectin as opposed to types I and II collagen, which have previously been used to guide human scaffold-free self-organization (160). Fibronectin is also the earliest expressed and a necessary extracellular matrix molecule for cell condensation (151,218). We sought to promote self-organization and guide cell condensation utilizing fibronectin as a necessary substrate to define tissue geometry into a flattened disc as opposed to a pellet.

Low oxygen has previously been shown to be detrimental to the development of scaffold-free neocartilage (159); though, we posit that the noted central void in scaled-up tissue culture was the result of tissue anoxia from nutrient deprivation, which has previously been characterized by both diffusion modeling and oxygen delivery experiments (221,224). In our system, we generated thick tissues without a central void through optimization of cell seeding density and culture media volume. In accordance with our previous data from re-differentiation of expanded human chondrocytes in pellet culture (178), lowered oxygen promoted the stable articular cartilage phenotype for ACs in the scaffold-free disc model, especially at the gene level. Lowering oxygen stabilizes hypoxia-

inducible factors (HIFs), which are otherwise targeted for proteosomal degradation in the presence of oxygen. HIFs, in turn, regulate transcription factors and genes with hypoxia responsive elements (HRE), drive chondrogenesis toward the articular chondrocyte phenotype, and modulate extracellular matrix metabolism (177). In physioxia, ACs significantly upregulated genes with HREs, including *SOX9* and *PRG4*, which also led to a downstream increase in SOX-9 targets: *COL2A1* and *ACAN*. Although all ACP clones upregulated *COL2A1* in physioxia, the response was not significant. ACPs did not significantly modify any other genes of the articular chondrocyte phenotype. We have previously shown that the response of human-derived stem cells to lowered oxygen depends on the intrinsic chondrogenic differentiation capacity, and highly chondrogenic ACP clones, such as those used in the present work, were less responsive at the gene level than poorly chondrogenic clones (Chapter 3). The only significant change in gene expression from culture in hyperoxia to physioxia for ACPs was a decrease *SOX9*, which was possibly a consequence of examining gene expression only after 28 days of culture—a time point much later than the induction of differentiation by TGF- β or physioxia culture when *SOX9* is first promoted. Both cell types consistently downregulated *COL10A1* of the hypertrophic chondrocyte phenotype, but only ACs significantly downregulated *COL1A1* and *MMP13*; results also consistent with our previous work exploring the role of physioxia in regulation of the hypertrophic phenotypes of chondrogenic cells (Chapter 3) (178).

Compared with culture in hyperoxia, physioxia significantly increased the bulk equilibrium modulus for AC-derived neocartilage following a concomitant increase in total GAG production. While compressive stiffness directly correlates with proteoglycan content in native tissue (25), a greater than 10-fold higher equilibrium modulus of ACP-

relative to AC-derived tissue was not attributable only to proteoglycan content based on equivalent GAG levels in physioxia. Thus, differences in compressive stiffness are due to other constituents of the extracellular matrix: potentially including collagen, which primarily contributes to tensile, shear, and dynamic stiffness. In these tissues, there were not only differences in the total collagen content but also in the types of collagen between AC- and ACP-derived tissues, with more type II collagen in ACP-derived neocartilage. Further, increased overall collagen may be complemented by collagen crosslinking in physioxia through lysyl oxidase, which has an HRE in its gene promoter region, to drive a further increase in compressive modulus similar to mechanisms of post-natal native tissue maturation (23). However, we were unable to detect mature collagen crosslinks in these tissues. Previous studies have shown that lowered oxygen increases collagen crosslinking in maturing scaffold-free tissues generated from primary bovine chondrocytes (153). In physioxia, both AC- and ACP-derived neocartilage exhibited strain stiffening behavior—a property of the collagen network of mature articular cartilage that immature postnatal tissues lack (23)—indicating potential evidence for enhanced collagen crosslinking. Unlike the compressive equilibrium modulus, the dynamic modulus was no different between tissue types nor with change in oxygen level. In native tissue, dynamic modulus is traditionally proportional to collagen content (25); though, ACP-derived neocartilage did not have a significantly higher dynamic modulus despite increased collagen content in physioxia.

Further investigation of the extracellular matrix revealed that the collagen expression profile was improved with culture in physioxia relative to hyperoxia for neocartilage from both ACs and ACPs—maintaining global type II collagen expression but

decreasing types I and X collagen throughout the tissues. These results are consistent with those for pellet culture of each cell type (Chapter 3) (178). Regardless of oxygen tension, AC-derived neocartilage did not show evidence of pericellular matrix localization of type VI collagen or perlecan, and these proteins were expressed throughout the bulk of the matrix. ACP-derived neocartilage displayed similar perlecan expression to AC-derived neocartilage; however, ACPs localized type VI collagen to the pericellular matrix after 28 days in physioxia and hyperoxia. Both perlecan and type VI collagen may serve as additional markers of tissue maturity in scaffold-free neocartilage, as these proteins are globally expressed in neonatal cartilage and subsequently localized to the pericellular matrix with maturation (43,46), potentially suggesting greater matrix maturity for ACP-derived than AC-derived neocartilage. Independent of oxygen level, ACs produced abundant lubricin that was localized primarily to one surface of the neocartilage disc. In contrast, ACPs did not produce detectible amounts of lubricin. Chondroprogenitors have recently been identified by *PRG4* expression (20) or lubricin production (136,225) *in vivo*, but this is the first study to investigate lubricin and *PRG4* expression during *in vitro* differentiation or tissue engineering of ACPs. Lack of *PRG4* and lubricin expression in these tissues is of concern and indicates that these cells may be subject to phenotypic modification when isolated, cloned, expanded, and differentiated *in vitro*, and *PRG4* expression may be attenuated following differentiation toward the articular chondrocyte phenotype. Alternatively, the cells isolated from the adult human tissue through differential fibronectin adhesion may represent a progenitor population up- or down-stream in the chondrocyte lineage from the *PRG4*-expressing lineage identified *in vivo* (20,21), or the cell populations may be entirely distinct; these remain future topics for investigation in our

laboratory to work toward the goal of producing a tissue of biomechanical equivalence to native tissue.

4.6 CONCLUSIONS:

Taken together, our results regarding biochemical and biomechanical properties, gene expression, and protein expression indicate that culture in physioxia relative to hyperoxia is beneficial for AC neocartilage development toward the articular cartilage phenotype. Although they were less responsive to changes in oxygen, highly chondrogenic ACPs clones produced a robust tissue that was mechanically superior and more mature than tissues derived from ACs, and unlike ACs, these tissues were derived from a single cell following clonal isolation and expansion. The ability to produce large-scale scaffold-free constructs of a defined geometry from adult human cell sources, especially from clonal chondroprogenitors, may eventually allow us to offer personalized and autologous therapies to a large population suffering from focal articular cartilage injuries. With further development, this scaffold-free tissue engineering approach may enable us to generate tissues with an extracellular matrix that suits both structural and functional demands required of a repair tissue.

CHAPTER 5:
SCAFFOLD-FREE NEOCARTILAGE MATURATION UNDER
DYNAMIC COMPRESSIVE STIMULATION

Devon E. Anderson,¹ Constance Pritchard,¹ Robert L. Mauck,² and Brian Johnstone¹

¹Oregon Health & Science University, Department of Orthopaedics & Rehabilitation

²University of Pennsylvania, Department of Orthopaedic Surgery

Work presented at Gordon Research Conference in Musculoskeletal Biology and Bioengineering, August 2016.

Devon executed all aspects of this project from experimental design through data collection and analysis.

5.1 ABSTRACT:

Introduction: Mechanically stimulated reorganization of the extracellular matrix is thought to drive both depth-dependent anisotropy and pericellular matrix development in native articular cartilage. Scaffold-free neocartilage tissues derived from adult human chondrocytes and chondroprogenitors exhibit structural immaturity similar to neonatal mammalian cartilage. The objective of this project was not only to define the role of a dynamic mechanical environment in driving maturation of biochemical constituents and biomechanical properties of scaffold-free neocartilage, but also to investigate the role of endogenous fibroblast growth factors (FGF) in modulating the metabolic reorganization of the extracellular matrix toward anisotropy in response to dynamic load.

Methods: Human adult chondrocyte- and chondroprogenitor-derived scaffold-free neocartilage was grown for 28 days in free-swelling culture. Tissues were subsequently subjected to either dynamic compressive load in a custom bioreactor or free-swelling culture for an additional 14 days in the presence or absence of an FGF receptor inhibitor.

Results: The custom bioreactor was able to both measure tissue thickness and load tissues throughout a defined dynamic compressive regime. Tissues derived from both chondrocytes (ACs) and chondroprogenitors (ACPs) did not experience a significant change in bulk biochemical properties, including collagen and proteoglycan content, or gene expression with perturbation of time, load, or FGF receptor inhibition. Additional time in culture, but not load nor FGF receptor inhibition, enhanced the biomechanical properties of neocartilage. Endogenous FGF signaling was efficiently blocked with the

receptor inhibitor but was ineffective in promoting tissue reorganization with respect to extracellular matrix molecule distribution.

Conclusions: This was the first experiment to load scaffold-free tissues derived from human cell sources. Unlike cells cultured in a stiff biomaterial substrate, scaffold-free tissues cannot bear load until the cells produce a robust extracellular matrix, and a pre-load culture period substantially increases overall experimental duration compared with biomaterial-based tissue engineering. Relative to free-swelling controls, dynamic compression for 14 days following a 28-day pre-load culture period, did not significantly enhance the biochemical or biomechanical properties of AC- or ACP-derived neocartilage, nor did it influence localization of extracellular matrix molecules. Based on previous work with chondrocytes, tissue maturation in the mechanical environment may require a time scale longer than that employed in the current loading regime. Ultimately, the ability to generate tissues of the mature articular cartilage phenotype utilizing a scaffold-free approach from a single human cell origin may improve the functional properties and therapeutic potential of neocartilage destined for autologous repair.

5.2 INTRODUCTION:

Mature native articular cartilage demonstrates distinct depth-dependent anisotropy with respect to cell distribution and morphology, collagen arrangement, and extracellular matrix molecule distribution, and the tissue can be histologically divided into superficial, middle, and deep zones based on these characteristics. Within all zones, the extracellular matrix is organized into distinct regions from the cell outward, creating another anisotropic

arrangement of the tissue (32,33) While it is well known that the anisotropic structural organization of articular cartilage facilitates tissue function (25,40), the development of structural anisotropy largely remains an unknown process.

Similarly, the mechanisms that drive articular cartilage development *in utero* remain unclear; recent results in a rodent model indicate that the tissue is potentially derived from clonal articular cartilage progenitors (ACPs) through appositional growth (20). Further evidence from animal models indicates that mechanical signals throughout the duration of embryologic development are necessary for cartilage tissue formation. Synovial joints fail to develop with early chemically-induced neuromuscular paralysis of chick embryos *in ovo* (7,22). Later induction of neuromuscular paralysis results in articular cartilage of decreased extracellular matrix content and reduced biomechanical stiffness in comparison with non-paralyzed controls (226). Following tissue development *in utero*, postnatal mammalian tissue is immature and relatively isotropic with more homogeneous extracellular matrix distribution than adult articular cartilage as evidenced in histological analysis (16,18,23,38,227,228). Mechanically stimulated reorganization is hypothesized to drive both depth-dependent zonal organization and pericellular matrix development (33,180). Based on analyses of regional variation in cartilage from newborn, juvenile, and adult mammals, multiple groups have validated that areas of increased loading within a single specimen as well as the same location between specimens of increased age exhibit greater tissue stiffness (37,229). An increase in tissue stiffness with age appears to correspond with the temporal establishment of anisotropy and maturation of the collagen network over the same time scale (23,230).

In mature cartilage, each zone throughout the tissue depth has a structure suited for the mechanical environment, and the pericellular matrix surrounding each cell translates mechanical signals into biological events through mechanotransduction (33,40). The spatial relationship of matrix molecules in the pericellular matrix, including type VI collagen and perlecan, is thought to govern cellular mechanotransduction events (44). These molecules, however, are found throughout the bulk of the matrix in postnatal mammalian cartilage and are subsequently localized to the pericellular matrix through unknown mechanisms of tissue remodeling (43), revealing potential markers of tissue maturity in both native and tissue-engineered cartilage. In mature cartilage, there exists an extracellular pool of basic fibroblast growth factor (FGF2) that is bound to the heparan sulfate glycosaminoglycan chains of perlecan and that signals through extracellular-regulated kinase (ERK) pathways in the adjacent cell following release under mechanical perturbation (44,231,232). Exogenous application of both FGF2 and TGF- β 1 to immature cartilage explants in the absence of a mechanical environment induces precocious maturation of native mammalian cartilage with remodeling toward anisotropy (231,232). These studies indicate that tissue reorganization into distinct zones and development of the pericellular matrix in the mechanical environment is likely not simply a passive process driven only by mechanical forces at each zone; rather, these processes, similar to development or degeneration, are driven by a balance of anabolic and catabolic mediators in response to chemical signals. For example, FGF2 is known to upregulate catabolic enzymes including matrix metalloproteinases 1 and 3 (MMP1, MMP3) and anti-catabolic factors including tissue inhibitor of metalloproteinases 1 (TIMP1) in response to cartilage injury through induction of the mitogen-activated protein kinase (MAPK) pathway

(233,234). Another consequence of FGF2-induced MAPK signaling is upregulation of *INHBA*, the gene for activin A, which is a member of the TGF- β superfamily and inhibits proteoglycan degradation through suppression of aggrecanases (ADAMTS) (234,235). FGF2 has further been shown to regulate chondrocyte hypertrophy by upregulating *RUNX2*, and subsequently *MMP13*, through the PKC δ pathway (236,237). The enzyme MMP13 degrades type II collagen in articular cartilage during tissue remodeling to facilitate endochondral ossification. Taken together, these defined pathways indicate that mobilization of FGF2 from the pericellular matrix in the mechanical environment, including during both physiologic loading in developing cartilage and supra-physiologic loading in injury, drives downstream regulation of catabolic and anti-catabolic mediators to remodel the collagen and proteoglycan constituents of the extracellular matrix.

FGF2 has been investigated as an exogenously added chemical mediator of cell proliferation, differentiation, and metabolism in tissue-engineered articular cartilage (28,238); however, the role of endogenous FGF2 bound to heparan sulfate in tissue engineered cartilage has not been investigated as a potential mediator of tissue-engineered neocartilage maturation in a mechanical environment. Scaffold-free neocartilage tissues derived from human adult chondrocytes and chondroprogenitors exhibit structural immaturity and lack both depth-dependent and cell-outward anisotropy of native mature cartilage. The objective of the current study was not only to define the role of a dynamic mechanical environment in driving maturation of biochemical constituents and biomechanical properties of scaffold-free neocartilage, but also to investigate the role of endogenous FGF2 in modulating the metabolic reorganization of the extracellular matrix toward anisotropy in response to dynamic load. To test the hypothesis that FGF2 release

and signaling drive tissue maturation in the mechanical environment, we compared dynamically loaded tissues with free-swelling controls in the presence or absence of a pan-FGF receptor inhibitor.

5.3 MATERIALS & METHODS:

Cell & Tissue Culture: Articular cartilage progenitors (ACPs) and articular chondrocytes (ACs) (n = 3 each, all male age 16-33) were isolated from healthy human cartilage according to methods described in Chapter 2. Briefly, full thickness articular cartilage was dissected from the femoral condyles of healthy human donors, and the total chondrocyte population was isolated through enzymatic digestion of minced tissue. ACPs were further isolated from the total chondrocyte population through differential adhesion to fibronectin coated plates, and clonal populations were selected and expanded. Expanded populations of ACPs and ACs were plated onto fibronectin-coated Transwell inserts to generate scaffold-free neocartilage discs according to methods described in Chapter 2. Neocartilage discs from at least 3 biologic replicates of each cell type were differentiated in serum-free chondrogenic differentiation medium and cultured in free-swelling conditions for 28 days before being separated into treatment groups according to Table 5.1, with at least 5 discs per group.

Cell seeding density was defined for each cell type prior to the loading experiment and was scaled to 3×10^6 cells per disc for ACPs and 2×10^6 cells per disc for ACs to facilitate growth of the thickest possible construct over a 28-day differentiation pre-culture period without development of a central void from poor nutrient diffusion. Groups receiving the FGF receptor inhibitor from day 29 to day 42 were cultured with 250 nM of

a small molecule inhibitor of FGF receptor types 1 and 3 (FGFRI) (Sigma-Aldrich, PD173074) in 7 μ M DMSO (Sigma-Aldrich), concentrations previously validated for tissue culture (44). Tissues not receiving FGFRI treatment were cultured with equivalent concentrations of DMSO as a vehicle control over the same period.

Week	1	2	3	4	5	6	7
D28 baseline	Expansion	Pre-culture 28 days					
D42 unloaded						Free Swelling	
D42 + Load						Load	
D42 + FGFRI						FGFRI	
D42 + Load + FGFRI						Load + FGFRI	

Bioreactor Design and Validation: A custom dynamic compression bioreactor (Figure 5.1) was designed according to specifications previously developed by Mauck et al. (182,183), with modifications to integrate load monitoring capabilities. Specifically, a stepper motor and integrated linear stage (ATS0300-BMS-U, AeroTech, Pittsburgh, PA) were driven by a uniaxial controller (Soloist, AeroTech). A through-hole donut load cell (THA-50-P, Transducer Technologies, Inc., Temecula, CA) was integrated between a horizontal stage extension and a sterile polysulfone loading platen, and it was integrated to a custom LabView graphical user interface (GUI) through a low-voltage transmitter (SST-LV, Transducer Technologies). The custom LabView GUI (Ashford Solutions, Beaverton, OR) integrated position and load to measure tissue thickness through differential load detection and to monitor load over a dynamic compression regime (Figure 5.2). These two functions were validated with a preliminary experiment to monitor parameters (load and displacement) during a loading regime consisting of 1 Hz dynamic compression at 10 %

strain superimposed on a 5% pre-strain for agarose discs (A9414, Sigma-Aldrich) of increasing percent weight by volume, testing the hypothesis that substrate stiffness, corresponding to % w/v agarose, will correlate to the load required to compress discs to a standard percent strain.

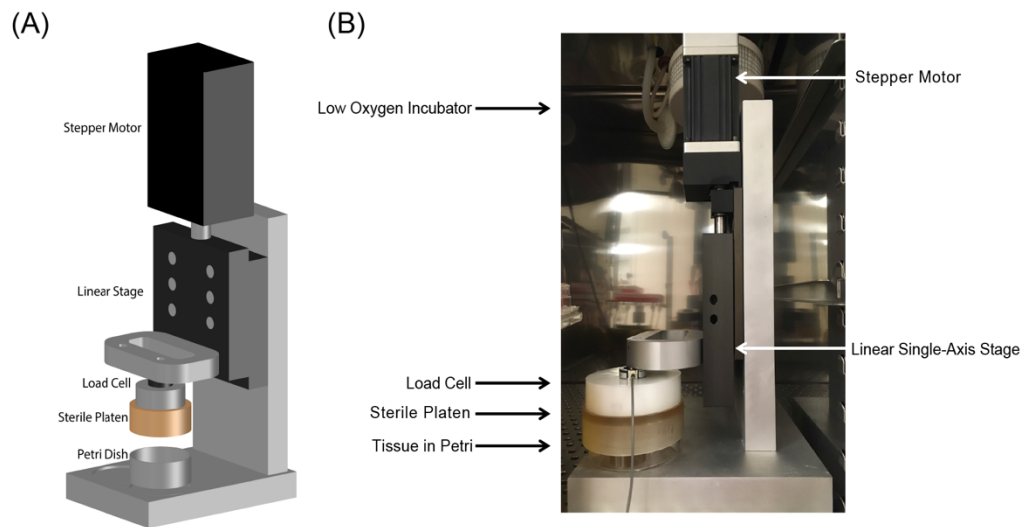


FIGURE 5.1 – BIOREACTOR FOR DYNAMIC MECHANICAL STIMULATION. (A) Schematic and (B) image of custom dynamic compressive bioreactor.

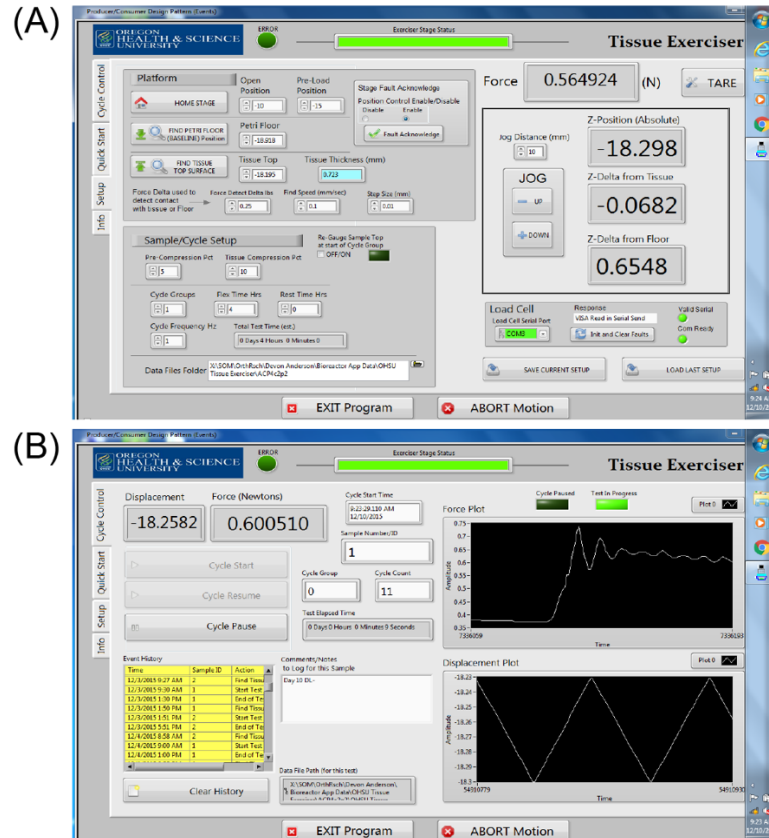


FIGURE 5.2 – BIOREACTOR SOFTWARE GRAPHICAL USER INTERFACE.

Layout of the (A) experimental set-up and (B) load cycle control panels of the custom graphical user interface (GUI) for the dynamic compressive bioreactor.

Mechanical Stimulation: Tissues subjected to mechanical stimulation were cultured for a 28-day differentiation period in free-swelling culture. Starting on day 29, tissues were subjected to 14 days of dynamic compression for 4 hours per day. The loading regime consisted of a 10% peak-to-peak 1 Hz dynamic strain of a triangle waveform superimposed on a 5% pre-strain to engage tissues and to maintain contact over the loading period. When not under stimulation, tissues were removed from the bioreactor and cultured on an orbital shaker at 1 Hz, which represents the conditions used for free-swelling controls over the same 14-day culture period. The platen was rinsed with 100% ethanol and sterile 1X PBS before and after loading each group.

Biochemical and Biomechanical Analyses: Biochemical assays including glycosaminoglycan, DNA, and hydroxyproline quantification and biomechanical tests to derive the bulk tissue compressive equilibrium and dynamic moduli were conducted using triplicate sample replicates according to methods described in Chapter 2.

Gene Expression Analyses: RNA was isolated from one quarter of two or three pooled sample replicates in each condition with the RNeasy Mini Kit according to manufacturer's instructions and methods of Chapter 2. Quantitative polymerase chain reaction (qPCR) was performed using reverse transcribed cDNA and TaqMan assay primers (Table 2.1) to the following gene targets: *COL1A1*, *COL2A1*, *COL6A1*, *COL9A1*, *COL10A1*, *COL11A2*, *ACAN*, *VCAN*, *MTN3*, *PRG4*, *SOX9*, *LOX*, *MMP1*, *MMP13*, *TIMP1*, *INHBA*, *TRPV4*, and *PIEZO1*. RNA was collected from loaded tissues within 2 hours of the final loading regime based on previously published work to define the temporal regulation of genes following loading of human chondrocytes (239). Gene expression was calculated using the $2^{-\Delta Ct}$ method relative to the most stably expressed housekeeping gene for each cell type—*TBP* for ACPs and *18S* for ACs—from 3 evaluated candidates. Thus, comparisons of gene expression were not made between cell types. Gene expression for each group was normalized to the baseline condition at day 28. Fold change (Log 2) from baseline was calculated for each gene of each experimental group for each cell type, and both unscaled and clustered heatmaps were generated using a R Studio.

Protein Analyses: Qualitative immunohistochemistry was performed on cross-sectional thin sections of neocartilage tissues from each condition and each cell type according to the methods and antibody parameters described in Chapter 2. Specifically, tissues were probed for types I, II, VI, and X collagen, perlecan, FGF2, and lubricin according to the antibody specifications in Table 2.2. Tissue lysates were collected by flash freezing neocartilage in liquid nitrogen, crushing the tissue with a pestle, and immediately lysing with RIPA buffer with 1% Triton X-100, 1% Tween 20, protease inhibitor, and phosphatase inhibitor. Total protein concentration was quantified through a BCA Assay, and equal quantities were loaded onto 10 or 15% polyacrylamide gels. Gels were run and transferred to PVDF membranes, blocked with 5% BSA to avoid phospho-protein cross-reactivity of casein, and probed for ERK1/2, phospho-ERK1/2, and FGF2 according to the antibody specifications in Table 2.2.

Statistical Analyses: All statistical analyses were performed using GraphPad Prism v7.0 (GraphPad, La Jolla, CA, USA). For each biochemical assay or biomechanical test, the five experimental groups within a given cell type were compared in a one-way analysis of variance (ANOVA) with multiple comparisons corrected with a Tukey's post-hoc analysis for significant tests. Each experimental condition was compared between cell types using an unpaired t-test. For all statistical analyses, significance was determined at $p < 0.05$. Values are reported as mean \pm standard deviation.

5.4 RESULTS:

The custom bioreactor loads tissues. To more accurately measure tissue thickness at the start of each loading period and to monitor stresses generated on tissues throughout a loading regime, a load cell was integrated into the dynamic compressive bioreactor through a custom LabView program. The bioreactor reliably measured tissue thickness within 10% error based on comparison between the measured thickness of agarose discs with digital calipers and the average of at least 3 thickness readings from the bioreactor. To validate tissue loading, the average load (N) was recorded from the mean of the first 50 cycles of agarose discs loaded in dynamic compression at 10% peak-to-peak strain on top of 5% static strain. The resultant stress was calculated by normalizing load by disc surface area. For agarose discs of increasing percent weight, substrate stiffness—measured as the compressive equilibrium modulus—was highly correlated to stresses generated within the bioreactor within a given loading regime (Figure 5.3). When the same measurements for tissue stiffness and bioreactor stress were calculated for all replicates of scaffold-free neocartilage subjected to the same dynamic loading regime, the majority of tissues exhibited a biomechanical response close to that of the agarose discs.

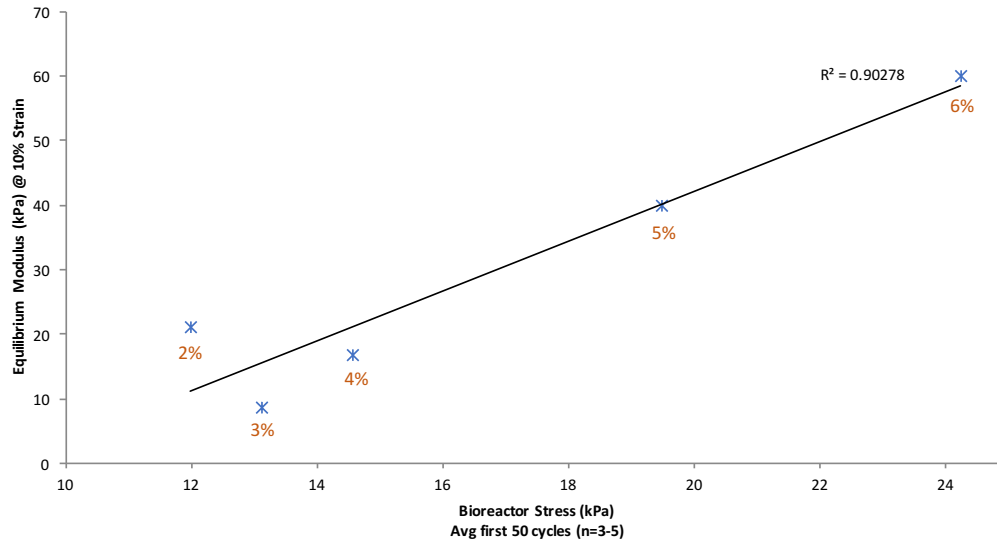


FIGURE 5.3 – BIOREACTOR VALIDATION WITH AGAROSE HYDROGELS.

Validation of the bioreactor through loading agarose discs of increasing % w/v demonstrate a relationship between substrate stiffness and stresses generated by each hydrogel in the defined dynamic loading regime.

Biochemical composition of scaffold-free neocartilage is unchanged with time, mechanical stimulation, or FGF receptor inhibition. Qualitative histologic analysis of tissues for total proteoglycan content revealed that loaded tissues are slightly thinner with higher metachromasia (Figure 5.4). Decreased metachromasia for AC-derived tissues cultured in FGFR1 relative to other groups was inconsistent with quantitative measures for GAG content. Following 14 days of free-swelling culture, dynamic loading, FGF receptor inhibition (FGFR1), or a combination of loading and FGFR1, there were no statistically significant changes to the total GAG, DNA, or hydroxyproline content of the extracellular matrix when compared with either the baseline tissues from day 28 or with one another, except for an increase in total GAG content for AC-derived neocartilage cultured with FGFR1 relative to baseline (Figure 5.5). There was wide variation in quantitative biochemistry across the three replicates of ACP-derived neocartilage, driving a lack of

significance for comparisons between AC- and ACP-derived tissues for GAG/DNA and hydroxyproline content, which were higher in ACP-derived tissues.

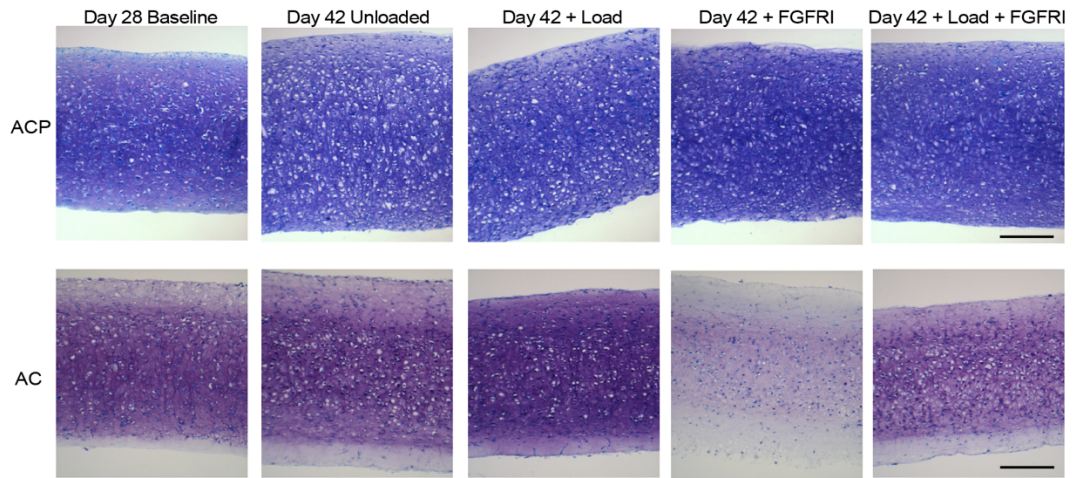


FIGURE 5.4 – PROTEOGLYCAN DISTRIBUTION IN STIMULATED NEOCARTILAGE.

Qualitative assessment of proteoglycan distribution by toluidine blue staining of paraffin-embedded tissue cross-sections demonstrates tissue compaction and increased metachromasia with load, and decreased metachromasia with FGF receptor inhibition. Scale = 100 μ m.

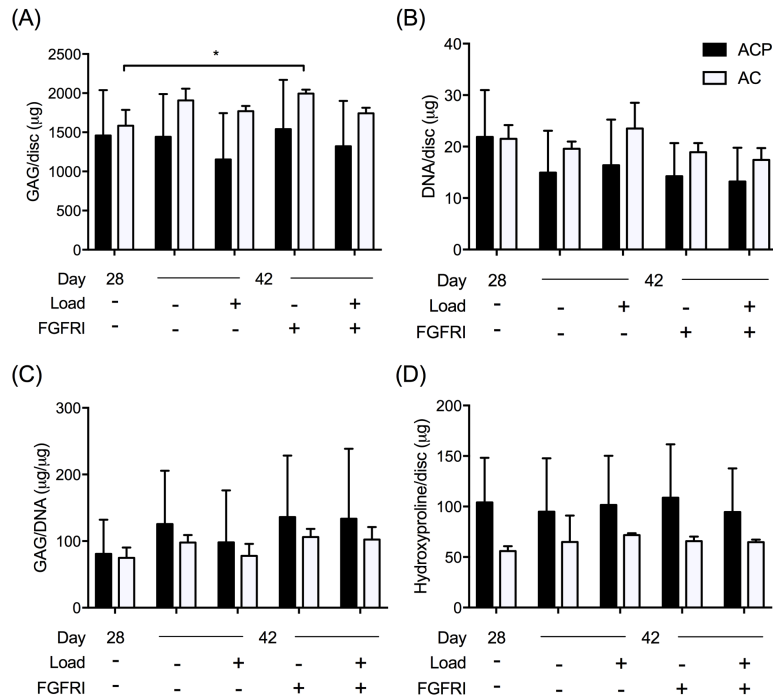


FIGURE 5.5 – BIOCHEMICAL ANALYSIS OF STIMULATED NEOCARTILAGE.

Composition of scaffold-free neocartilage derived from ACPs and ACs—including: (A) total GAG content, (B) total DNA content, (C) GAG/DNA, and (D) total collagen content—was unchanged with time, load, or FGF receptor inhibition. Statistical significance defined as $*p < 0.05$.

Time has the greatest impact on the bulk mechanical properties of scaffold-free neocartilage. Although not statistically significant because of wide variation in adult human-derived tissues, the additional 14 days of culture enhanced both the equilibrium modulus and dynamic modulus of ACP- and AC-derived neocartilage at consecutive 10% strain ramps in stress relaxation (Figure 5.6A, B). These tissues demonstrated strain stiffening behavior consistent with results from studies in physioxia (Chapter 4). The addition of dynamic compressive loading did not enhance the biomechanical properties any more than time. The addition of the FGFR1 decreased the equilibrium modulus of ACP-derived tissues, but adding dynamic load with the inhibitor reversed this reduction. There

were no differences in the peak stress—generated by each tissue in stress relaxation tests at 10% strain—across all conditions of either cell type; though, day 28 ACP-derived tissues had a significantly higher peak stress than day 28 AC-derived tissues (Figure 5.6C).

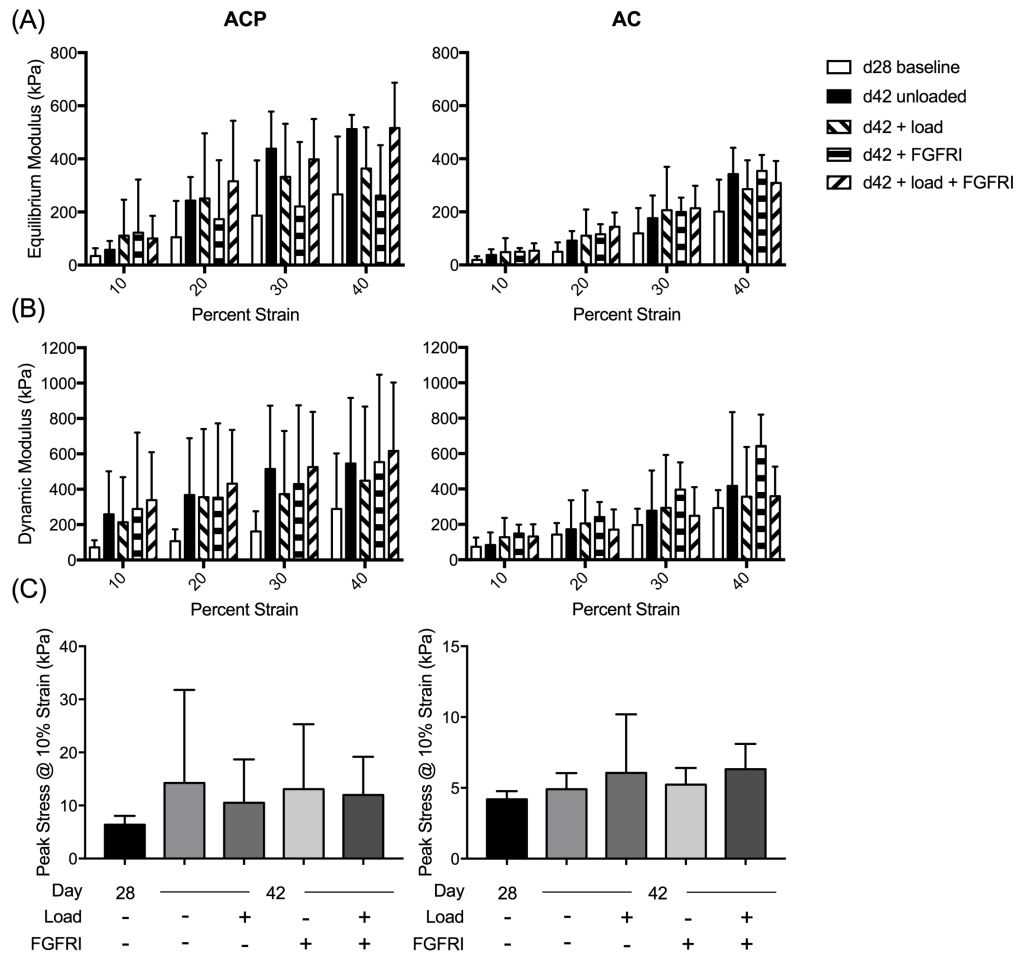


FIGURE 5.6 – BIOMECHANICAL ANALYSIS OF STIMULATED NEOCARTILAGE.

Bulk mechanical properties including (A) equilibrium compressive modulus and (B) dynamic compressive modulus at 1 Hz and 1% strain are increased with additional time in culture, but unchanged with load or FGF receptor inhibition. (C) Peak stress generated by the tissue at 10% strain is unchanged with time, load, or FGF receptor inhibition.

Gene expression was stable with respect to time, loading, and FGF2 signaling (Figure 5.7). When assessed relative to the baseline tissues harvested after a 28-day pre-experimental culture period, all ACP replicates upregulated genes of the chondrogenic phenotype including *COL2A1*, *ACAN* and *MTN3* with time, load, and inhibition of FGF2 signaling. ACs replicates similarly upregulated *MTN3* under all conditions, *COL2A1* with load, and *ACAN* with a combination of load and FGF2 inhibition. Time and loading caused an increase in *PRG4* expression for ACPs, though the expression relative to housekeeping genes was low. Across ACP replicates, FGF receptor inhibition decreased expression of *COL1A1* and *COL10A1*—genes representative of the fibro- and hypertrophic chondrocyte phenotypes, respectively—but increased *COL1A1* expression with load. ACs downregulated *COL1A1* with both time and FGF receptor inhibition but upregulated *COL1A1* with load; *COL10A1* was undetectable in all AC-derived tissues. Similarly, both *MMP1* and *MMP13*, genes coding for matrix metalloproteinases downstream of FGF receptor signaling, were undetectable across replicates of ACPs and ACs. For both cell types, *TIMP1* was downregulated with inhibition of FGF receptors. There were no trends in gene expression across replicates or experimental groups for other genes including *COL6A1*, *COL11A2*, *VCAN*, *SOX9*, *LOX*, or *INHBA*. Similarly, genes coding for mechano-sensitive ion channels, *PIEZO1* and *TRPV4*, were unchanged with loading across replicates of either cell type. When experimental groups were clustered based on relative changes in gene expression from baseline, each cell type clustered based on the presence or absence of the FGF receptor inhibitor (Figure 5.8).

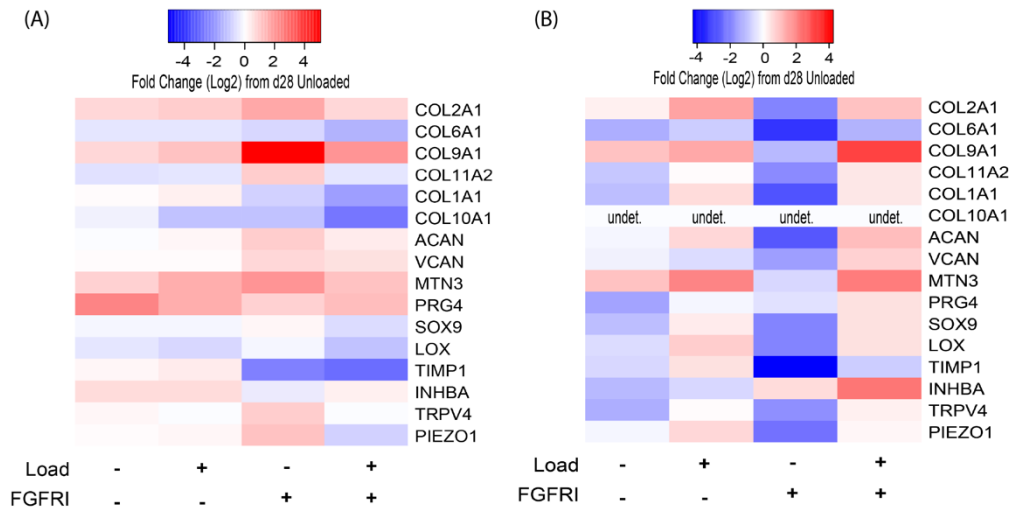


FIGURE 5.7 – CHONDROGENIC GENE EXPRESSION OF STIMULATED NEOCARTILAGE. (A) ACPs and (B) ACs show similar fold-change in gene expression relative to 28 days in culture in response to load and FGF receptor inhibition.

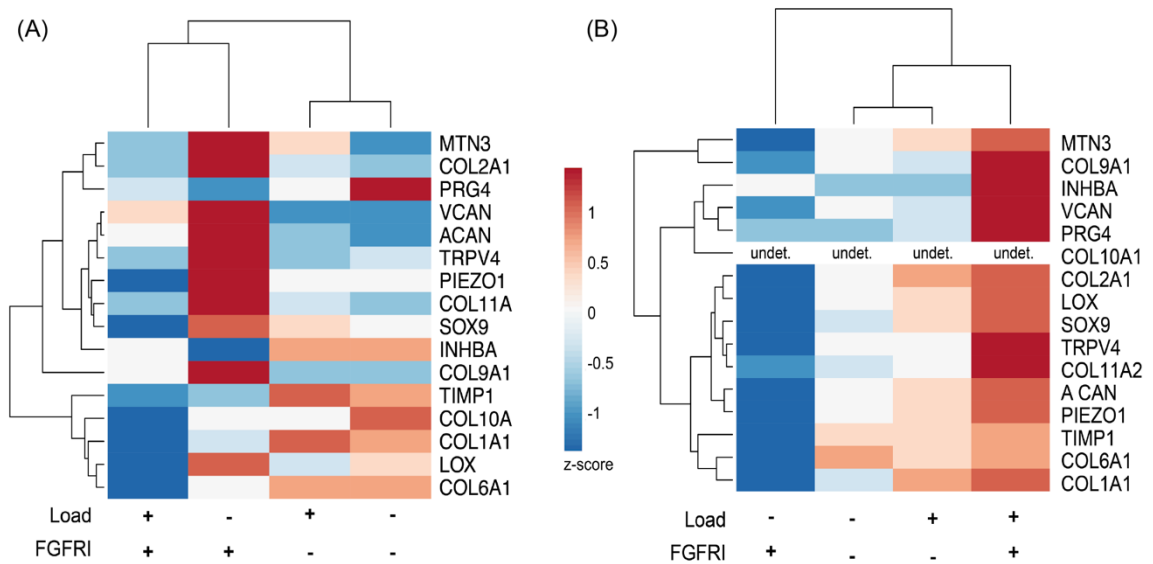


FIGURE 5.8 – CHONDROGENIC GENE EXPRESSION CLUSTERING. Clustering of experimental groups for (A) ACPs and (B) ACs based on relative fold-change gene expression from baseline indicated that groups were most closely related based on the presence or absence of the FGF receptor inhibitor.

FGF receptor inhibition blocked signaling at the protein level. To verify that the small molecule FGF receptor inhibitor was active, western blots were performed to probe for phosphorylation of ERK proteins relative to the total unphosphorylated protein level across all experimental groups for both cell types (Figure 5.9). Addition of the FGF receptor inhibitor blocked ERK phosphorylation regardless of loading conditions. Unlike native tissue (44), both ACP- and AC-derived neocartilage had high phospho-ERK levels at baseline in unloaded conditions, and load did not further increase ERK phosphorylation. Total FGF2 protein levels were consistent across all experimental groups for both cell types.

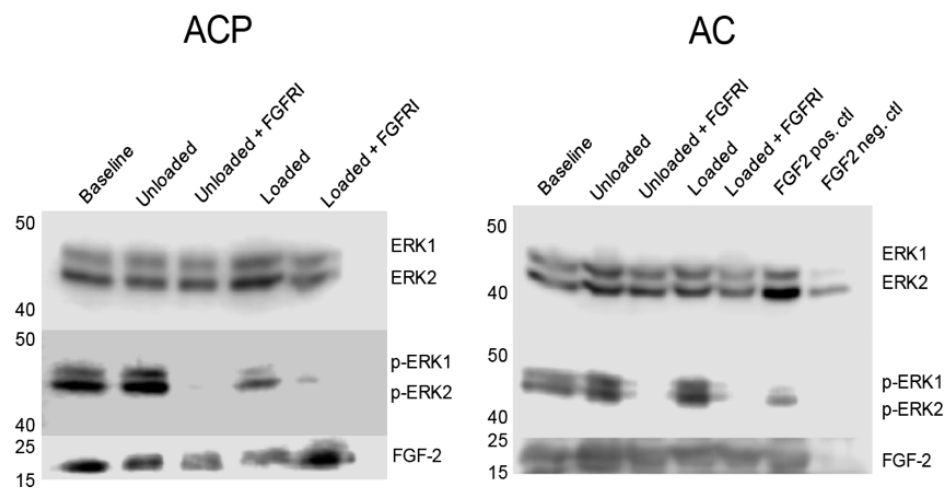


FIGURE 5.9 – PROTEIN ANALYSIS FOR FGF SIGNALING.

Representative western blots performed on total tissue lysates showed that inhibition of FGF receptors abrogated ERK1/2 phosphorylation when loaded for consistent total ERK1/2 levels across all groups for each cell type. Total FGF2 content was not different between groups for either cell type.

Collagens of the extracellular matrix matured toward the stable articular cartilage tissue phenotype with time but were unresponsive to load or FGF2 signaling. Both ACP- and AC-derived neocartilage increased type II collagen protein expression from day 28 to day 42 in free-swelling culture. Type II collagen was unresponsive to additional changes, neither increased nor decreased, with loading or FGF receptor inhibition. AC-derived neocartilage decreased types I and X collagen with an additional 14 days of free-swelling culture, but were again unresponsive to additional changes with other experimental conditions. ACP-derived neocartilage had minimal to no type X collagen expression that varied among biologic replicates and was unchanged across all conditions. ACPs-derived tissues similarly did not change type I collagen expression with load or FGF receptor inhibition, but these tissue showed a wide range of expression between replicates from minimal extracellular protein to type I collagen throughout the bulk of the tissue (Figure 5.10).

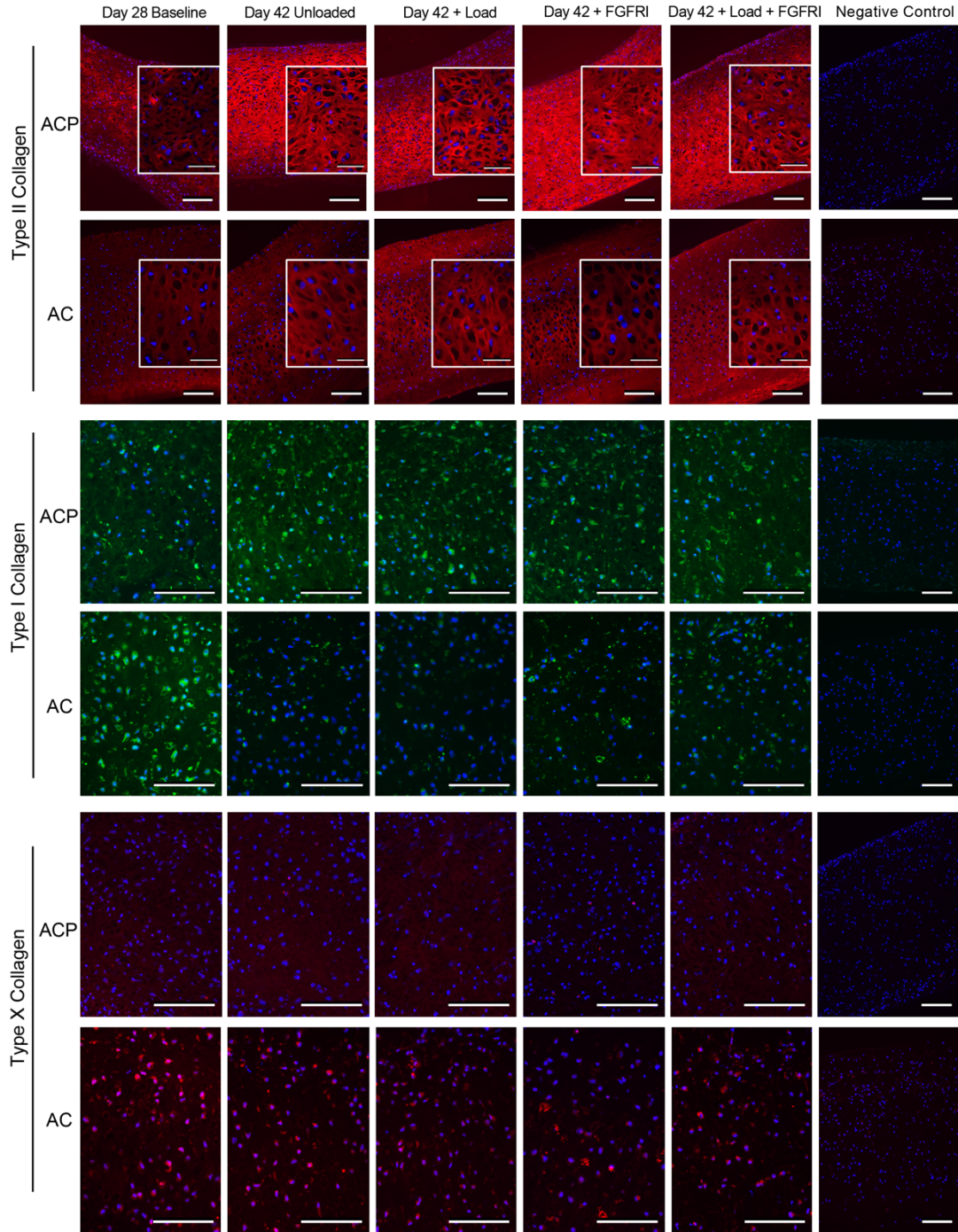


FIGURE 5.10 – COLLAGEN ANALYSIS OF STIMULATED NEOCARTILAGE.

Representative immunohistochemistry revealed that an additional 14 days in culture increased type II collagen and decreased type I collagen; though, there was not an appreciable difference for either collagen with application of load or an FGF receptor inhibitor. Type X collagen was undetectable in ACP-derived neocartilage and was decreased with time in AC-derived neocartilage. Nuclei were counterstained blue with DAPI. Scale = 100 μ m for all panels except type II collagen inserts where scale = 10 μ m.

Markers of tissue anisotropy demonstrated subtle changes with time, load, and FGF2 signaling. Neither loading nor FGF receptor inhibition changed the distribution of perlecan or FGF2 in the extracellular matrix; these molecules were expressed throughout the bulk of the tissue. Type VI collagen, however, stained with higher intensity in the pericellular region of tissues derived from both ACPs and ACs and was decreased in the presence of the FGF receptor inhibitor. Lubricin was absent from ACP-derived tissues, but was increased with load in AC-derived neocartilage in comparison with very low expression at baseline (Figure 5.11).

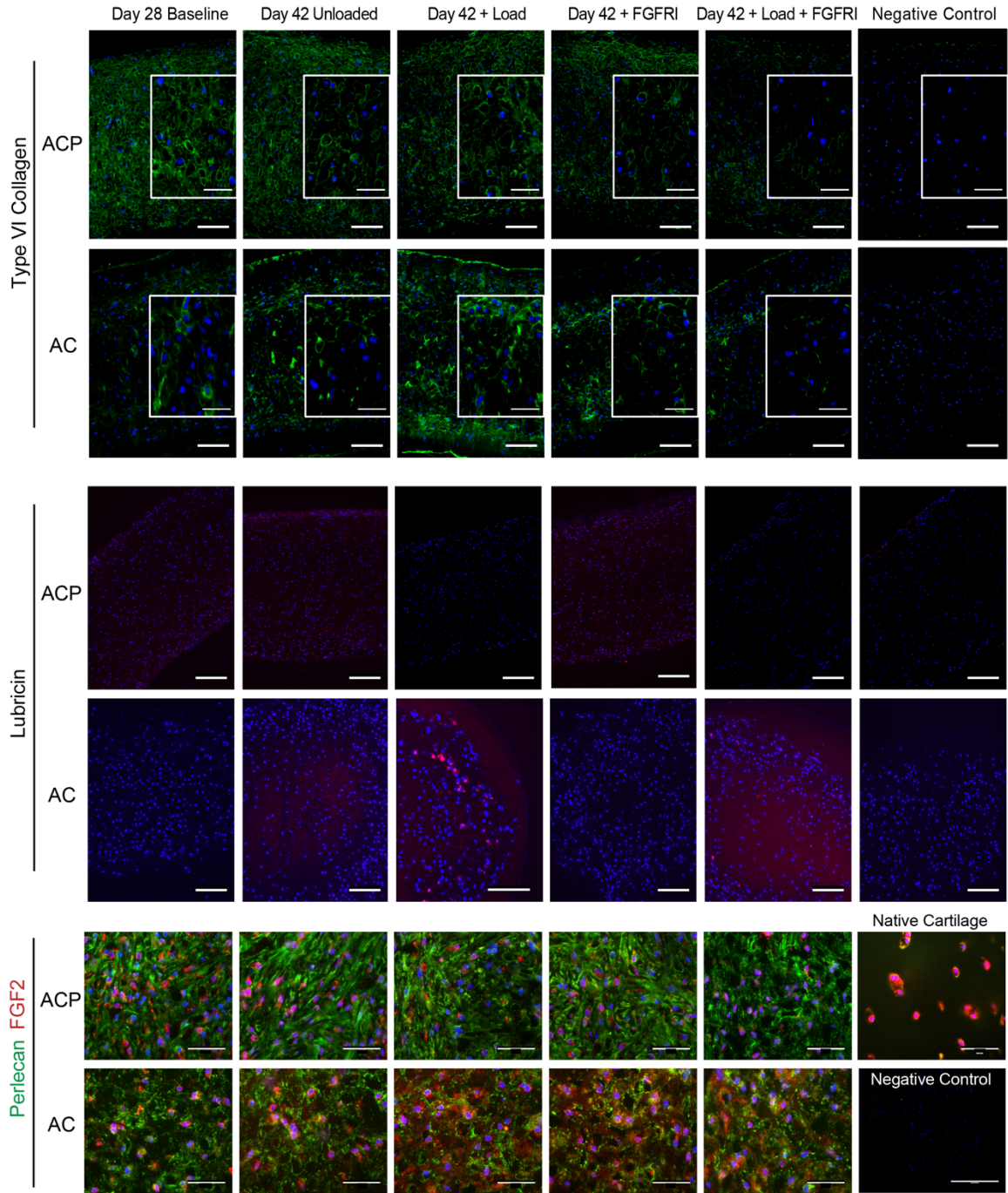


FIGURE 5.11 – EXTRACELLULAR MATRIX MOLECULES OF STIMULATED NEOCARTILAGE. Representative immunohistochemistry revealed that type VI collagen was decreased with FGF receptor inhibition for both cell types, lubricin was absent in ACP-derived neocartilage and increased with load for AC-derived neocartilage, and perlecan and FGF2 distribution were abundant throughout the extracellular matrix for neocartilage derived from both cell types regardless of time, load, or FGF receptor inhibition. Nuclei were counterstained blue with DAPI. Scale = 100 μ m for lubricin and type VI collagen, and scale = 10 μ m for type VI collagen inserts and perlecan/FGF2.

5.5 DISCUSSION:

Little is known about the processes that govern both articular cartilage development *in utero* and postnatal tissue maturation toward anisotropy. As scaffold-free tissues derived from adult human cell sources, including expanded chondrocytes and clonally-derived and expanded articular cartilage progenitor cells, are structurally immature following 28 days of development *in vitro*, we sought to characterize tissue maturation in a dynamic mechanical environment such as that experienced by chondrocytes in the postnatal period. In collaboration with Dr. Mauck at University of Pennsylvania, we designed and built a custom unconfined dynamic compression bioreactor, which was based on a bioreactor he and his laboratory previously validated for use on cell-laden hydrogels (182,183). Unlike hydrogels of defined thickness, scaffold-free tissue thickness was governed by cellular matrix production and varied between biologic donors. Thus, we modified the bioreactor to include load monitoring capabilities to measure tissue thickness for accurate loading based on percent strain and to monitor load over the entire loading duration to ensure constant contact between the tissue and the loading platen. We validated the load monitoring function of the modified bioreactor by loading agarose discs of known dimensions and mechanical properties and generating a standard curve for tissue stiffness versus stresses generated by the bioreactor. In addition to defining the role of dynamic mechanical stimulation in driving tissue reorganization, we further sought to define the role of endogenous growth factors in mediating catabolic and anti-catabolic tissue reorganization through the use of an FGF receptor inhibitor to block the FGF2 signaling following mobilization in the mechanical environment.

To date, dynamic mechanical stimulation has been employed in two other scaffold-free tissue models: one for articular cartilage and one for fibrocartilaginous meniscus (240,241). For scaffold-free engineering of articular cartilage, neonatal porcine primary chondrocytes were driven toward self-organization and cultured in a combined perfusion and dynamic compression system following a 10-day consolidation period (240). Perfusion of the tissue greatly enhanced the biochemical and biomechanical properties in comparison with static culture; however, dynamic loading did not have any additive benefit to perfusion. For scaffold-free fibrocartilage tissues generated from neonatal bovine primary chondrocytes (articular cartilage-derived) and fibrochondrocytes (meniscus-derived) in a self-assembly model and pre-cultured for either 10 or 17 days, a combined tensile and compressive dynamic loading regime did not promote biochemical anabolism or enhance bulk biomechanical properties (241). The addition of a chemical cocktail of anabolic TGF- β 1 and catabolic chondroitinase ABC, however, ultimately enhanced biochemical and biomechanical tissue properties upon mechanical stimulation. A follow-up study utilizing the same chemical cocktail sought to define the development of tissue anisotropy in scaffold-free fibrocartilage generated for the temporomandibular disc (242); although, this study employed passive axial compression, not a dynamic mechanical regime. Passive strain confined tissue morphology and was sufficient to drive changes in the properties of the collagen network, but the addition of chemical stimuli was necessary to cause significant changes to bulk tissue properties, including collagen alignment, under this loading regime. In contrast to these studies that all used primary cells harvested from neonatal tissues, we utilized expanded cell populations derived from adult human donors, which are known to be comparatively metabolically limited (103). Despite major

differences in scaffold-free system, we too did not find significant changes to the bulk biochemical composition or biomechanical properties of scaffold-free neocartilage tissues following application of a dynamic loading regime, especially with intra-donor variability. Additional time in culture from 28 to 42 days, however, increased tissue stiffness with maintenance of strain stiffening properties, and time further promoted an increase in type II collagen and a decrease of type I collagen of the extracellular matrix.

Native articular cartilage resides in a complex biomechanical environment with contributions not only from dynamic compression and passive strain, but also from shear, hydrostatic pressure, and fluid flow. Multiple groups have shown benefit of hydrostatic loading on the bulk biochemical and biomechanical properties of scaffold-free tissues in comparison with free-swelling controls; although, time had a significant influence on these responses (154,243). Increases in GAG and hydroxyproline content, along with aggregate modulus, under hydrostatic loading were most prominent over short-term culture duration, but these differences were diminished with longer-term culture; Young's modulus gradually improved over long-term culture (243). At the gene level, hydrostatic loading significantly increased *COL2* and *ACAN* gene expression relative to unloaded controls only after 3 weeks of culture, but these changes were not matched with significant differences in the bulk composition of the extracellular matrix; gene expression for molecules within the pericellular matrix, including perlecan and CD44, were unchanged with hydrostatic loading at all time points (154). The variation in response to hydrostatic loading, specifically with time, indicate that loading duration is potentially the most influential parameter for a given loading regime.

The influence of mechanical loading on neocartilage generated within scaffold-free systems is limited to experiments described here; however, loading of chondrocytes seeded within scaffold- and matrix-based biomaterials has been extensively studied. We have identified over 80 independent studies that loaded chondrocytes in dynamic compression. Results from these experiments, when considered together, do not provide conclusive evidence for the influence of mechanical loading on neocartilage tissue growth and maturation. This may be related to the wide variation in both tissue engineering and bioreactor systems as well as loading regimes. In studies that used a similar loading regime to ours, longer-term mechanical stimulation significantly enhanced biochemical and biomechanical properties of chondrocyte-laden agarose hydrogels relative to free-swelling controls (244,245). These studies did not require a pre-loading culture period because agarose hydrogels exhibit stiffness necessary to support load, and the total culture duration was equivalent to the loading duration. Scaffold-free systems require a pre-loading culture duration sufficient to allow for extracellular matrix elaboration and tissue formation. We defined a loading duration of 14 days, which was much shorter than the total loading duration of 28 or 42 days used previously within the similar regime. Similarly, the only other study to dynamically load ACPs, which were seeded in a fibrin-polyurethane composite scaffold, noted a significant increase in GAG content and *ACAN* expression following 28 days of loading (246). In the context of these long-duration studies, we speculate that tissue remodeling in response to dynamic compression is a time-intensive process and longer loading regimes are necessary to allow for tissue maturation.

While bulk changes to the extracellular matrix in response to dynamic mechanical loading were of interest in the present system, we further sought to characterize a potential

mechanism of neocartilage maturation and reorganization in response to dynamic load. We hypothesized that the mechanical environment would mobilize FGF2 from the extracellular matrix, and FGF2 would signal to neighboring cells to mediate tissue reorganization. To validate that the FGF receptor inhibitor was active within the system and that loading promoted FGF2 signaling, we probed tissue lysates for ERK phosphorylation. Unlike unloaded native tissue explants or chondrocytes seeded within a stiff hydrogel (44,45), scaffold-free neocartilage exhibited high ERK phosphorylation in free-swelling culture, and retained this activity with loading; FGF receptor inhibition efficiently blocked ERK phosphorylation. The tissues had abundant FGF2, which was co-localized with perlecan throughout the extracellular matrix, and the relative amount of FGF2 did not change between experimental groups, regardless of loading or receptor inhibition. When probed for downstream gene targets of MAPK signaling, cells cultured with FGF receptor inhibitor decreased *TIMP1*, did not change *INHBA* expression, and *MMP1* and *MMP13*—matrix metalloproteinase targets—were undetectable. Based on the necessary addition of a metabolic cocktail to cause significant changes in previous studies (241,247), we anticipated FGF2 signaling to promote catabolic and anti-catabolic control of tissue reorganization in the mechanical environment, but our results do not support that this occurred within the stimulatory time-frame based on quantification of extracellular matrix constituents and gene expression analyses. We did not anticipate that these tissues would not express genes coding for catabolic enzymes; as a result, a primary metric of potential FGF2-mediated catabolic control was lost in this system. Further, we did not anticipate that scaffold-free tissues would exhibit high MAPK pathway activity in the unloaded environment, and the ability to differentiate the specific role of FGF2 signaling from

loading in comparison with free-swelling controls was diminished. A final limitation of FGF receptor inhibition for endogenous FGF signaling is the inability to isolate the effect of just FGF2, as other FGF molecules, most notably FGF18, may also be bound to heparan sulfate, direct chondrocyte differentiation and cartilage tissue development, and signal in response to mechanical loading in this system (248-250). Evaluation of tissues at the gross level indicated that neither loading nor FGF receptor inhibition detectably affected extracellular matrix molecule distribution or tissue isotropy over the 14-day stimulation period.

5.6 CONCLUSIONS:

The overall objective of this study was to define the role of dynamic mechanical stimulation in the maturation of scaffold-free neocartilage derived from adult human donors and to establish the role of endogenous FGF2 signaling in tissue reorganization. Overall, additional time in free-swelling culture was of benefit to scaffold-free tissues, but neither dynamic compressive load nor FGF receptor inhibition significantly influenced tissue maturation within the bulk of the extracellular matrix. Since time was the most influential variable for scaffold-free tissue growth in free-swelling culture and for chondrocyte-laden biomaterials in long-term loading studies, we reason that these tissues may exhibit significant structural reorganization with increased loading time. Ultimately, we hope to identify conditions to direct structural maturation of scaffold-free neocartilage toward anisotropy of native tissue in order to grow autologous tissues that can properly function in the complex biomechanical environment of the joint when used for repair of focal articular cartilage defects.

CHAPTER 6: CONCLUSIONS & FUTURE DIRECTIONS

The overall objective of the research detailed in this dissertation was to develop a novel scaffold-free approach to generate mature neocartilage from a single human cell toward the eventual goal of autologous focal articular cartilage repair. The recent success of osteochondral allograft (OCA) transplantation for restoration of focal articular cartilage defects has informed us that an autologous approach to tissue regeneration will require an implant of comparable biomechanical function and structural organization to native tissue (251). However, OCA is limited by tissue availability and poor cartilage integration with adjacent native tissue. The chapters presented in this dissertation represent work carried out in development of the three aspects of tissue engineering including: characterization and selection of highly chondrogenic cells; generation of large-scale scaffold-free neocartilage tissues composed of an endogenously produced extracellular matrix scaffold; and determination of the role of stimulating factors, specifically physioxia and dynamic mechanical compression, in driving structural and functional tissue maturation *in vitro*. Just as this project advanced our ability to generate large-scale neocartilage tissues from adult human-derived cell sources, so too did the research generate many more questions regarding cells, scaffold, and signals. These three elements of the tissue engineering triad are highly interconnected, and eventual *in vivo* application of a scaffold-free tissue for the repair of focal articular cartilage defects will depend on successful development of the entire system. Clinical application will further depend on meeting specifications including scalability, manufacturability, cost, regulatory approval, and clinical efficacy; none of which were explored in this research.

6.1 CELL CHONDROGENICITY

Among the variety of candidate cells with which to generate neocartilage in a tissue engineering system, we focused on a novel cell candidate, articular cartilage progenitor cells (ACPs), comparing them with expanded articular chondrocytes (ACs) and mesenchymal stem cells (MSCs). We derived all three cell types from healthy adult human donors. Employing standard chondrogenic assays, we sought to define the intrinsic chondrogenic differentiation capacity of each of the two progenitor cells types, ACPs and MSCs, with reference to the redifferentiation capacity of articular chondrocytes, which we had previously characterized (178). Compared with the relatively consistent chondrogenic redifferentiation of ACs between human donors, we found that there was a wide range of chondrogenicity for progenitor cells between both individual human donors and clonal populations derived from a single donor (Figure 3.1). We further found that this variation predicted the response of cells to variations in oxygen level and likely explains wide discrepancies in the literature regarding the modulation of the hypertrophic phenotype of MSCs with culture in physioxia (reviewed in Chapter 3). Importantly, this was the first study to investigate the response of ACPs to culture in physioxia and to report the wide variation in chondrogenicity across ACP replicates and clones. Advantages of ACPs over MSCs include the ability to generate clonal populations from a single cell without loss of phenotypic plasticity, favored chondrogenic differentiation among potential connective tissue lineages, and lack of chondrocyte hypertrophy (19,138). ACPs are advantageous in comparison with ACs because of the potential to generate large autologous cell populations through *in vitro* expansion of clonal cells isolated from a limited tissue harvest site, such as a biopsy. Our results, however, indicate that not all ACP clones are suitable candidates

for tissue engineering application: we identified some clones that expanded poorly *in vitro* following clonal isolation and some clones that produced hypertrophic neocartilage containing type X collagen. Since we are the first to report ACP hypertrophy, we are following up these results to investigate the phenotype of a larger number of clones from additional biologic replicates in future studies. We further discovered, and report for the first time, that all ACP clones lacked lubricin expression at the gene and protein level once expanded *in vitro*. As ACPs were most recently identified *in situ* by lineage tracing studies using the *PRG4* gene locus, the lack of *PRG4* and lubricin expression *in vitro* generates new questions for investigation in future research.

6.1.1 ARTICULAR CARTILAGE PROGENITOR CELLS

ACPs used in the present work were isolated from fresh cadaveric donor tissue, which is a relatively sparse resource. ACs were derived from more readily available allograft tissue that had been preserved for at least 14 days following harvest from the donor. We have most recently successfully isolated clonal cell populations from preserved allograft donor tissue, and we are presently working to characterize the morphology, expansion, and chondrogenic differentiation of these cells relative to ACPs derived from fresh cadaveric tissues. This new cell source will allow our laboratory to conduct future experiments with ACPs and to continue to define intra- and inter-donor variation in ACPs derived from healthy human articular cartilage, especially with regard to type X collagen expression.

In both pellet and disc culture systems, we found that all ACP clones lacked *PRG4* gene expression and lubricin protein expression. These results have recently been

corroborated by another group (Qian Laboratory, Brown University, unpublished results), who attributed the result to potential variability between cells derived from osteoarthritic tissue from a single adult human donor. No other groups, to our knowledge, have reported *PRG4* or lubricin expression during *in vitro* analysis of ACPs. For ACs, we found that the relative level of lubricin expression in immunohistochemical analysis corresponded to *PRG4* gene expression levels, and we are confident that all ACP clones we used throughout this dissertation research lacked expression. Lack of *PRG4*/lubricin in ACPs is a curious result, for the most recent study to identify ACPs *in situ* used a reporter at the *PRG4* gene locus to trace appositional growth of articular cartilage during *in utero* and post-natal mouse limb development and maturation (20). Based on these disparate results, we have generated two hypotheses about ACP *PRG4*/lubricin expression: [1] *in vitro* expansion conditions drive phenotypic modulation and loss of *PRG4*/lubricin in ACPs prior to chondrogenesis, or [2] the cells identified as tissue progenitors using a *PRG4* reporter are different (either up- or down-stream in a progenitor cell lineage or entirely distinct) from those isolated *in vitro* through the fibronectin adhesion method that we used.

In the initial characterization of ACPs derived from healthy adult human cartilage, our collaborators found that these cells required exogenous FGF2 and TGF- β , fetal bovine serum, and conditioned medium all be added to the medium to maintain proliferation and chondrogenic differentiation potential during expansion (19). It is well known that FGF2 and TGF- β induce downstream stabilization of β -catenin through interactions and stimulation of canonical Wnt signaling pathways (252-255). Within the context of chondrogenesis, activation of β -catenin is required during both joint specification and chondrogenic differentiation for the production of lubricin (256,257). However, excessive

β -catenin activity in osteoarthritic articular cartilage causes loss of lubricin *in vivo* (258,259), and high levels of exogenously added Wnt3a causes a dose-dependent loss of lubricin *in vitro* (260). Wnt16 is a weak activator of canonical β -catenin activity, but it functions to regulate excessive β -catenin levels in osteoarthritis and can independently rescue lubricin expression in human articular chondrocytes *in vitro* (259). Taken together, these studies indicate that homeostatic regulation of canonical Wnt signaling, and downstream β -catenin activity, likely controls *PRG4*/lubricin expression during *in vitro* chondrogenesis, and we hypothesize that excessive β -catenin activation from the addition of exogenous FGF2 and TGF- β during expansion is responsible for the modulation of ACP phenotype toward loss of *PRG4*/lubricin expression (Figure 6.1). To test this hypothesis, we intend to expand both ACs and ACPs—derived from the same human—in the presence or absence of exogenous growth factors and evaluate *COL2A1*, *ACAN*, *PRG4* and *Wnt3a* gene expression before and after pellet chondrogenesis. Preliminary results reveal that expansion in the presence of exogenous growth factors decreases chondrocyte *PRG4* expression relative to expansion without growth factors. Following pellet chondrogenesis, ACs significantly increased *COL2A1* and *ACAN* expression but decreased *PRG4* expression when expanded with FGF2 and TGF- β (Figure 6.2). Based on these preliminary results, we are conducting a larger study with multiple biologic replicates to compare expansion of both ACs and ACPs in the presence or absence of FGF2 and TGF- β .

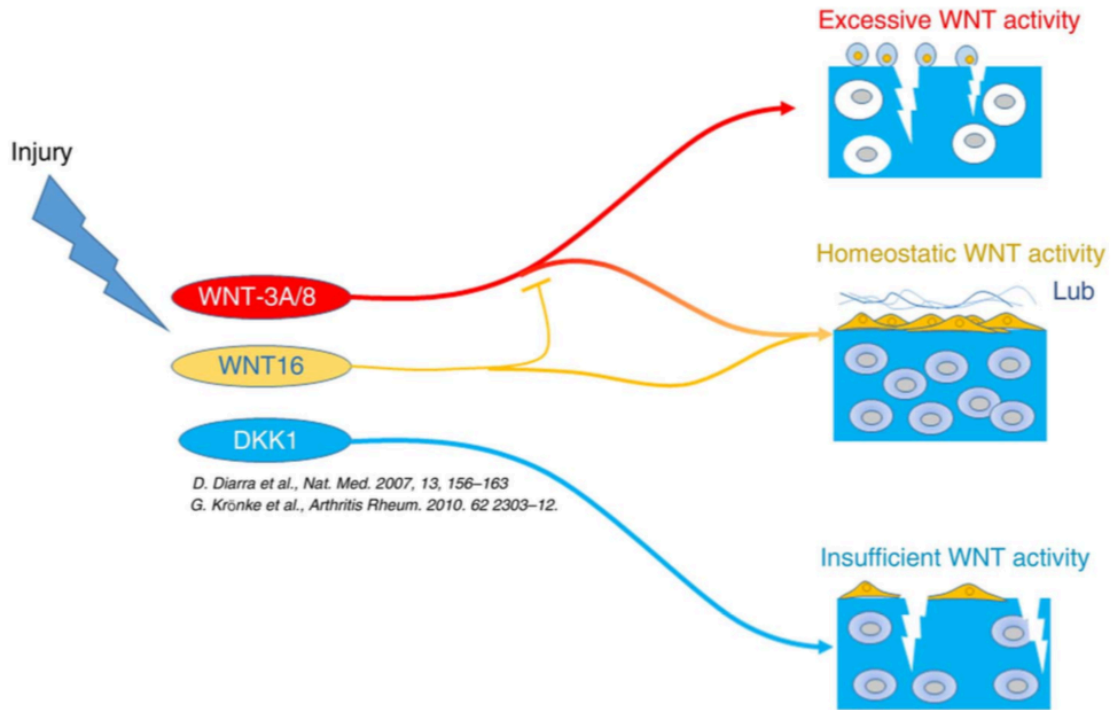


FIGURE 6.1 – WNT HOMEOSTASIS.

Cartilage injury causes activation of WNT signaling through downregulation of antagonists and upregulation of several agonists such as WNT16 and WNT8. WNT16 buffers the canonical WNT activation to homeostatic levels through its capacity to directly support a weak activation and preventing excessive activation induced by other ligands. Excessive canonical WNT activation causes cartilage breakdown by driving inappropriate maturation particularly within the superficial zone progenitor cells, whereas homeostatic levels of activation are necessary for supporting the superficial progenitor population and lubricin expression. Reproduced with permission from Nalesso et al. © 2016, BMJ Publishing Group (259).

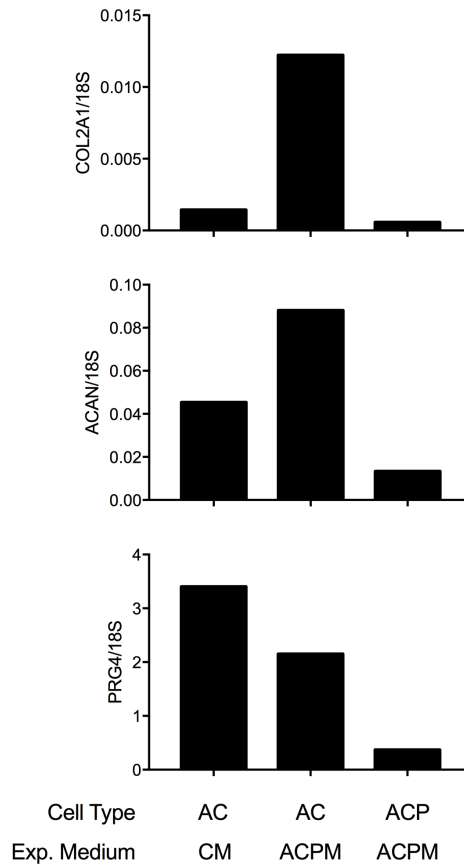


FIGURE 6.2 – EFFECT OF ADDING GROWTH FACTORS DURING EXPANSION.

ACP expansion medium (ACPM) includes the addition of exogenous FGF2 and TGF- β to the traditional chondrocyte expansion medium (CM). Preliminary data ($n = 1$) from culture of ACs in ACPM increased subsequent gene expression of *COL2A1* and *ACAN* during pellet chondrogenesis but decreased *PRG4*. This result potentially indicates that adding growth factors during expansion may cause phenotypic modulation during chondrogenesis and may explain lack of *PRG4* expression by ACPs.

Based on the alternative hypothesis, lack of ACP *PRG4*/lubricin expression *in vitro* despite *in situ* lineage tracing through the *PRG4* gene locus calls into question the identity and congruence of the *in situ* cell population identified in lineage tracing with the ACPs that are isolated *in vitro* by differential adhesion to fibronectin. Specifically, Kozhemyakina et al. (2015) showed that cells expressing the *PRG4* gene locus are fetal progenitors that give rise to articular chondrocytes, but this study does not test whether

PRG4-expressing cells of the superficial zone are the same as stable progenitors that reside in adult cartilage (21). Thus, the *PRG4* gene locus may have been turned on during the sequence of chondrocyte differentiation, which would fail to identify the true progenitors upstream of *PRG4*-producing cells. Alternatively, *PRG4* expression may be a marker of the stem cells in the superficial zone, and the gene is subsequently downregulated later in the chondrocyte lineage. Co-localization of progenitor cells and lubricin-producing cells, however, does not clearly indicate a common cell nor does it specify whether superficial zone chondrocytes arise in the same appositional pattern, or in a separate pattern, from cells that do not produce lubricin in deeper zones. To validate that chondroprogenitors selected through fibronectin adhesion *in vitro* are the same as those identified through *PRG4* lineage tracing *in vivo*, the total chondrocyte population could be harvested from the *PRG4*-reporter mouse femoral condyle, subjected to fibronectin adhesion, and recombined *in vitro*. However, if loss of *PRG4* expression results from *in vitro* expansion in the presence of high dose growth factors (according to the first hypothesis), a negative result may mask evaluation needed for comparison of proposed *in vivo* and *in vitro* cell populations. Further, this experiment must be preceded by a feasibility study to establish whether progenitor cells can even be isolated from mouse cartilage, which is of limited volume in comparison with larger mammals for which the method has been validated. Ultimately, the mechanism for ACP loss of *PRG4* expression *in vitro* needs to be reconciled within the context of *PRG4*-based lineage tracing to elucidate the true identity of these cells *in vivo* and to generate ACP-derived tissues that produce lubricin.

6.2 SCAFFOLD-FREE TISSUE ENGINEERING

To overcome historical challenges in biomaterial-based tissue engineering for articular cartilage repair, we sought to develop a scaffold-free tissue engineering system with which to generate large-scale neocartilage tissues from adult human-derived cells. We were particularly interested in applying clonally-derived ACPs in a scaffold-free system for the first time; the ability to build large-scale tissues from a single cell origin would overcome significant challenges associated with cell availability. To date, scaffold-free tissue engineering systems have been well characterized using neonatal primary chondrocytes (31,148,149,161,240), but fewer studies have reported similar methods for adult human-derived cells (156,157,160), which differ in metabolic capacity (103). Unlike ACs and MSCs, we discovered that ACPs required a substrate on which to bind in order to define tissue geometry; thus, we facilitated cellular self-organization on a fibronectin-coated membrane. Control over tissue geometry was a primary specification in development of our methodology in order to generate a tissue that can not only be subjected to compressive loading *in vitro* but also fill a focal cartilage defect *in vivo*. Over 28 days of culture, we found that all three cell types—ACs, ACPs, and MSCs—formed large-scale tissues composed of a dense cartilaginous extracellular matrix (Chapter 4, Appendix D). Preliminary work to grow AC- and ACP-derived tissues over a longer time scale *in vitro* demonstrated that tissues continue to grow in thickness, and future studies to characterize tissue growth will better inform us of limitations to construct size intended for clinical application. Ultimately, the scaffold-free technique presented in this dissertation has enabled our laboratory to reliably produce large three-dimensional tissues from a variety of adult human-derived cells; moreover, we envision using this platform to build more

complex osteochondral tissues to facilitate translation to clinical practice. There may be a tradeoff, however, between neocartilage complexity and maturity with integration into neighboring native tissue following implantation, and this relationship must be investigated prior to clinical application. Toward the eventual goal of clinical translation, we intend to conduct studies to determine if these tissues maintain a cartilaginous phenotype *in vivo* following subcutaneous implantation and to determine the performance of scaffold-free neocartilage in articular cartilage repair following *in situ* implantation.

6.2.1 CULTURE DURATION

As a preliminary study, we cultured ACP-derive neocartilage discs over an extended duration (150 days) to evaluate tissue maturation with time. The tissues continued to grow in thickness while maintaining a constant diameter. Upon harvest, the tissues did not show evidence of central necrosis, which is a common limitation in generating thick tissues through high cell seeding density because of impaired nutrient diffusion (159,261-263). Consistent with the literature, we found that increasing cell seeding density from 2×10^6 to 4×10^6 ACPs generated tissues with central necrosis, yet culture of neocartilage containing 2×10^6 ACPs for extended duration facilitated an increase in tissue thickness without central necrosis (Figure 6.3). These results indicate that time, not cell number, is likely an important variable in generating tissues of a clinically relevant thickness [1.7-2.5cm for knee (264)] for repair of focal lesions in adult human cartilage. Longer range studies will inform our understanding of size limitations in the scaffold-free system.

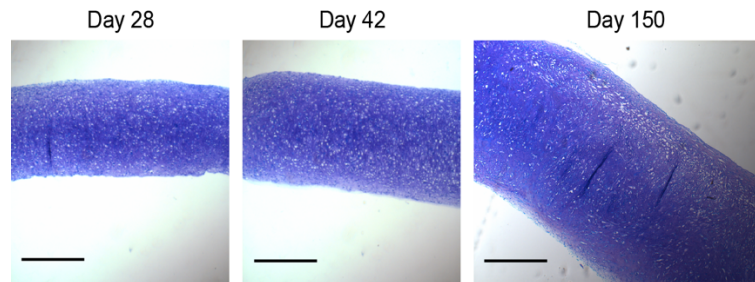


FIGURE 6.3 – EFFECT OF EXTENDED CULTURE DURATION.

Preliminary experiments showed that with increased time in culture from day 28 to day 48 to day 150, ACP neocartilage continued to grow in thickness with maintenance of the proteoglycans throughout the depth of the tissue. Scale = 500 μ m.

6.2.1 OSTEOCHONDRAL INTEGRATION

While the primary overall objective of this research is to grow autologous tissues for the repair of focal cartilage defects, we recognize that success of a chondral implant will ultimately depend on its integration with and functional performance within the native joint, specifically, at the adjacent articular cartilage and the underlying subchondral bone. We have shown that cells within scaffold-free neocartilage build a robust extracellular matrix (Chapter 4), which will likely limit cell migration at the tissue margins and, thus, limit integration capacity with neighboring tissues following implantation. To facilitate integration with the subchondral bone, we could culture bilaminar neocartilage discs by seeding bone marrow-derived MSCs on the basal surface and articular cartilage-derived ACPs on the apical surface. We hypothesize that each cell type would produce a distinct, yet integrated, tissue throughout the total depth; wherein, MSCs generate a tissue of the hypertrophic cartilage phenotype and ACPs generate a tissue of the articular cartilage phenotype during chondrogenic differentiation. Upon implantation to the subchondral bone within a full thickness cartilage defect, we further hypothesize that the hypertrophic MSC-

derived tissue would ossify, integrate, and anchor into the subchondral bone based on recent data that indicate MSC-derived cartilage pellets facilitate *in vivo* fracture repair through sequential ossification and integration into the host tissue (265).

Just as integration into the subchondral bone is necessary to anchor a transplanted tissue into a full-thickness cartilage defect, so too is integration into the adjacent articular cartilage necessary to facilitate biomechanical function of the implant in the native joint environment. We have shown that increased time in culture drives an overall increase in scaffold-free tissue stiffness, thickness, and extracellular matrix content (Chapter 5), thus tissue maturity; however, the literature suggests that there may be a trade-off between *in vitro* tissue maturity and *in vivo* integration capacity (Figure 6.4) (266). Extensive review of the outcomes following osteochondral allograft transplantation, which necessarily includes implantation of mature adult tissues, showed that cartilage integration is universally minimal, if not absent; although, underlying osseous integration anchors the cartilage to provide a functional fill and to improve clinical outcomes (251). Without integration into adjacent cartilage, stresses become concentrated at the tissue boundaries and lead to not only implant failure but also to adjacent native tissue degeneration. As reviewed by Khan et al. (2008), factors known to contribute to integration at the cartilage interface include: cell viability in the neocartilage and native tissue; initial cell origin and cell phenotype following differentiation; maturity and extent of the collagenous and proteoglycan networks of the ECM; and properties of the scaffold employed in the tissue engineering system (267). Functional integration of neocartilage into adjacent native tissue is best evaluated following implantation into a defect *in situ*, which encompasses the complex biomechanical environment; however, structural integration can be evaluated *in*

vitro through implantation of neocartilage into a native tissue explant. To our knowledge, neocartilaginous scaffold-free tissues have not been implanted to fill a cartilage defect *in situ*, but a single study to characterize integration of a scaffold-free tissue into a cartilage explant found structural integration of proteoglycans and type II collagen across the tissue interface and functional integration that generated substantial peak stress (400kPa) at mechanical failure (162). To investigate integration of scaffold-free tissues generated from adult human cells, we could design a similar explant study. Specifically, we would harvest osteochondral tissue explants from allogeneic human donor tissue and create a full thickness cartilage defect using a biopsy punch of the same diameter as the scaffold-free tissues (7mm). We would suture the upper edge of the neocartilage to the rim of the explant defect in order to maintain tissue congruence in free-swelling culture. After four weeks of implantation, the tissues would be harvested to investigate cell viability with a live/dead assay, structural integration with histology and immunohistochemistry, and functional integration with a mechanical push-out test to measure peak stress at failure.

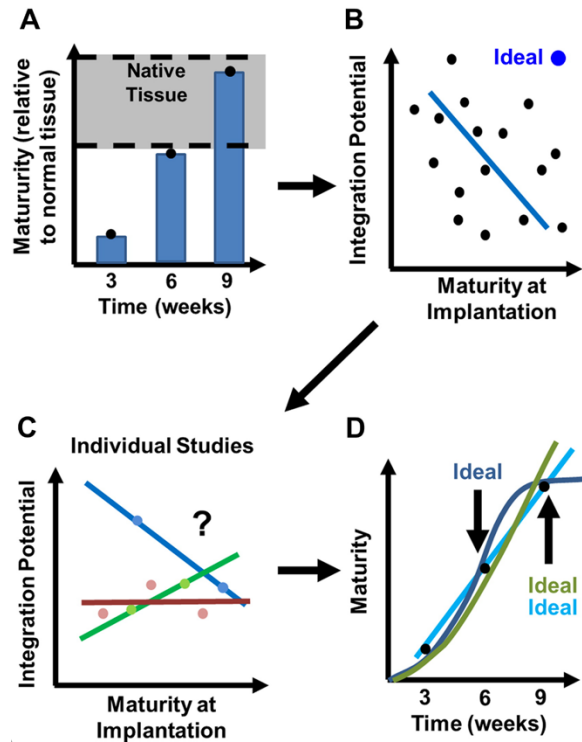


FIGURE 6.4 – TRADEOFF BETWEEN MATURITY AND INTEGRATION.

Schematic illustration of the question of construct state versus trajectory. (A) Current practice in cartilage tissue engineering allows for the formation of constructs with some properties matching native tissue. (B) While there is a general negative correlation between construct maturity and its ability to integrate with native tissue, (C) individual studies are less clear regarding this trend and are limited by few data points. (D) One important factor in correlating construct maturity and integration potential might be its “trajectory” or time-dependent properties, however, the shape of maturation for these constructs has yet to be elucidated, which could influence the ideal time for implantation. Reproduced with permission from Fisher et al. © 2013, Elsevier (266).

6.2.2 IN VIVO IMPLANTATION

Prior to clinical application, the performance of scaffold-free neocartilage tissues derived from adult cell sources needs to be evaluated *in vivo* to determine: [1] tissue phenotype following subcutaneous implantation of a xenograft, [2] tissue immunogenicity following *in situ* implantation of an allograft, and [3] functional performance and structural integration following *in situ* implantation of either an autograft or an allograft, dependent on results of immune characterization. Following experimental design of and prior to

starting animal experiments, we would seek approval from the Institutional Animal Care and Use Committee (IACUC) to conduct all animal studies. To investigate tissue phenotype *in vivo*, we could implant adult human-derived tissues subcutaneously onto the dorsal side of athymic nude mice for a minimum of 28 days according to methods outlined by Nemoto et al. (2015) (268). Following animal sacrifice, we would harvest tissues and perform standard assays described in Chapter 2 to assess tissue properties including measurement of cell viability, quantification of proteoglycan and collagen content, and further characterization of the extracellular matrix through histology and immunohistochemistry. Translation of potential cartilage therapies from animal models into clinical practice is primarily limited by the difficulty of finding an animal with comparable tissue thickness and joint morphology to humans. Yucatan miniature pigs, which have thick cartilage and large stifle joints, have recently been employed as a large animal model to investigate cartilage repair (269). In the next *in vivo* study, we could investigate structural and functional outcomes following transplantation of scaffold-free neocartilaginous allografts into full-thickness cartilage defects in comparison with untreated defects, microfracture-treated defects, and native tissue, all in the mini pig model. We would characterize the local immune environment for all conditions, with emphasis on determining the immunogenicity of allogeneic tissues. Should allogeneic tissues elicit acute rejection in the host animal, we would revise the study to generate autologous scaffold-free tissues through a two-stage procedure, similar to ACI, for implantation into a cartilage defect. These future studies represent the classic progression from the laboratory to clinical practice; however, a large number of *in vitro* studies to fully understand scaffold-free tissue maturation must precede *in vivo* application.

6.3 STIMULATING FACTORS FOR TISSUE MATURATION

After characterizing the cells and extracellular matrix in the novel scaffold-free tissue engineering system, we sought to establish the role of stimulating factors representative of those within the native joint environment, including physioxia and dynamic compression, in driving maturation of neocartilage *in vitro*. Physioxia promoted biochemical anabolism and biomechanical stiffening of AC-derived neocartilage in the scaffold-free system. ACPs of high chondrogenicity were less responsive than ACs to changes in oxygen level, but we anticipated this result based on the investigation of these cells in pellet culture. Ultimately, highly chondrogenic ACPs produced a tissue of superior biochemical content and biomechanical stiffness to ACs regardless of oxygen level; however, these tissues lacked lubricin expression: a result we intend to investigate in future experiments described earlier in this chapter. In addition to residing in a low oxygen environment, native articular cartilage develops, matures and functions in a dynamic biomechanical environment. We hypothesized that dynamic compressive stimulation would induce structural reorganization of scaffold-free neocartilage, specifically through endogenous FGF2 control of enzymes that remodel the native extracellular matrix. The loading regime was designed based on commonly used parameters for dynamic compression of tissue engineered neocartilage; however, this was the first study to employ the loading regime to scaffold-free tissues derived from human- and adult-derived cells. With our readouts, we did not see clear responses with loading nor with inhibition of FGF signaling; thus, we have designed future experiments to extend the loading duration and to develop and to employ novel microscopy techniques to investigate tissue maturation across various length scales.

6.3.1 MECHANICAL STIMULATION

This was the first study to evaluate the response of adult human cell-derived scaffold-free neocartilage to dynamic loading, and our results indicated that time, not necessarily dynamic load nor inhibition of FGF2 signaling influenced tissue maturation. Maturation of native tissue is a time intensive process that occurs over months, if not years, in the post-natal period (23) and requires reorganization of relatively stable biomolecules of the extracellular matrix through catabolic and anabolic matrix remodeling. Our collaborators, and others, have found that chondrocytes cultured in various tissue engineering systems enhance biochemical and biomechanical measures in dynamic compression relative to free swelling controls, but the magnitude of response is significantly increased with increased duration of dynamic stimulation, with significance arising within a range of 21-39 days (244,245,270-272). Other tunable variables in a dynamic compression loading regime include percent strain (if the motor is displacement-driven or load if the motor is load-driven), frequency, and intermittent loading duration. Alterations to peak-to-peak strain and frequency for a dynamic loading cycle are limited by the time needed for tissue rebound between loading cycles, and 10% strain and 1Hz frequency have been well defined as parameters to maintain tissue-platen contact throughout loading duration and elicit cellular responses (245,273). Since ours was among the first studies to investigate maturation of scaffold-free tissues in the mechanical environment, we designed our initial experiment to include a mid-range dynamic stimulation period from the literature (14 days) following a 28-day cell differentiation and tissue formation period, which was necessary for the neocartilage tissues to build a matrix that could bear load. Based on inconclusive results from this first experiment, we now

hypothesize that chondrocytes within the scaffold-free tissues are relatively stable, and biochemical and biomechanical measures will increase proportionally with long-term dynamic stimulation. We intend to employ the same experimental protocol as those defined in Chapter 5, but we will increase the total duration of loading to 20 and 30 days for comparison with free-swelling controls according to the experimental design in Table 6.1.

Week	1	2	3	4	5	6	7	8	9	10	11	12	
Baseline													
DL14	Expansion	Pre-culture				*harvest							
FS20						Free Swelling		*					
DL20						DL 20 days (4 wks, 5d/wk)		*					
FS30						Free Swelling		*					
DL30						DL 30 days (6 wks, 5d/wk)		*					
								*					

6.3.2 ADVANCED MICROSCOPY

Native articular cartilage is composed of a highly structured extracellular matrix that demonstrates both depth-dependent and cell-outward anisotropy. In the final aim of this research, we sought to drive structural maturation of scaffold-free neocartilage toward the organization of native tissue using dynamic mechanical stimulation. Based on the post-natal maturation of native articular cartilage in the mechanical environment (23,43), we specifically hypothesized that the mechanical environment would induce development of the pericellular matrix and macromolecular reorganization of the collagen network. A secondary aim of this project was to develop advanced microscopy techniques with which to evaluate extracellular matrix reorganization including: [1] super-resolution microscopy (SRM) to measure the development of the pericellular matrix and [2] second harmonic generation (SHG) microscopy to quantify collagen fiber size, distribution, and alignment.

Our current understanding of the organization of the pericellular matrix stems from localization of proteins through immunohistochemistry with confocal imaging and identification of protein interactions through analytical biochemistry. To date, matrix biologists have generated vast libraries of reliable antibodies and immunohistochemical methods to identify antigens within the complex and organized extracellular matrix, yet the field has been limited by the relatively slow adoption of novel microscopy techniques with which to visualize and characterize spatial relationships of molecules, such as those of the PCM. Within the past decade, the advent of super-resolution microscopy techniques has enabled investigation of spatial relationships of intracellular molecules at the nanoscale (274,275), yet, to our knowledge, these techniques have only been applied to the extracellular matrix to evaluate the nanoscale organization of the glomerular basement membrane of the kidney (276) and, very recently, the molecular architecture of fibronectin fibril formation (277). To elucidate spatial relationships of molecules within the pericellular matrix of native human cartilage, we have been working in collaboration with Dr. Xiaolin Nan's laboratory at OHSU to develop a workflow to apply stochastic optical reconstruction microscopy (STORM) to probe for molecules with antibodies that we have optimized for use on native human articular cartilage in the Johnstone Laboratory. STORM is a technique that enables single molecule localization by targeting a molecule of interest with an antibody-based photoswitchable fluorophore that can be detected in the activated state and temporospatially resolved from neighboring fluorophores (275). Capture of individual fluorophores that are separated in time and space allows resolution of individual molecules that reside within the diffraction limit of light that limits resolution during traditional immunofluorescence imaging of cells and tissues (Figure 6.5). To achieve

characterization of native cartilage with STORM, we have optimized tissue processing and sectioning, antigen retrieval, antibody conditions, and imaging parameters to probe for a host of targets in the PCM, including type VI collagen, perlecan, fibronectin, laminin, and FGF2. We are now employing multi-stochastic STORM to image multiple targets simultaneously with photoswitchable fluorophores of differing excitation and emission wavelengths (Figure 6.6). We plan to build a map of the pericellular matrix in a combinatorial approach using dual-color STORM to infer relationships according to target pairs specified in Figure 6.7. Our eventual goal is to characterize the development of the PCM in scaffold-free neocartilage with reference to that of native tissue as a readout for *in vitro* maturation.

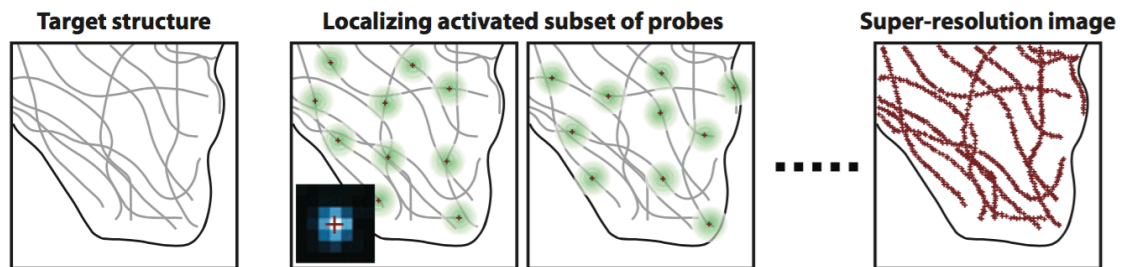


FIGURE 6.5 – PRINCIPLES OF SUPER-RESOLUTION MICROSCOPY.

The principle of stochastic optical reconstruction microscopy (STORM), photoactivated localization microscopy (PALM), and fluorescence photoactivation localization microscopy (FPALM). Different fluorescent probes marking the sample structure are activated at different time points, allowing subsets of fluorophores to be imaged without spatial overlap and to be localized to high precision. Iterating the activation and imaging process allows the position of many fluorescent probes to be determined and a super-resolution image is then reconstructed from the positions of a large number of localized probe molecules. The lower left inset of the second panel shows an experimental image of a single fluorescent dye (*blue*) and the high-precision localization of the molecule (*red cross*). Reproduced with permission from Huang et al. © 2009, Annual Reviews (275).

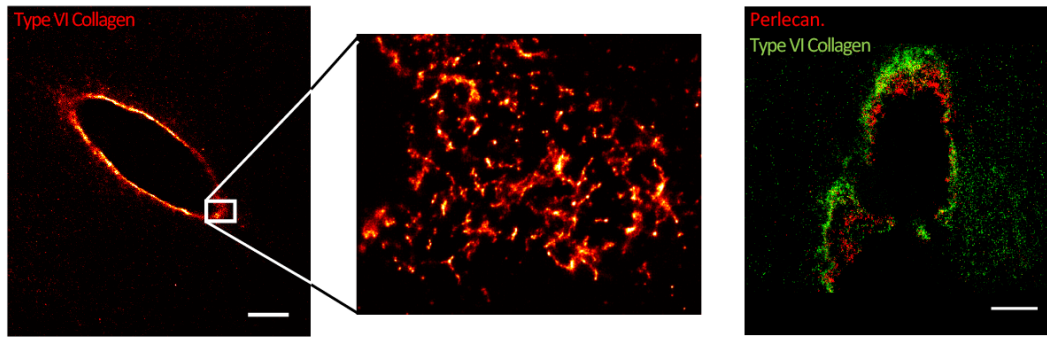


FIGURE 6.6 – SUPER-RESOLUTION MICROSCOPY OF THE PERICELLULAR MATRIX. SRM allows for resolution of individual antigens, including type VI collagen and perlecan, which can be spatially resolved in the pericellular matrix of native articular cartilage. Images compliments of Jing Wang and Dr. Xiaolin Nan, OHSU. Scale = 5 μ m.

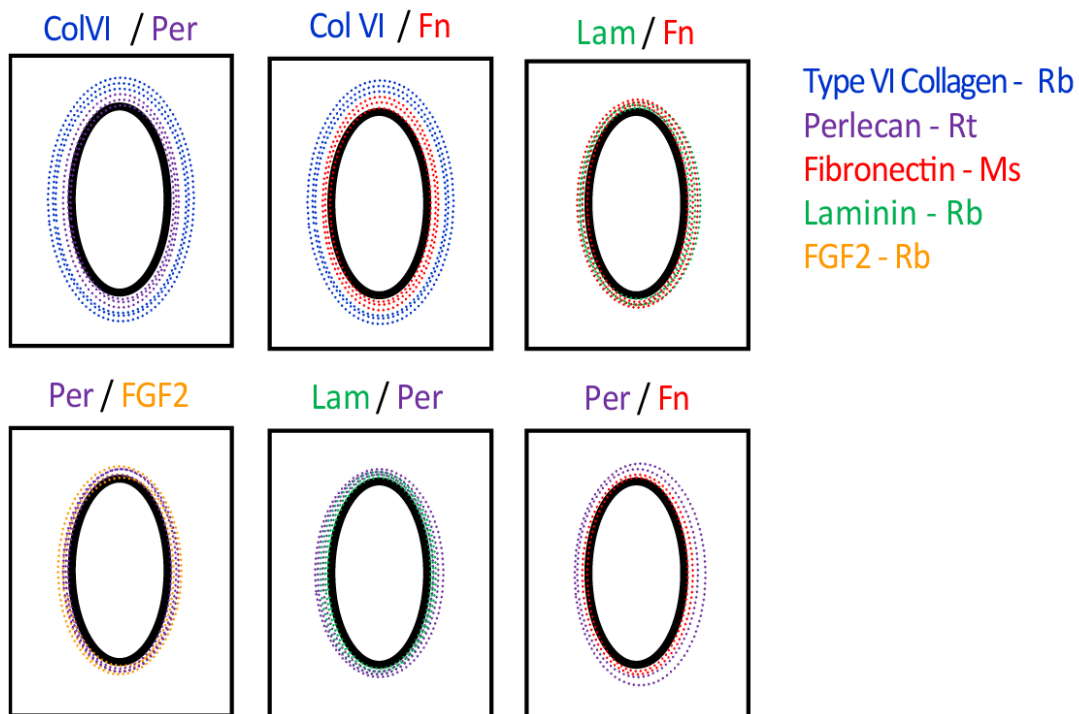


FIGURE 6.7 – SUPER-RESOLUTION MICROSCOPY EXPERIMENTAL DESIGN. Using multi-spectral super-resolution microscopy to resolve multiple antigens simultaneously, we intend to build a map of the pericellular matrix based on a combinatorial approach with paired targets. Target pairs were identified in fluorescent microscopy based on lack of cross-reactivity between primary antibodies for targets in native articular cartilage. Diagram compliments of Constance Pritchard, OHSU.

Just as the PCM is established during post-natal tissue maturation, so too is the collagen network organized into distinct zonal regions in response to the biomechanical environment. We seek to characterize collagen maturation of scaffold-free neocartilage during *in vitro* dynamic mechanical stimulation. Specifically, we intend to apply second harmonic generation (SHG) microscopy to quantify changes in collagen size, orientation, and distribution following mechanical stimulation. SHG is a non-linear optical process that can resolve the second-order symmetry and polarization of collagen (278). The ordered structure of collagen generates an emission pattern composed of forward and backward scattering photons, and photon detection allows for quantitation of fiber size and orientation based on the ratio of directional scattering (279). Integration of a confocal reflectance microscope into an SHG system allows for simultaneous detection of cells by collecting light that is reflected from cells within the dense extracellular matrix (280). In collaboration with Dr. Steven Jacques' laboratory at OHSU, we are developing methods to image both formalin-fixed paraffin-embedded (FFPE) sections and formalin-fixed whole tissue cross-sections of scaffold-free neocartilage for comparison with native cartilage. Our preliminary data suggest that the collagen matrix in native tissue may be too dense and mature to quantify collagen properties; however, we can resolve individual collagen fibers in scaffold-free neocartilage (Figure 6.8). Numerical methods for quantification of collagen properties are presently being developed by the Jacques Laboratory to afford a novel, yet important, metric to characterize maturation of scaffold-free neocartilage *in vitro*.

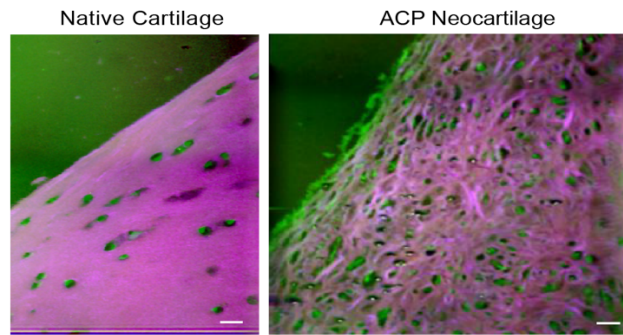


FIGURE 6.8 – SECOND HARMONIC GENERATION MICROSCOPY OF CARTILAGE.

Resolution and quantification of individual collagen structures in native articular cartilage with SHG microscopy is limited based on the signal from the mature and dense collagen network. Quantification of properties of the collagen network in scaffold-free neocartilage may be possible based on preliminary images acquired with SHG microscopy. Images compliments of Drs. Ravi Samatham and Steven Jacques, OHSU. Scale = 10 μ m.

6.4 FINAL REMARKS

Articular cartilage has limited capacity for intrinsic repair, and focal damage to the tissue in injury causes significant disability and leads to osteoarthritis when left unrepaired. Failures of both current surgical methods and biomaterial-based tissue engineering systems to generate a tissue of the correct structure and function to restore articular cartilage demands novel techniques to develop cell-based therapeutics. Scaffold-free neocartilage tissues generated from a single chondroprogenitor cell show promising characteristics of the articular cartilage tissue phenotype, but we still have a large amount of *in vitro* and *in vivo* work to optimize the system and to characterize the tissues prior to potential translation to clinical therapy. I am hopeful that, within my career, we will successfully apply decades of tissue engineering research to build neocartilage tissues that exhibit structure and function comparable to native tissue in order to surgically restore focal defects and to treat a large population suffering from articular cartilage pathology.

APPENDIX A:
ARTHROSCOPIC MECHANICAL CHONDROPLASTY
OF THE KNEE IS BENEFICIAL FOR TREATMENT OF FOCAL CARTILAGE LESIONS
IN THE ABSENCE OF CONCURRENT PATHOLOGY

Devon E. Anderson¹, Michael Rose¹, Aaron J. Wille¹, Jack Wiedrick², and Dennis C. Crawford¹

¹Oregon Health & Science University, Department of Orthopaedics & Rehabilitation

²Oregon Health & Science University, Biostatistics and Design Program

The objective of this study was to define the clinical efficacy of arthroscopic mechanical chondroplasty, which is the most commonly performed surgery to repair focal cartilage defects. We specifically sought to characterize outcomes following this surgery performed on a general population and in isolation, as it has only been studied as a primary treatment for osteoarthritis or in subjects who underwent concurrent procedures at the time of chondroplasty. This study has been presented in the following venues:

- Anderson, DE, M Rose, AJ Wille, J Wiedrick, and DC Crawford. *Arthroscopic Mechanical Chondroplasty of the Knee is Beneficial for Treatment of Focal Cartilage Lesions in the Absence of Concurrent Pathology*. Manuscript submitted to *Journal of Bone and Joint Surgery*. June 2016.
- Anderson, DE, M Rose, AJ Wille, J Wiedrick, and DC Crawford. *Mechanical Chondroplasty of the Knee is Beneficial for Treatment of Focal Cartilage Lesions in the Absence of Concurrent Pathology*. Abstract presented at the International Cartilage Repair Society (ICRS) World Congress, Sorrento, Italy. September 2016. Poster Presentation.

Devon executed all aspects of this project including study design, IRB approval, data collection, data analysis, and manuscript preparation.

Introduction: The high prevalence of focal articular cartilage lesions necessitates effective therapies to treat acute injuries before chronic degeneration. Arthroscopic mechanical debridement (chondroplasty) represents the majority of cartilage procedures; however, limited data exist regarding outcomes following chondroplasty performed in isolation of concurrent procedures or not as a primary treatment for osteoarthritis.

Methods: Subjects who met inclusion criteria were identified by billing data over a 3-year period in a single surgeon practice. Osteoarthritis was quantified through Kellgren-Lawrence (KL) scoring. Subjective patient reported outcomes (PROs), including IKDC, KOOS, WOMAC, Tegner, Lysholm, and VR-12, were collected pre-operatively and at follow-up intervals. International Cartilage Repair Society (ICRS) grade and lesion size were determined at arthroscopy. Linear regression was used to determine the effect of baseline score on final follow-up score. Correlated regression equations were used to assess the relationship of covariates and change in PRO scores.

Results: Sixty-two percent of subjects completed post-operative questionnaires at an average of 31.5 months (range 11.5-57). Average age was 37.3 ± 9.7 , average BMI was 27.7 ± 5.6 , and 62% were women. The average treated lesion size was $3.3 \pm 1.9 \text{ cm}^2$, 68% were ICRS grade 2 or 3, and 79% had a KL score of 0-2. On average, the cohort demonstrated significant improvement from baseline for almost all PRO scores. Regression analysis of change in score versus baseline indicated subjects with lower pre-operative scores gained more benefit from chondroplasty. Correlated regression equations showed high KL score and male sex had the most consistent positive effect on change in

PRO scores, high ICRS grade had the most consistent negative effect, and lesion size, age, and obesity did not have an effect. Eight subjects (15%) required further surgical intervention within the follow-up period.

Conclusions: The clinical efficacy of chondroplasty in isolation has not been studied. Our data show that on average, arthroscopic mechanical chondroplasty is beneficial to subjects. Additionally, response to surgical intervention is correlated to baseline PRO scores, sex, ICRS grade, and KL score.

Study Design: Case series; level of evidence, 4.

APPENDIX B:

NEOCART SURGICAL THERAPY AS A PRIMARY REPARATIVE

TREATMENT FOR KNEE CARTILAGE INJURY

Devon E. Anderson¹ Riley J. Williams III,² Thomas M. DeBerardino,³ Dean C. Taylor,⁴ C. Benjamin Ma,⁵ Marie S. Kane,¹ Dennis C. Crawford¹

¹Oregon Health & Science University, Department of Orthopaedics & Rehabilitation

²Hospital for Special Surgery, Sports Medicine Service / Institute for Cartilage Repair

³University of Connecticut, Department of Orthopaedic Surgery

⁴Duke University, Department of Orthopaedic Surgery

⁵University of California San Francisco, Department of Orthopaedic Surgery

The objective of this study was to define the clinical efficacy of a novel next-generation matrix-associated chondrocyte implantation (MACI) therapeutic in Phase II FDA clinical trials through objective clinical, subjective patient-reported, and magnetic resonance imaging outcomes. This work has been presented in the following venues:

- Anderson, DE, RJ Williams III, TM DeBerardino, DC Taylor, CB Ma, MS Kane, and DC Crawford. Magnetic Resonance Imaging (MRI) Characterization and Clinical Outcomes following NeoCart Surgical Therapy as a Primary Reparative Treatment for Knee Cartilage Injury. Manuscript accepted to *American Journal of Sports Medicine*. August 2016.
- Kane, MS, RJ Williams III, TM DeBerardino, DC Taylor, CB Ma, DE Anderson, and DC Crawford. NeoCart in Comparison to Microfracture after Five Years: A Report of Primary Outcome Measures at Study Conclusion from the “Exploratory” Phase II FDA Regulated Randomized Clinical Trial. Manuscript submitted to *Journal of Bone and Joint Surgery*. July 2016.

Devon executed data analysis, data interpretation, and manuscript preparation for these projects.

Study 1: Magnetic Resonance Imaging (MRI) Characterization and Clinical Outcomes following NeoCart Surgical Therapy as a Primary Reparative Treatment for Knee Cartilage Injury.

Introduction: Autologous cartilage tissue implants (ACTI), including the NeoCart implant, are intended to repair focal articular cartilage lesions. We report five-year follow-up clinical and MRI data for patients treated with NeoCart and identify the implant as an efficacious primary treatment for cartilage injury and a safe surgically applied cell-based therapeutic. We hypothesized that quantitative magnetic resonance imaging (MRI) analysis would reveal NeoCart tissue maturation through 5-year follow-up.

Methods: Patients with symptomatic full thickness cartilage lesions of the distal femoral condyle were treated with NeoCart in FDA clinical trials. Safety and efficacy were evaluated prospectively by MRI and clinical patient reported outcomes (PROs) through 60-month follow-up. Qualitative MRI metrics were quantified according to modified MOCART (magnetic resonance observation of cartilage repair tissue) criteria, with independent evaluation of repair tissue signal intensity. Subjective PROs and objective range of motion (ROM) were obtained at baseline and through 60 months.

Results: Twenty-nine patients treated with NeoCart were followed over 52 ± 15.5 (median=60) months. MOCART analyses indicated significant improvement ($p < 0.001$) in the cartilage quality from 3 to 24 months, with stabilization from 24 to 60 months. Signal intensity of the repair tissue evolved from hyperintense at early follow-up to isointense

after 6 months and to hypointense after 24 months. All PROs, including International Knee Documentation Committee (IKDC), Short Form (SF-36) Health Survey, and all 5 domains of the Knee Injury and Osteoarthritis Outcome Score (KOOS) significantly improved ($p < 0.001$) at all time points from 24 to 60 months and at final follow-up, when compared with baseline values. Significant decreases from baseline in VAS pain scores by 6 months were sustained through 5 years ($p < 0.0001$). ROM improved by 9 ± 10 degrees at final follow-up ($p < 0.0001$).

Conclusion: Longitudinal MRI analysis demonstrated NeoCart based repair tissue is durable and evolves over time, with corresponding improvement in clinical measures. Results from safety and exploratory clinical trials indicate that NeoCart is a safe and effective treatment for articular cartilage lesions through 5-year follow-up.

Study Design: Case series; level of evidence, 4.

Study 2: NeoCart in Comparison to Microfracture after Five Years: A Report of Primary Outcome Measures at Study Conclusion from the “Exploratory” Phase II FDA Regulated Randomized Clinical Trial.

Introduction: NeoCart, an autologous cartilage tissue-engineered implant, reduced pain and increased function compared with microfracture at 3-24 months following primary treatment of grade III ICRS cartilaginous knee lesions. We report the continued evaluation of the safety and efficacy of NeoCart in comparison to Microfracture through 5 years.

Methods: Patients with full thickness cartilage injury were randomized to NeoCart (n=21) or microfracture (n=9) treatment. Patient outcome surveys were assessed annually throughout the 5-year study.

Results: Average follow-up time was 51 ± 14 months. Adverse event rates did not differ between treatment arms. Mean age, injury acuity and lesion size were similar at baseline, although BMI and VAS pain scores were higher in the NeoCart cohort, and KOOS Sports & Recreation was higher in the microfracture cohort ($p < 0.05$). Outcome score change from baseline for the NeoCart cohort was greater than microfracture for the two study primary end points; IKDC at 1 and 2 years and KOOS Pain at 1, 3 and 4 years, as well as QOL, Symptoms, and Sports & Recreation until 2-4 years. At 5 years, IKDC score, KOOS Pain, ADL, and QOL, and SF-36 Physical scores for both treatment arms had improved significantly ($p < 0.05$) from baseline. These improvements for NeoCart were significant throughout the study period, while improvements for microfracture began later. The

NeoCart but not microfracture group also improved significantly in KOOS Symptoms, Sports & Recreation, and VAS scores. At final follow-up, the difference in change from baseline scores between the NeoCart and microfracture groups was only significant for VAS Average scores. Responder analysis identified significantly more NeoCart patients with clinical improvement at 1 year ($p=0.046$). All non-responders in the microfracture group dropped out prior to 5 years.

Conclusion: NeoCart implantation has a safety and efficacy profile over 5 years supporting further consideration of this therapy as a primary cartilage treatment.

Study Design: Randomized clinical trial; level of evidence, level 1.

APPENDIX C:
EFFECTS OF CELL DENSITY AND MEDIA VOLUME ON
CHONDROGENIC DIFFERENTIATION IN PHYSIOXIA

Introduction: Our laboratory has previously shown that chondrogenic differentiation of adult human-derived cells in a three-dimensional pellet culture largely depends on the oxygen tension within the *in vitro* culture system (178), likely because articular cartilage resides in a physiologically low oxygen environment (physioxia). The results in the literature, however, vary substantially with respect to the effect of lowered oxygen on chondrogenesis, and the variability becomes increasingly large when culture systems are scaled up (reviewed in chapters 3 & 4). Along with variability in results, we have identified that studies to evaluate pellet chondrogenesis in low oxygen also substantially vary in both cell seeding density and volume of chondrogenic medium, which provides nutrients for a chondrogenic fate. Thus, we hypothesized that variations in the ratio of cell density to media volume leads to significantly different anabolic capacity of cells during chondrogenic differentiation in pellet culture.

Methods: Human articular chondrocytes (n=4) were isolated from adult human donors and redifferentiated in pellet culture according to methods in Chapter 2. Cells were seeded at a density of 100K cells per pellet and maintained in increasing amounts of defined chondrogenic induction medium (60, 120, and 240 μ l) at either 20% (hyperoxic) or 2% (physioxic) oxygen over a 14-day differentiation period prior to harvest for biochemical analyses detailed in Chapter 2. Statistical analyses were performed with a one-way

ANOVA using Tukey's *post-hoc* analysis for multiple comparisons between different media volumes at a given oxygen level and with an unpaired t-test for comparison between oxygen levels at a given media volume.

Results: Relative to culture in hyperoxia for all media volumes, culture in physioxia significantly increased the total amount of glycosaminoglycans (GAG) produced by each pellet, an increase that was retained when normalized to DNA content (Figure C.1A, B). Lowering oxygen did not change total collagen content, measured by hydroxyproline residues per pellet, or DNA content (Figure C.1C, D, E). Only in physioxia, increasing the media volume significantly increased both the total GAG content and the total collagen content (Figure C.1A, C), but significance was not retained when these measures were normalized to DNA content (Figure C.1B, D).

Discussion: Consistent with our laboratory's previous study (178), we found that relative to culture in hyperoxia, culture in physioxia significantly enhanced the biochemical anabolism of GAGs, thus proteoglycans, but had no effect on collagen content. Adding to this previous finding, we found that increasing the media volume caused a significant increase in both GAGs and hydroxyproline. Taken together, we now know that the biochemical anabolism of chondrocytes during chondrogenic redifferentiation in 3D pellet culture is influenced not only by oxygen tension but also by overall nutrient availability. These findings indicate that cell seeding density and media volume are not trivial variables, and they may influence cellular response to other experimental variables, such as oxygen level. Consequently, I used this knowledge to employ the maximum possible media volume

(240 μ l) for all pellet culture studies (Chapter 3) and scaled the cell density to media volume ratio in development of the disc culture system (Chapter 4 & 5) used throughout this dissertation.

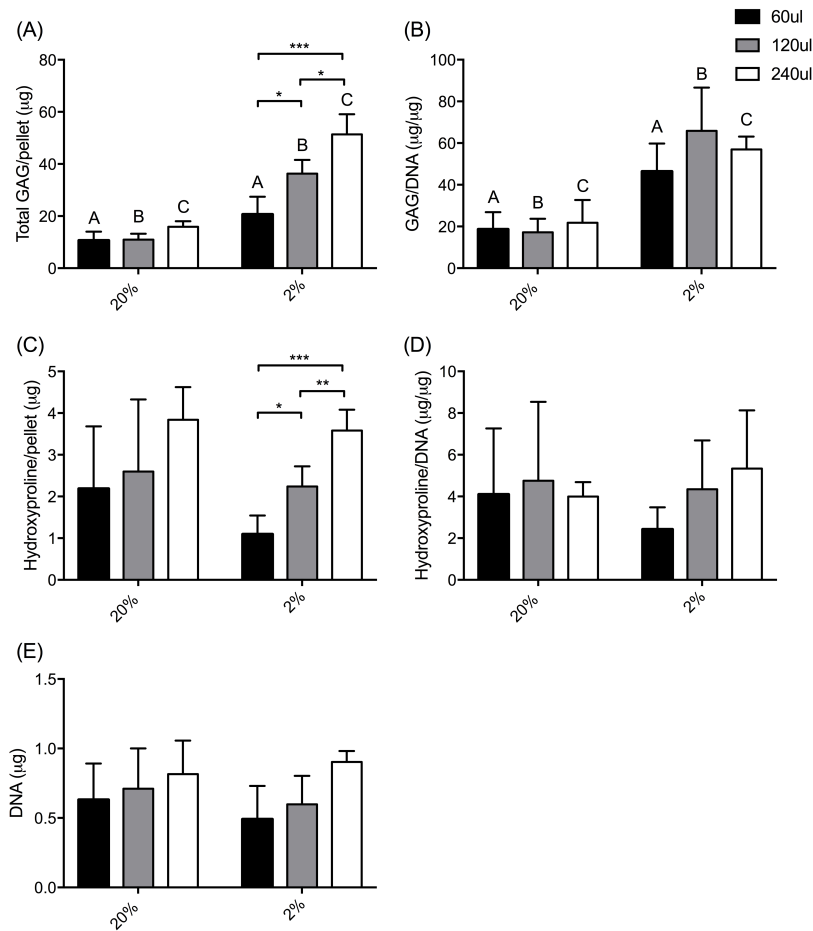


FIGURE C.1 – EFFECT OF CELL NUMBER PER MEDIA VOLUME ON CHONDROGENESIS. Quantitative measures of (A) total glycosaminoglycan (GAG) content, (B) GAG/DNA, (C) total hydroxyproline content per pellet as a readout for total collagen content, (D) hydroxyproline/DNA, and (E) DNA content of neocartilage pellets derived from healthy human articular chondrocytes demonstrate that both oxygen level and media volume influence extracellular matrix anabolism during chondrogenesis. Statistical significance was defined as * $p < 0.05$, ** $p < 0.01$, *** $p < 0.001$, and bars with matching letters (A, B, C) are significantly different from one another with $p < 0.05$.

APPENDIX D:

MESENCHYMAL STEM CELL-BASED SCAFFOLD-FREE NEOCARTILAGE

Introduction: Mesenchymal stem cells (MSCs) represent a widely available and easily harvested adult human cell source with which to potentially generate autologous tissues for connective tissue therapies. Since our laboratory first identified the conditions that drive MSCs chondrogenic differentiation *in vitro* (129,130), we have consistently seen that MSCs continue differentiation toward a hypertrophic chondrocyte lineage, marked by the production of type X collagen and matrix metalloproteinase 13 (MMP13). In contrast to these results, the original work to culture large-scale scaffold-free neocartilage tissues derived from MSCs in a Transwell-based system reported that the resultant tissue expressed minimal type X collagen (157). We sought to reproduce these methods in our scaffold-free system, with the primary aim to investigate the hypertrophic phenotype of adult human MSC-derived tissues following 28 days of scaffold-free tissue culture.

Methods: Bone marrow-derived MSCs were isolated from adult human donors, differentiated in scaffold-free disc culture, and assessed by qualitative histology and immunohistochemistry according to methods in Chapter 2.

Results: When cultured on a fibronectin-coated Transwell membrane, MSCs produced a thick discoid tissue that had proteoglycans distributed throughout the depth (Figure D.1). When probed for collagens by immunohistochemistry, MSC neocartilage exhibited even distribution of both type II and type X collagen throughout the depth. An acellular layer of

extracellular matrix at the basal surface of the tissues contained abundant fibronectin that the cells produced in response to extended culture on a fibronectin-coated membrane.

Discussion: When cultured in the scaffold-free system developed and utilized throughout this dissertation research, adult human bone marrow-derived MSCs formed a robust extracellular matrix with abundant proteoglycans and type II collagen; however, in contrast to prior studies that seeded human MSCs into scaffold-free tissue culture (156,157,162), we found that MSCs produce substantial type X collagen representative of the hypertrophic cartilage tissue phenotype. In the interest of producing a tissue representative of the articular cartilage tissue phenotype, we focused our subsequent studies on articular chondrocytes and tissue-derived chondroprogenitors that produce minimal, if any, type X collagen. Employing MSCs in the scaffold-free system, however, helped us to identify that the acellular matrix produced by all three cell types, when cultured for a 28 days in the Transwell insert, was composed of fibronectin. Based on this finding, we modified our methods to release the discs at day 10 of culture, prior to the secretion of a fibronectin-rich matrix between the tissues and the fibronectin-coated membrane; this change resulted in tissues that lacked the acellular layer upon harvest at 28 days. Ultimately, while MSCs may represent a cell source for tissue engineering human articular cartilage, our inability to control their progression toward hypertrophy limits the current utility of the cells for regeneration of stable articular cartilage.

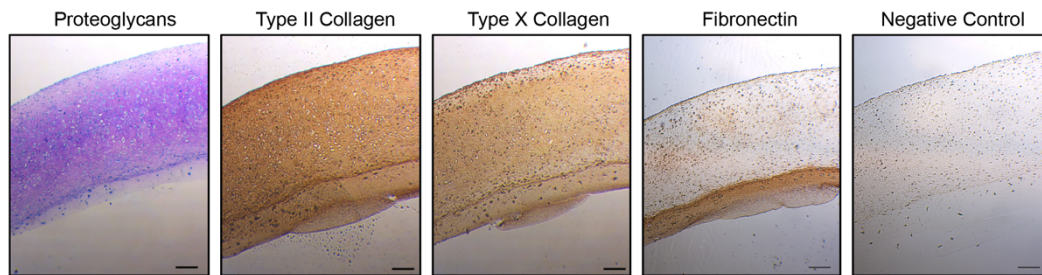


FIGURE D.1 – MESENCHYMAL STEM CELL-BASED SCAFFOLD-FREE NEOCARTILAGE. Representative histology and DAB immunohistochemistry to demonstrate the distribution of extracellular matrix molecules in scaffold-free neocartilage derived from adult human bone marrow-derived MSCs. Proteoglycans represented by toluidine blue staining of glycosaminoglycan side chains. Scale = 100 μ m.

REFERENCES

1. Mescher AL. Cartilage. In: Junqueira's Basic Histology, 14e. New York, NY: McGraw-Hill Education; 2016.
2. Archer CW, Dowthwaite GP, Francis-West P. Development of synovial joints. *Birth Defects Res C*. 2003;69(2):144–55.
3. Khan IM, Redman SN, Williams R, Dowthwaite GP, Oldfield SF, Archer CW. The Development of Synovial Joints. In: *Current Topics in Developmental Biology*. Elsevier; 2007. pp. 1–36.
4. Moskalewski S, Hyc A, Jankowska-Steifer E, Osiecka-Iwan A. Formation of synovial joints and articular cartilage. *Folia Morphol*. 2013;72(3):181–7.
5. Grassel S, Aszodi A, editors. *Cartilage*. Switzerland: Springer; 2016. 275 p.
6. Archer CW, Morrison H, Pitsillides AA. Cellular aspects of the development of diarthrodial joints and articular cartilage. *J Anat*. 1994;184:447–56.
7. Roddy KA, Prendergast PJ, Murphy P. Mechanical Influences on Morphogenesis of the Knee Joint Revealed through Morphological, Molecular and Computational Analysis of Immobilised Embryos. *PLoS ONE*. 2011;6(2):e17526–14.
8. Nowlan NC, Sharpe J, Roddy KA, Prendergast PJ, Murphy P. Mechanobiology of embryonic skeletal development: Insights from animal models. *Birth Defects Res C*. 2010;90(3):203–13.
9. Shea CA, Rolfe RA, Murphy P. The importance of foetal movement for coordinated cartilage and bone development in utero. *Bone Joint Res*. 2015;7:105–16.
10. Gilbert SF. *Developmental Biology*. 6 ed. Sunderland, MA: Sinauer Associates; 2006.
11. Long F, Ornitz DM. Development of the Endochondral Skeleton. *Cold Spring Harbor Perspectives in Biology*. 2013;5(1).
12. Park J, Gebhardt M, Golovchenko S, Perez-Branguli F, Hattori T, Hartmann C, et al. Dual pathways to endochondral osteoblasts: a novel chondrocyte-derived osteoprogenitor cell identified in hypertrophic cartilage. *Biol Open*. 2015;4(5):608–21.
13. Zhou X, Mark von der K, Henry S, Norton W, Adams H, de Crombrughe B. Chondrocytes Transdifferentiate into Osteoblasts in Endochondral Bone during Development, Postnatal Growth and Fracture Healing in Mice. *PLoS*

Genet. 2014;10(12):e1004820–0.

14. de Crombrughe B, Lefebvre V, KazuhisaNakashima. Regulatory mechanisms in the pathways of cartilage and bone formation. *Curr Opin Cell Biol.* 2001;13:721–7.
15. Pacifici M, Koyama E, Shibukawa Y, Wu C, Tamamura Y, Enomoto-Iwamoto M, et al. Cellular and Molecular Mechanisms of Synovial Joint and Articular Cartilage Formation. *Ann N Y Acad Sci.* 2006;1068(1):74–86.
16. Hayes AJ, MacPherson S, Morrison H, Dowthwaite GP, Archer CW. The development of articular cartilage: evidence for an appositional growth mechanism. *Anat Embryol.* 2001;203:469–79.
17. Dowthwaite GP, Bishop JC, Redman SN, Khan IM, Rooney P, Evans DJR, et al. The surface of articular cartilage contains a progenitor cell population. *J Cell Sci.* 2004;117(6):889–97.
18. Hunziker EB, Kapfinger E, Geiss J. The structural architecture of adult mammalian articular cartilage evolves by a synchronized process of tissue resorption and neof ormation during postnatal development. *Osteoarthr Cartilage.* 2007;15(4):403–13.
19. Williams R, Khan IM, Richardson K, Nelson L, McCarthy HE, Analbelsi T, et al. Identification and Clonal Characterisation of a Progenitor Cell Sub-Population in Normal Human Articular Cartilage. *PLoS ONE.* 2010;5(10):e13246.
20. Kozhemyakina E, Zhang M, Ionescu A, Ayturk UM, Ono N, Kobayashi A, et al. Identification of a Prg4-Expressing Articular Cartilage Progenitor Cell Population in Mice. *Arthritis Rheum.* 2015;67(5):1261–73.
21. Lefebvre V, Bhattaram P. Editorial: Prg4-Expressing Cells: Articular Stem Cells or Differentiated Progeny in the Articular Chondrocyte Lineage? *Arthritis Rheum.* 2015;67(5):1151–4.
22. Responde DJ, Lee JK, Hu JC, Athanasiou KA. Biomechanics-driven chondrogenesis: from embryo to adult. *FASEB J.* 2012;26(9):3614–24.
23. Gannon AR, Nagel T, Bell AP, Avery NC, Kelly DJ. Postnatal changes to the mechanical properties of articular cartilage are driven by the evolution of its collagen network. *Eur Cells Mater.* 2015;29:105–23.
24. Vinatier C, Mrugala D, Jorgensen C, Guicheux J, Noël D. Cartilage engineering: a crucial combination of cells, biomaterials and biofactors. *Trends Biotechnol.* 2009;27(5):307–14.
25. Van C Mow, Gu WY, Chen FH. Structure and Function of Articular Cartilage

- and Meniscus. In: Mow VC, Huijskes R, editors. *Basic Orthopaedic Biomechanics & Mechano-biology*. 3rd ed. Philadelphia: Lippincott Williams & Wilkins; 2005. pp. 181–258.
26. Chubinskaya S, Malfait A-M, Wimmer M. Form and Function of Articular Cartilage. In: O'Keefe RJ, Jacobs JJ, Chu CR, Einhorn TA, editors. *Orthopaedic Basic Science*. Rosemont, IL: AAOS; 2013. pp. 183–97.
 27. Heinegård D, Paulsson M. Structure and Metabolism of Proteoglycans. In: Piez KA, Reddi AH, editors. *Extracellular Matrix Biochemistry*. New York: Elsevier; 1984. pp. 277–328.
 28. Athanasiou KA. *Articular Cartilage Tissue Engineering*. Morgan & Claypool; 2010. 182 p.
 29. Hayes AJ, Tudor D, Nowell MA, Caterson B, Hughes CE. Chondroitin Sulfate Sulfation Motifs as Putative Biomarkers for Isolation of Articular Cartilage Progenitor Cells. *J Histochem Cytochem*. 2007;56(2):125–38.
 30. Klein TJ, Malda J, Sah RL, Hutmacher DW. Tissue engineering of articular cartilage with biomimetic zones. *Tissue Eng Pt B*. 2009;15(2):143–57.
 31. Hayes AJ, Hall A, Brown L, Tubo R, Caterson B. Macromolecular Organization and In Vitro Growth Characteristics of Scaffold-free Neocartilage Grafts. *J Histochem Cytochem*. 2007;55(8):853–66.
 32. Poole CA. Articular cartilage chondrons: form, function and failure. *J Anat*. 1997;191:1–13.
 33. Zhang Z. Chondrons and the Pericellular Matrix of Chondrocytes. *Tissue Eng Pt B*. 2014; 21(3)267-77.
 34. Thompson JC. *Netter's Concise Orthopaedic Anatomy*. 2nd ed. Philadelphia, PA: Elsevier; 2010.
 35. Heinegård D, Saxne T. The role of the cartilage matrix in osteoarthritis. *Nat Rev Rheumatol*. 2010;7(1):50–6.
 36. Mansour JM. Biomechanics of Cartilage. In: Oatis CA, editor. *Kinesiology: the mechanics and pathomechanics of human movement*. Lippincott, Williams & Wilkens; 2003. pp. 66–79.
 37. Brommer H, Brama PAJ, Laasanen MS, Helminen HJ, van Weeren PR, Jurvelin JS. Functional adaptation of articular cartilage from birth to maturity under the influence of loading: a biomechanical analysis. *Equine Vet J*. 2005;37(2):148–54.
 38. Quinn TM, Häuselmann HJ, Shintani N, Hunziker EB. Cell and matrix

- morphology in articular cartilage from adult human knee and ankle joints suggests depth-associated adaptations to biomechanical and anatomical roles. *Osteoarthr Cartilage*. 2013;21(12):1904–12.
39. Klein TJ, Chaudhry M, Bae WC, Sah RL. Depth-dependent biomechanical and biochemical properties of fetal, newborn, and tissue-engineered articular cartilage. *J Biomech*. 2007;40(1):182–90.
 40. Wong M, Carter DR. Articular cartilage functional histomorphology and mechanobiology: a research perspective. *Bone*. 2003;33(1):1–13.
 41. Flannery CREA. Articular Cartilage Superficial Zone Protein (SZP) Is Homologous to Megakaryocyte Stimulating Factor Precursor and Is a Multifunctional Proteoglycan with Potential Growth-Promoting, Cytoprotective, and Lubricating Properties in Cartilage Metabolism. *Biochem Bioph Res Co*. 1999;254:535–41.
 42. Wilusz RE, Sanchez-Adams J, Guilak F. The structure and function of the pericellular matrix of articular cartilage. *Matrix Biol*. 2014;39:25–32.
 43. Kvist AJ, Nyström A, Hultenby K, Sasaki T, Talts JF, Aspberg A. The major basement membrane components localize to the chondrocyte pericellular matrix — A cartilage basement membrane equivalent? *Matrix Biol*. 2008;27(1):22–33.
 44. Vincent TL, McLean CJ, Full LE, Peston D, Saklatvala J. FGF-2 is bound to perlecan in the pericellular matrix of articular cartilage, where it acts as a chondrocyte mechanotransducer. *Osteoarthr Cartilage*. 2007;15(7):752–63.
 45. Vincent TL, Hermansson MA, Hansen UN, Amis AA, Saklatvala J. Basic fibroblast growth factor mediates transduction of mechanical signals when articular cartilage is loaded. *Arthritis Rheum*. 2004;50(2):526–33.
 46. Zhang Z. Chondrons and the Pericellular Matrix of Chondrocytes. *Tissue Eng Pt B*. 2015;21(3):267–77.
 47. Youn I, Choi JB, Cao L, Setton LA, Guilak F. Zonal variations in the three-dimensional morphology of the chondron measured in situ using confocal microscopy. *Osteoarthr Cartilage*. 2006;14(9):889–97.
 48. Wilusz RE, DeFrate LE, Guilak F. A biomechanical role for perlecan in the pericellular matrix of articular cartilage. *Matrix Biol*. 2012;31(6):320–7.
 49. Briggs AM, Cross MJ, Hoy DG, Sánchez-Riera L, Blyth FM, Woolf AD, et al. Musculoskeletal Health Conditions Represent a Global Threat to Healthy Aging: A Report for the 2015 World Health Organization World Report on Ageing and Health. *Geront*. 2016;56(Suppl 2):S243–55.

50. Woolf AD, Erwin J, March L. The need to address the burden of musculoskeletal conditions. *Best Pract Res Cl Rh.* 2012;26(2):183–224.
51. Woolf AD, Pfleger B. Burden of major musculoskeletal conditions. *B World Health Organ.* 2003;81(9):1–11.
52. Yelin EH, Cisternas M, Watkins-Castillo SI. *The Burden of Musculoskeletal Diseases in the United States.* 3rd ed. Rosemont, IL: Bone & Joint Initiative; 2014. 2 p.
53. Hootman JM, Brault MW, Helmick CG, Theis KA, Armour BS. Prevalence and Most Common Causes of Disability Among Adults. *CDC Morbidity and Mortality Weekly Report.* 2009;58(16):421–6.
54. Grimm NL, Weiss JM, Kessler JI, Aoki SK. Osteochondritis Dissecans of the Knee. *Clin Sports Med.* 2014;33(2):181–8.
55. Komistek RD, Kane TR, Mahfouz M, Ochoa JA, Dennis DA. Knee mechanics: a review of past and present techniques to determine in vivo loads. *J Biomech.* 2005;38(2):215–28.
56. Aspden RM, Jeffrey JE, Burgin LV. Impact Loading of Articular Cartilage. *Osteoarthr Cartilage.* 2002;10(7):588–9.
57. McCormick F, Harris JD, Abrams GD, Frank R, Gupta A, Hussey K, et al. Trends in the Surgical Treatment of Articular Cartilage Lesions in the United States: An Analysis of a Large Private-Payer Database Over a Period of 8 Years. *Arthroscopy.* 2014;30(2):222–6.
58. Widuchowski W, Widuchowski J, Trzaska T. Articular cartilage defects: Study of 25,124 knee arthroscopies. *Knee.* 2007;14(3):177–82.
59. Hjelle K, Solheim E, Strand T, Muri R, Brittberg M. Articular cartilage defects in 1,000 knee arthroscopies. *Arthroscopy.* 2002;18(7):730–4.
60. Flanigan DC, Harris JD, TRINH TQ, Siston RA, BROPHY RH. Prevalence of Chondral Defects in Athletes' Knees. *Med Sci Sport Exer.* 2010;42(10):1795–801.
61. Heir S, Nerhus TK, Rotterud JH, Loken S, Ekeland A, Engebretsen L, et al. Focal Cartilage Defects in the Knee Impair Quality of Life as Much as Severe Osteoarthritis: A Comparison of Knee Injury and Osteoarthritis Outcome Score in 4 Patient Categories Scheduled for Knee Surgery. *Am J Sport Med.* 2010;38(2):231–7.
62. Jiang Y, Tuan RS. Origin and function of cartilage stem/progenitor cells in osteoarthritis. *Nat Rev Rheumatol.* 2014;11(4):206–12.

63. Barbour KE, Helmick CG, Theis KA, Murphy LB, Hootman JM, Brady TJ, et al. Prevalence of Doctor-Diagnosed Arthritis and Arthritis-Attributable Activity Limitation — United States, 2010–2012. *CDC Morbidity and Mortality Weekly Report*. 2013;62:1–24.
64. Murphy L, Schwartz TA, Helmick CG, Renner JB, Tudor G, Koch G, et al. Lifetime risk of symptomatic knee osteoarthritis. *Arthritis Rheum*. 2008;59(9):1207–13.
65. Murphy LB, Helmick CG, Schwartz TA, Renner JB, Tudor G, Koch GG, et al. One in four people may develop symptomatic hip osteoarthritis in his or her lifetime. *Osteoarthr Cartilage*. 2010;18(11):1372–9.
66. Vincent KR, Conrad BP, Fregly BJ, Vincent HK. The Pathophysiology of Osteoarthritis: A Mechanical Perspective on the Knee Joint. *Phys Med Rehabil*. 2012;4(5):S3–S9.
67. Arden N, Nevitt MC. Osteoarthritis: Epidemiology. *Best Pract Res Cl Rh*. 2006;20(1):3–25.
68. Brown TD, Johnston RC, Saltzman CL, Marsh JL, Buckwalter JA. Posttraumatic Osteoarthritis: A First Estimate of Incidence, Prevalence, and Burden of Disease. *J Orthop Trauma*. 2006;20(10):739–44.
69. Carbone A, Rodeo S. A review of current understanding of post-traumatic osteoarthritis resulting from sports injuries. *J Orthop Res*. 2016;In Press:1–25.
70. Anderson JM, Brown SA, Hoffman AS, Kowalski JB, Merritt K, Morrissey RF, et al. Implants, Devices, and Biomaterials: Issues Unique to this Field. In: Ratner BD, Hoffman AS, Schoen FJ, Lemons JE, editors. *Biomaterials Science*. San Diego, CA: Elsevier; 2004.
71. Moran CJ, Pascual-Garrido C, Chubinskaya S, Potter HG, Warren RF, Cole BJ, et al. Restoration of Articular Cartilage. *J Bone Joint Surg Am*. 2014;96(4):336–44.
72. Cole BJ, Pascual-Garrido C, Grumet RC. Surgical Management of Articular Cartilage Defects in the Knee. *J Bone Joint Surg*. 2009;91:1778–90.
73. Scillia AJ, Aune KT, Andrachuk JS, Cain EL, Dugas JR, Fleisig GS, et al. Return to Play After Chondroplasty of the Knee in National Football League Athletes. *Am J Sport Med*. 2015;43(3):663–8.
74. Montgomery SR, Foster BD, Ngo SS, Terrell RD, Wang JC, Petrigliano FA, et al. Trends in the surgical treatment of articular cartilage defects of the knee in the United States. *Knee Surg Sports Traumatol Arthrosc*. 2013;22(9):2070–5.

75. Mosely BJ, O'Malley K, Petersen NJ, Menke TJ, Brody BA, Kuykendall DH, et al. A controlled trial of arthroscopic surgery for osteoarthritis of the knee. *New Engl J Med.* 2002;347(2):81–8.
76. Spahn G, Hofmann GO, Engelhardt LV. Mechanical debridement versus radiofrequency in knee chondroplasty with concomitant medial meniscectomy: 10-year results from a randomized controlled study. *Knee Surg Sports Traumatol Arthrosc.* 2015;1–9.
77. Dervin GF, Stiell IG, Rody K, Grabowski J. Effect of Arthroscopic Débridement for Osteoarthritis of the Knee on Health-Related Quality of Life. *J Bone Joint Surg.* 2002;85(1):10–9.
78. Barber FA, Iwasko NG. Treatment of Grade III Femoral Chondral Lesions: Mechanical Chondroplasty Versus Monopolar Radiofrequency Probe. *Arthroscopy.* 2006;22(12):1312–7.
79. Merchan ECR, Galindo E. Arthroscope-Guided Surgery Versus Nonoperative Treatment for Limited Degenerative Osteoarthritis of the Femorotibial Joint in Patients Over 50 Years of Age: A Prospective Comparative Study. *Arthroscopy.* 1993;9(6):663–7.
80. Jackson RW. Arthroscopic surgery and a new classification system. *Am J Knee Surg.* 1998;11(1):51–4.
81. Kirkley A, Birmingham TB, Litchfield RB, Griffin R, Willits KR, Wong CJ, et al. A Randomized Trial of Arthroscopic Surgery for Osteoarthritis of the Knee. *New Engl J Med.* 2009;359(11):1097–107.
82. Tuan RS, Mauck RL. Articular Cartilage Repair and Regeneration. In: O'Keefe RJ, Jacobs JJ, Chu CR, Einhorn TA, editors. *Orthopaedic Basic Science.* Rosemont, IL: AAOS; 2013. pp. 309–27.
83. Mithoefer K, McAdams T, Williams RJ, Kreuz PC, Mandelbaum BR. Clinical Efficacy of the Microfracture Technique for Articular Cartilage Repair in the Knee: An Evidence-Based Systematic Analysis. *Am J Sport Med.* 2009;37(10):2053–63.
84. Orth P, Cucchiari M, Kohn D, Madry H. Alterations of the subchondral bone in osteochondral repair - translational data and clinical evidence. *Eur Cells Mater.* 2013;25:299–316.
85. Peterson L, Vasiliadis HS, Brittberg M, Lindahl A. Autologous Chondrocyte Implantation: A Long-term Follow-up. *Am J Sport Med.* 2010;38(6):1117–24.
86. Makris EA, Gomoll AH, Malizos KN, Hu JC, Athanasiou KA. Repair and tissue engineering techniques for articular cartilage. *Nat Rev Rheumatol.* 2014;11(1):21–34.

87. Wylie JD, Hartley MK, Kapron AL, Aoki SK, Maak TG. What Is the Effect of Matrices on Cartilage Repair? A Systematic Review. *Clin Orthop Relat R.* 2015;473(5):1673–82.
88. Crawford DC, Heveran CM, Cannon WD, Foo LF, Potter HG. An Autologous Cartilage Tissue Implant NeoCart for Treatment of Grade III Chondral Injury to the Distal Femur: Prospective Clinical Safety Trial at 2 Years. *Am J Sport Med.* 2009;37(7):1334–43.
89. Crawford DC, DeBerardino TM, Williams RJ. NeoCart, an Autologous Cartilage Tissue Implant, Compared with Microfracture for Treatment of Distal Femoral Cartilage Lesions. *J Bone Joint Surg Am.* 2012;94(11).
90. Bedi A, Feeley BT, Williams RJ. Management of Articular Cartilage Defects of the Knee. *J Bone Joint Surg.* 2010;92(4):994–1009.
91. Murphy CM, O'Brien FJ, Little DG, Schindeler A. Cell-Scaffold Interactions in the Bone Tissue Engineering Triad. *Eur Cells Mater.* 2013;26:120–32.
92. Chung C, Burdick JA. Engineering cartilage tissue. *Adv Drug Deliver Rev.* 2008;60(2):243–62.
93. Benya PD, Shaffer JD. Dedifferentiated chondrocytes reexpress the differentiated collagen phenotype when cultured in agarose gels. *Cell.* 1982 Aug;30(1):215–24.
94. Goessler UR, Bugert P, Bieback K, Baisch A, Sadick H, Verse T, et al. Expression of collagen and fiber-associated proteins in human septal cartilage during in vitro dedifferentiation. *Int J Mol Med.* 2004;14(6):1015–22.
95. Darling EM, Athanasiou KA. Rapid phenotypic changes in passaged articular chondrocyte subpopulations. *J Orthop Res.* 2005;23(2):425–32.
96. Goessler UR, Bieback K, Bugert P, Heller T, Sadick H, Hörmann K, et al. In vitro analysis of integrin expression during chondrogenic differentiation of mesenchymal stem cells and chondrocytes upon dedifferentiation in cell culture. *Int J Mol Med.* 2006;17(2):301–7.
97. Goessler UR, Bieback K, Bugert P, Naim R, Schafer C, Sadick H, et al. Human chondrocytes differentially express matrix modulators during in vitro expansion for tissue engineering. *Int J Mol Med.* 2005;16(4):509–15.
98. Goessler UR, Bugert P, Bieback K, Sadick H, Baisch A, Hörmann K, et al. In vitro analysis of differential expression of collagens, integrins, and growth factors in cultured human chondrocytes. *Otolaryngol Head Neck Surg.* 2006;134(3):510–5.
99. Malpeli M, Randazzo N, Cancedda R, Dozin B. Serum-free growth medium

- sustains commitment of human articular chondrocyte through maintenance of Sox9 expression. *Tissue Eng.* 2004;10(1-2):145–55.
100. Parsch D, Brümmendorf TH, Richter W, Fellenberg J. Replicative aging of human articular chondrocytes during ex vivo expansion. *Arthritis Rheum.* 2002;46(11):2911–6.
 101. Parsch D, Fellenberg J, Brümmendorf TH, Eschlbeck A-M, Richter W. Telomere length and telomerase activity during expansion and differentiation of human mesenchymal stem cells and chondrocytes. *J Mol Med.* 2004;82(1):49–55.
 102. Barbero A, Ploegert S, Heberer M, Martin I. Plasticity of clonal populations of dedifferentiated adult human articular chondrocytes. *Arthritis Rheum.* 2003;48(5):1315–25.
 103. Barbero A, Grogan S, Schäfer D, Heberer M, Mainil-Varlet P, Martin I. Age related changes in human articular chondrocyte yield, proliferation and post-expansion chondrogenic capacity. *Osteoarthr Cartilage.* 2004;12(6):476–84.
 104. Adkisson HD, Martin JA, Amendola RL, Milliman C, Mauch KA, Katwal AB, et al. The potential of human allogeneic juvenile chondrocytes for restoration of articular cartilage. *Am J Sport Med.* 2010;38(7):1324–33.
 105. Farr J, Cole BJ, Sherman S, Karas V. Particulated articular cartilage: CAIS and DeNovo NT. *J Knee Surg.* 2012;25(1):23–9.
 106. Adkisson HD, Milliman C, Zhang X, Mauch K, Maziarz RT, Streeter PR. Immune evasion by neocartilage-derived chondrocytes: Implications for biologic repair of joint articular cartilage. *Stem Cell Res.* 2010;4(1):57–68.
 107. Liu H, Zhao Z, Clarke RB, Gao J, Garrett IR, Margerrison EEC. Enhanced Tissue Regeneration Potential of Juvenile Articular Cartilage. *Am J Sport Med.* 2013;41(11):2658–67.
 108. Sommaggio R, Uribe-Herranz M, Marquina M, Costa C. Xenotransplantation of pig chondrocytes: therapeutic potential and barriers for cartilage repair. *Eur Cells Mater.* 2016;32:24–39.
 109. Niemietz T, Zass G, Hagmann S, Diederichs S, Gotterbarm T, Richter W. Xenogeneic transplantation of articular chondrocytes into full-thickness articular cartilage defects in minipigs: fate of cells and the role of macrophages. *Cell Tissue Res.* 2014;358(3):749–61.
 110. Stone KR, Walgenbach AW, Abrams JT, Nelson J, Gillett N, Galili U. Porcine and bovine cartilage transplants in cynomolgus monkey: I. A model for chronic xenograft rejection. *Transplantation.* 1997;63(5):640–5.

111. Owen M. Marrow stromal stem cells. *J Cell Sci Suppl.* 1988;10:63–76.
112. Caplan AI. The mesengenic process. *Clin Plast Surg.* 1994;21(3):429–35.
113. Pittenger MF, Mackay AM, Beck SC, Jaiswal RK, Douglas R, Mosca JD, et al. Multilineage potential of adult human mesenchymal stem cells. *Science.* 1999;284(5411):143–7.
114. Murray IR, West CC, Hardy WR, James AW, Park TS, Nguyen A, et al. Natural history of mesenchymal stem cells, from vessel walls to culture vessels. *Cell Mol Life Sci.* 2014;71(8):1353–74.
115. Dennis JE, Merriam A, Awadallah A, Yoo JU, Johnstone B, Caplan AI. A quadripotential mesenchymal progenitor cell isolated from the marrow of an adult mouse. *J Bone Miner Res.* 1999;14(5):700–9.
116. De Miguel MP, Fuentes-Julián S, Blázquez-Martínez A, Pascual CY, Aller MA, Arias J, et al. Immunosuppressive properties of mesenchymal stem cells: advances and applications. *Curr Mol Med.* 2012;12(5):574–91.
117. Adesida AB, Mulet-Sierra A, Jomha NM. Hypoxia mediated isolation and expansion enhances the chondrogenic capacity of bonemarrow mesenchymal stromal cells. *Stem Cell Res Ther.* 2012;3(2):9.
118. Russell KC, Lacey MR, Gilliam JK, Tucker HA, Phinney DG, O'Connor KC. Clonal analysis of the proliferation potential of human bone marrow mesenchymal stem cells as a function of potency. *Biotechnol Bioeng.* 2011;108(11):2716–26.
119. Russell KC, Phinney DG, Lacey MR, Barrilleaux BL, Meyertholen KE, O'Connor KC. In Vitro High-Capacity Assay to Quantify the Clonal Heterogeneity in Trilineage Potential of Mesenchymal Stem Cells Reveals a Complex Hierarchy of Lineage Commitment. *Stem Cells.* 2010;28(4):788–98.
120. Muraglia A, Cancedda R, Quarto R. Clonal mesenchymal progenitors from human bone marrow differentiate in vitro according to a hierarchical model. *J Cell Sci.* 2000;113(7):1161–6.
121. Stenderup K, Justesen J, Clausen C, Kassem M. Aging is associated with decreased maximal life span and accelerated senescence of bone marrow stromal cells. *Bone.* 2003;33:919–26.
122. Simonsen JL, Rosada C, Serakinici N, Justesen J, Stenderup K, Rattan SIS, et al. Telomerase expression extends the proliferative life-span and maintains the osteogenic potential of human bone marrow stromal cells. *Nat Biotechnol.* 2002;20:592–6.
123. Crisan M, Yap S, Casteilla L, Chen C-W, Corselli M, Park TS, et al. A

Perivascular Origin for Mesenchymal Stem Cells in Multiple Human Organs. *Cell Stem Cell*. 2008;3(3):301–13.

124. Herrmann M, Bara JJ, Sprecher CM, Menzel U, Jalowiec JM, Osinga R, et al. Pericyte plasticity - comparative investigation of the angiogenic and multilineage potential of pericytes from different human tissues. *Eur Cells Mater*. 2016;31:236–49.
125. Ito T, Sawada R, Fujiwara Y, Seyama Y, Tsuchiya T. FGF-2 suppresses cellular senescence of human mesenchymal stem cells by down-regulation of TGF- β 2. *Biochem Bioph Res Co*. 2007;359(1):108–14.
126. Ito T, Sawada R, Fujiwara Y, Tsuchiya T. FGF-2 increases osteogenic and chondrogenic differentiation potentials of human mesenchymal stem cells by inactivation of TGF- β signaling. *Cytotechnology*. 2007;56(1):1–7.
127. Cheng T, Yang C, Weber N, Kim HT, Kuo AC. Fibroblast growth factor 2 enhances the kinetics of mesenchymal stem cell chondrogenesis. *Biochem Bioph Res Co*. 2012;426(4):544–50.
128. Handorf AM, Li W-J. Fibroblast growth factor-2 primes human mesenchymal stem cells for enhanced chondrogenesis. *PLoS ONE*. 2011;6(7):e22887.
129. Johnstone B, Hering T, Caplan AI, Goldberg VM, Yoo JU. In vitro chondrogenesis of bone marrow-derived mesenchymal progenitor cells. *Exp Cell Res*. 1998;238:265–72.
130. Yoo JU, Barthel TS, Nishimura K, Solchaga L, Caplan AI, Goldberg VM, et al. The Chondrogenic Potential of Human Bone-Marrow-Derived Mesenchymal Progenitor Cells. *J Bone Joint Surg*. 1998;80-A(12):1745–57.
131. Derfoul A, Perkins GL, Hall DJ, Tuan RS. Glucocorticoids Promote Chondrogenic Differentiation of Adult Human Mesenchymal Stem Cells by Enhancing Expression of Cartilage Extracellular Matrix Genes. *Stem Cells*. 2006;24(6):1487–95.
132. Ustunel I, Ozenci AM, Sahin Z, Ozbey O, Acar N, Tanriover G, et al. The immunohistochemical localization of notch receptors and ligands in human articular cartilage, chondroprogenitor culture and ultrastructural characteristics of these progenitor cells. *Acta Histochemica*. 2008;110(5):397–407.
133. Jones PH, Watt FM. Separation of Human Epidermal Stem Cells from Transit Amplifying Cells on the Basis of Differences in Integrin Function and Expression. *Cell*. 1993;73:713–24.
134. Nelson L, McCarthy HE, Fairclough J, Williams R, Archer CW. Evidence of a Viable Pool of Stem Cells within Human Osteoarthritic Cartilage. *Cartilage*.

- 2014;5(4):203–14.
135. Alsalameh S, Amin R, Gemba T, Lotz M. Identification of mesenchymal progenitor cells in normal and osteoarthritic human articular cartilage. *Arthritis Rheum.* 2004;50(5):1522–32.
 136. Seol D, McCabe DJ, Choe H, Zheng H, Yu Y, Jang K, et al. Chondrogenic progenitor cells respond to cartilage injury. *Arthritis Rheum.* 2012;64(11):3626–37.
 137. Koelling S, Kruegel J, Irmer M, Path JR, Sadowski B, Miro X, et al. Migratory Chondrogenic Progenitor Cells from Repair Tissue during the Later Stages of Human Osteoarthritis. *Stem Cell.* 2009;4(4):324–35.
 138. Jayasuriya CT, Chen Q. Potential benefits and limitations of utilizing chondroprogenitors in cell-based cartilage therapy. *Connect Tissue Res.* 2015;56(4):265–71.
 139. McCarthy HE, Bara JJ, Brakspear K, Singhrao SK, Archer CW. The comparison of equine articular cartilage progenitor cells and bone marrow-derived stromal cells as potential cell sources for cartilage repair in the horse. *Vet J.* 2012;192(3):345–51.
 140. Frisbie DD, McCarthy HE, Archer CW, Barrett MF, McIlwraith CW. Evaluation of Articular Cartilage Progenitor Cells for the Repair of Articular Defects in an Equine Model. *J Bone Joint Surg.* 2015;97(6):484–93.
 141. Smith BD, Grande DA. The current state of scaffolds for musculoskeletal regenerative applications. *Nat Rev Rheumatol.* 2015;11(4):213–22.
 142. Athanasiou KA, Eswaramoorthy R, Hadidi P, Hu JC. Self-Organization and the Self-Assembling Process in Tissue Engineering. *Annu Rev Biomed Eng.* 2013;15(1):115–36.
 143. Ahrens PB, Solursh M, Reiter RS. Stage-related capacity for limb chondrogenesis in cell culture. *Dev Biol.* 1977;60(1):69–82.
 144. Caplan AI. Effects of a nicotinamide-sensitive teratogen 6-aminonicotinamide on chick limb cells in culture. *Exp Cell Res.* 1972;70(1):185–95.
 145. McLachlan JC. Self-assembly of structures resembling functional organs by pure populations of cells. *Tissue Cell.* 1986;18(3):313–20.
 146. Mello MA, Tuan RS. High density micromass cultures of embryonic limb bud mesenchymal cells: an in vitro model of endochondral skeletal development. *In Vitro Cell Dev B.* 1999;35:262–9.
 147. Denker AE, Nicoll SB, Tuan RS. Formation of cartilage-like spheroids by

- micromass cultures of murine C3H10T1/2 cells upon treatment with transforming growth factor- β 1. *Differentiation*. 1995;59(1):25–34.
148. Hu JC, Athanasiou KA. A Self-Assembling Process in Articular Cartilage Tissue Engineering. *Tissue Eng*. 2006;12(4):1–12.
 149. Novotny JE, Turka CM, Jeong C, Wheaton AJ, Li C, Presedo A, et al. Biomechanical and Magnetic Resonance Characteristics of a Cartilage-like Equivalent Generated in a Suspension Culture. *Tissue Eng*. 2006;12(10):2755–64.
 150. Foty RA, Steinberg MS. The differential adhesion hypothesis: a direct evaluation. *Dev Biol*. 2005;278(1):255–63.
 151. Singh P, Schwarzbauer JE. Fibronectin and stem cell differentiation - lessons from chondrogenesis. *J Cell Sci*. 2012;125(16):3703–12.
 152. Ofek G, Revell CM, Hu JC, Allison DD, Grande-Allen KJ, Athanasiou KA. Matrix Development in Self-Assembly of Articular Cartilage. *PLoS ONE*. 2008;3(7):e2795.
 153. Makris EA, Hu JC, Athanasiou KA. Hypoxia-induced collagen crosslinking as a mechanism for enhancing mechanical properties of engineered articular cartilage. *Osteoarthr Cartilage*. 2013;21(4):634–41.
 154. Kraft JJ, Jeong C, Novotny JE, Seacrist T, Chan G, Domzalski M, et al. Effects of Hydrostatic Loading on a Self-Aggregating, Suspension Culture-Derived Cartilage Tissue Analog. *Cartilage*. 2011;2(3):254–64.
 155. Mohanraj B, Farran AJ, Mauck RL, Dodge GR. Time-dependent functional maturation of scaffold-free cartilage tissue analogs. *J Biomech*. 2014;47(9):2137–42.
 156. Murphy MK, Huey DJ, Hu JC, Athanasiou KA. TGF- β 1, GDF-5, and BMP-2 Stimulation Induces Chondrogenesis in Expanded Human Articular Chondrocytes and Marrow-Derived Stromal Cells. *Stem Cells*. 2015;33(3):762–73.
 157. Murdoch AD, Grady LM, Ablett MP, Katopodi T, Meadows RS, Hardingham TE. Chondrogenic Differentiation of Human Bone Marrow Stem Cells in Transwell Cultures: Generation of Scaffold-Free Cartilage. *Stem Cells*. 2007;25(11):2786–96.
 158. Lee WD, Hurtig MB, Kandel RA, Stanford WL. Membrane Culture of Bone Marrow Stromal Cells Yields Better Tissue Than Pellet Culture for Engineering Cartilage-Bone Substitute Biphasic Constructs in a Two-Step Process. *Tissue Eng Pt C Met*. 2011;17(9):939–48.

159. Qu C, Lindeberg H, Ylärinne JH, Lammi MJ. Five percent oxygen tension is not beneficial for neocartilage formation in scaffold-free cell cultures. *Cell Tissue Res.* 2012;348(1):109–17.
160. Rutgers M, Saris DB, Vonk LA, van Rijen MH, Akrum V, Langeveld D, et al. Effect of Collagen Type I or Type II on Chondrogenesis by Cultured Human Articular Chondrocytes. *Tissue Eng Pt A.* 2013;19(1-2):59–65.
161. DuRaine GD, Brown WE, Hu JC, Athanasiou KA. Emergence of Scaffold-Free Approaches for Tissue Engineering Musculoskeletal Cartilages. *Ann Biomed Eng.* 2014;43(3):543–54.
162. Bhumiratana S, Eton RE, Oungoulian SR, Wan LQ, Ateshian GA, Vunjak-Novakovic G. Large, stratified, and mechanically functional human cartilage grown in vitro by mesenchymal condensation. *Proc Natl Acad Sci.* 2014;111(19):6940-5.
163. Tuli R, Tuli S, Nandi S, Huang X, Manner PA, Hozack WJ, et al. Transforming growth factor-beta-mediated chondrogenesis of human mesenchymal progenitor cells involves N-cadherin and mitogen-activated protein kinase and Wnt signaling cross-talk. *J Biol Chem.* 2003;278(42):41227–36.
164. Kwon H, Paschos NK, Hu JC, Athanasiou K. Articular cartilage tissue engineering: the role of signaling molecules. *Cell Mol Life Sci.* 2016;73(6):1173–94.
165. Ornitz DM, Marie PJ. Fibroblast growth factor signaling in skeletal development and disease. *Gene Dev.* 2015;29(14):1463–86.
166. Solchaga LA, Penick K, Porter JD, Goldberg VM, Caplan AI, Welter JF. FGF-2 enhances the mitotic and chondrogenic potentials of human adult bone marrow-derived mesenchymal stem cells. *J Cell Physiol.* 2005;203(2):398–409.
167. Im H-J, Maddasani P, Natarajan V, Schmid TM, Block JA, Davis F, et al. Basic Fibroblast Growth Factor Stimulates Matrix Metalloproteinase-13 via the Molecular Cross-talk between the Mitogen-activated Protein Kinases and Protein Kinase C Pathways in Human Adult Articular Chondrocytes. *J Biol Chem.* 2007;282(15):11110–21.
168. Alexander S, Watt F, Sawaji Y, Hermansson M, Saklatvala J. Activin A is an anticatabolic autocrine cytokine in articular cartilage whose production is controlled by fibroblast growth factor 2 and NF- κ B. *Arthritis Rheum.* 2007;56(11):3715–25.
169. Chia S-L, Sawaji Y, Burleigh A, McLean C, Inglis J, Saklatvala J, et al. Fibroblast growth factor 2 is an intrinsic chondroprotective agent that

- suppresses ADAMTS-5 and delays cartilage degradation in murine osteoarthritis. *Arthritis Rheum.* 2009;60(7):2019–27.
170. Hakki SS, Hakki EE, Nohutcu RM. Regulation of matrix metalloproteinases and tissue inhibitors of matrix metalloproteinases by basic fibroblast growth factor and dexamethasone in periodontal ligament cells. *J Periodontal Res.* 2009;44(6):794–802.
171. Johnstone B, Alini M, Cucchiari M, Dodge GR, Eglin D, Guilak F, et al. Tissue Engineering for Articular Cartilage Repair - The State of the Art. *Eur Cells Mater.* 2013;25:248–67.
172. Carreau A, Hafny-Rahbi BE, Matejuk A, Grillon C, Kieda C. Why is the partial oxygen pressure of human tissues a crucial parameter? Small molecules and hypoxia. *J Cell Mol Med.* 2011;15(6):1239–53.
173. Spencer JA, Ferraro F, Roussakis E, Klein A, Wu J, Runnels JM, et al. Direct measurement of local oxygen concentration in the bone marrow of live animals. *Nature.* 2014;508(7495):269–73.
174. Lund-Olesen K. Oxygen tension in synovial fluids. *Arthritis Rheum.* 1970;13(6):769–76.
175. Brighton CT, Heppenstall RB. Oxygen tension in zones of the epiphyseal plate, the metaphysis and diaphysis. An in vitro and in vivo study in rats and rabbits. *J Bone Joint Surg Am.* 1971;53(4):719–28.
176. Lafont JE. Lack of oxygen in articular cartilage: consequences for chondrocyte biology. *Int J Exp Pathol.* 2010;91(2):99–106.
177. Murphy CL, Thomas BL, Vaghjiani RJ, Lafont JE. HIF-mediated articular chondrocyte function: prospects for cartilage repair. *Arthritis Res Ther.* 2009;11(213):1–7.
178. Markway BD, Cho H, Johnstone B. Hypoxia promotes redifferentiation and suppresses markers of hypertrophy and degeneration in both healthy and osteoarthritic chondrocytes. *Arthritis Res Ther.* 2013;15(4):R92.
179. Responde DJ, Lee JK, Hu JC, Athanasiou KA. Biomechanics-driven chondrogenesis: from embryo to adult. *FASEB J.* 2012;26(9):3614–24.
180. O'Connor CJ, Case N, Guilak F. Mechanical regulation of chondrogenesis. *Stem Cell Res Ther.* 2013;4(4):61.
181. Buschmann MD, Gluzband YA, Grodzinsky AJ, Hunziker EB. Mechanical compression modulates matrix biosynthesis in chondrocyte/agarose culture. *J Cell Sci.* 1995;108:1497–508.

182. Mauck RL, Byers BA, Yuan X, Tuan RS. Regulation of Cartilaginous ECM Gene Transcription by Chondrocytes and MSCs in 3D Culture in Response to Dynamic Loading. *Biomech Model Mechanobiol*. 2006;6(1-2):113–25.
183. Huang AH, Farrell MJ, Kim M, Mauck R. Long-term dynamic loading improves the mechanical properties of chondrogenic mesenchymal stem cell-laden hydrogels. *Eur Cells Mater*. 2010;19:72–85.
184. Huang AH, Baker BM, Ateshian GA, Mauck RL. Sliding contact loading enhances the tensile properties of mesenchymal stem cell-seeded hydrogels. *Eur Cells Mater*. 2012;24:29–45.
185. Grad S, Eglin D, Alini M, Stoddart MJ. Physical Stimulation of Chondrogenic Cells In Vitro: A Review. *Clin Orthop Relat R*. 2011;469(10):2764–72.
186. Markway BD, Cho H, Zilberman-Rudenko J, Holden P, McAlinden A, Johnstone B. Hypoxia-inducible factor 3-alpha expression is associated with the stable chondrocyte phenotype. *J Orthop Res*. 2015;33(11):1561–70.
187. Mauck R, Yuan X, TUAN R. Chondrogenic differentiation and functional maturation of bovine mesenchymal stem cells in long-term agarose culture. *Osteoarthr Cartilage*. 2006;14(2):179–89.
188. Gawlitta D, van Rijen MHP, Schrijver EJM, Alblas J, Dhert WJA. Hypoxia Impedes Hypertrophic Chondrogenesis of Human Multipotent Stromal Cells. *Tissue Eng Pt A*. 2012;18(19-20):1957–66.
189. Duval E, Baugé C, Andriamanalijaona R, Bénateau H, Leclercq S, Dutoit S, et al. Molecular mechanism of hypoxia-induced chondrogenesis and its application in in vivo cartilage tissue engineering. *Biomaterials*. 2012;33(26):6042–51.
190. Leijten J, Georgi N, Moreira Teixeira L, van Blitterswijk CA, Post JN, Karperien M. Metabolic programming of mesenchymal stromal cells by oxygen tension directs chondrogenic cell fate. *Proc Natl Acad Sci*. 2014;111(38):13954–9.
191. Felka T, SchAfer R, Schewe B, Benz K, Aicher WK. Hypoxia reduces the inhibitory effect of IL-1beta on chondrogenic differentiation of FCS-free expanded MSC. *Osteoarthr Cartilage*. 2009;17(10):1368–76.
192. Muller J, Benz K, Ahlers M, Gaissmaier C, Mollenhauer J. Hypoxic conditions during expansion culture prime human mesenchymal stromal precursor cells for chondrogenic differentiation in three-dimensional cultures. *Cell Transplant*. 2011;20(10):1589–602.
193. Bornes TD, Jomha NM, Mulet-Sierra A, Adesida AB. Hypoxic culture of bone marrow-derived mesenchymal stromal stem cells differentially enhances in

- vitro chondrogenesis within cell-seeded collagen and hyaluronic acid porous scaffolds. *Stem Cell Res Ther.* 2015;6(1):1–18.
194. Markway BD, Tan G-K, Brooke G, Hudson JE, Cooper-White JJ, Doran MR. Enhanced Chondrogenic Differentiation of Human Bone Marrow-Derived Mesenchymal Stem Cells in Low Oxygen Environment Micropellet Cultures. *Cell Transplant.* 2011;19(1):29–42.
 195. Meretoja VV, Dahlin RL, Wright S, Kasper FK, Mikos AG. The effect of hypoxia on the chondrogenic differentiation of co-cultured articular chondrocytes and mesenchymal stem cells in scaffolds. *Biomaterials.* 2013;34(17):4266–73.
 196. Gerter R, Kruegel J, Miosge N. New insights into cartilage repair — The role of migratory progenitor cells in osteoarthritis. *Matrix Biol.* 2012;31(3):206–13.
 197. Khan IM, Bishop JC, Gilbert S, Archer CW. Clonal chondroprogenitors maintain telomerase activity and Sox9 expression during extended monolayer culture and retain chondrogenic potential. *Osteoarthr Cartilage.* 2009;17(4):518–28.
 198. Mareddy S, Dhaliwal N, Crawford R, Xiao Y. Stem Cell-Related Gene Expression in Clonal Populations of Mesenchymal Stromal Cells from Bone Marrow. *Tissue Eng Pt A.* 2010;16(2):749–58.
 199. Pilgaard L, Lund P, Duroux M, Fink T, Ulrich-Vinther M, Søballe K, et al. Effect of oxygen concentration, culture format and donor variability on in vitro chondrogenesis of human adipose tissue-derived stem cells. *Regen Med.* 2009;4(4):539–48.
 200. Katopodi T, Tew SR, Clegg PD, Hardingham TE. The influence of donor and hypoxic conditions on the assembly of cartilage matrix by osteoarthritic human articular chondrocytes on Hyalograft matrices. *Biomaterials.* 2009;30(4):535–40.
 201. Farrell MJ, Shin JJ, Smith LJ, Mauck RL. Functional consequences of glucose and oxygen deprivation on engineered mesenchymal stem cell-based cartilage constructs. *Osteoarthr Cartilage.* 2015;23(1):134–42.
 202. Girkontaite I, Frischholz S, Lammi P, Wagner K, Swoboda B, Aigner T, et al. Immunolocalization of Type X Collagen in Normal Fetal and Adult Osteoarthritic Cartilage with Monoclonal Anti- bodies. *Matrix Biol.* 1996;15:231–8.
 203. Wagner K, Poschl E, Turnay J, Baik J-M, Pihlajaniemi T, Frischholz S, et al. Coexpression of α and β subunits of prolyl 4-hydroxylase stabilizes the triple helix of recombinant human type X collagen. *Biochem J.* 2000;352:907–11.

204. Saito T, Fukai A, Mabuchi A, Ikeda T, Yano F, Ohba S, et al. Transcriptional regulation of endochondral ossification by HIF-2 α during skeletal growth and osteoarthritis development. *Nat Med.* 2010;16(6):678–86.
205. Yang S, Kim J, Ryu J-H, Oh H, Chun C-H, Kim BJ, et al. Hypoxia-inducible factor-2 α is a catabolic regulator of osteoarthritic cartilage destruction. *Nat Med.* 2010;16(6):687–93.
206. Ruan MZC, Erez A, Guse K, Dawson B, Bertin T, Chen Y, et al. Proteoglycan 4 Expression Protects Against the Development of Osteoarthritis. *Sci Trans Med.* 2013;5(176):176ra34–4.
207. Lafont JE, Talma S, Hopfgarten C, Murphy CL. Hypoxia Promotes the Differentiated Human Articular Chondrocyte Phenotype through SOX9-dependent and -independent Pathways. *J Biol Chem.* 2007;283(8):4778–86.
208. Duval E, Leclercq S, Elissalde J-M, Demoor M, Galéra P, Boumédiène K. Hypoxia-inducible factor 1 α inhibits the fibroblast-like markers type I and type III collagen during hypoxia-induced chondrocyte redifferentiation. *Arthritis Rheum.* 2009;60(10):3038–48.
209. Erler JT, Bennewith KL, Nicolau M, Dornhöfer N, Kong C, Le Q-T, et al. Lysyl oxidase is essential for hypoxia-induced metastasis. *Nature.* 2006;440(7088):1222–6.
210. Hatta T, Kishimoto KN, Okuno H, Itoi E. Oxygen Tension Affects Lubricin Expression in Chondrocytes. *Tissue Eng Pt A.* 2014;20(19-20):2720–7.
211. Mhanna R, Öztürk E, Schlink P, Zenobi-Wong M. Probing the microenvironmental conditions for induction of superficial zone protein expression. *Osteoarthr Cartilage.* 2013;21(12):1924–32.
212. Bentovim L, Amarilio R, Zelzer E. HIF1 α is a central regulator of collagen hydroxylation and secretion under hypoxia during bone development. *Development.* 2012;139(23):4473–83.
213. Aspden RM. Fibre reinforcing by collagen in cartilage and soft connective tissues. *Proc Royal Soc London.* 2004;B:195–200.
214. Naumann A, Dennis JE, Aigner J, Coticchia J, Arnold J, Berghaus A, et al. Tissue Engineering of Autologous Cartilage Grafts in Three- Dimensional in vitro Macroaggregate Culture System. *Tissue Eng.* 2004;10(11/12):1695–706.
215. Elder SH, Cooley AJ, Borazjani A, Sowell BL, To H, Tran SC. Production of Hyaline-like Cartilage by Bone Marrow Mesenchymal Stem Cells in a Self-Assembly Model. *Tissue Eng Pt A.* 2009;15:3025–36.
216. Mayer-Wagner S, Schiergens TS, Sievers B, Docheva D, Betz OB, Jansson V,

- et al. Membrane-Based Cultures Generate Scaffold-Free Neocartilage In Vitro: Influence of Growth Factors. *Tissue Eng Pt A*. 2010;16(2):513–21.
217. Whitney GA, Mera H, Weidenbecher M, Awadallah A, Mansour JM, Dennis JE. Methods for Producing Scaffold-Free Engineered Cartilage Sheets from Auricular and Articular Chondrocyte Cell Sources and Attachment to Porous Tantalum. *BioResearch*. 2012;1(4):157–65.
218. Singh P, Schwarzbauer JE. Fibronectin matrix assembly is essential for cell condensation during chondrogenesis. *J Cell Sci*. 2014;127(20):4420–8.
219. Neumann AJ, Alini M, Archer CW, Stoddart MJ. Chondrogenesis of Human Bone Marrow-Derived Mesenchymal Stem Cells Is Modulated by Complex Mechanical Stimulation and Adenoviral-Mediated Overexpression of Bone Morphogenetic Protein 2. *Tissue Eng Pt A*. 2013;19(11-12):1285–94.
220. Munir S, Foldager CB, Lind M, Zachar V, Søballe K, Koch TG. Hypoxia enhances chondrogenic differentiation of human adipose tissue-derived stromal cells in scaffold-free and scaffold systems. *Cell Tissue Res*. 2013;355(1):89-102.
221. Armstrong JPK, Shakur R, Horne JP, Dickinson SC, Armstrong CT, Lau K, et al. Artificial membrane-binding proteins stimulate oxygenation of stem cells during engineering of large cartilage tissue. *Nat Commun*. 2016;6:1–6.
222. Avery NC, Sims TJ, Bailey AJ. Quantitative Determination of Collagen Cross-links. In: *Methods in Molecular Biology*. Even-Ram S, Artym V, editors. *Extracellular Matrix Protocols*. Totowa, NJ: Humana Press; 2009. pp. 103–21.
223. Wilson B, Novakofski KD, Donocoff RS, Liang YXA, Fortier LA. Telomerase Activity in Articular Chondrocytes Is Lost after Puberty. *Cartilage*. 2014;5(4):215–20.
224. Zhou S, Cui Z, Urban JPG. Factors influencing the oxygen concentration gradient from the synovial surface of articular cartilage to the cartilage-bone interface: A modeling study. *Arthritis Rheum*. 2004;50(12):3915–24.
225. Zhou C, Zheng H, Seol D, Yu Y, Martin JA. Gene expression profiles reveal that chondrogenic progenitor cells and synovial cells are closely related. *J Orthop Res*. 2014;32(8):981–8.
226. Mikic B, Isenstein AL, Chhabra A. Mechanical Modulation of Cartilage Structure and Function during Embryogenesis in the Chick. *Ann Biomed Eng*. 2004;32(1):18–25.
227. Chan EF, Harjanto R, Asahara H, Inoue N, Masuda K, Bugbee WD, et al. Structural and Functional Maturation of Distal Femoral Cartilage and Bone

- During Postnatal Development and Growth in Humans and Mice. *Orthop Clin North Am.* 2012;43(2):173–85.
228. Meller R, Schiborra F, Brandes G, Knobloch K, Tschernig T, Hankemeier S, et al. Postnatal maturation of tendon, cruciate ligament, meniscus and articular cartilage: A histological study in sheep. *Ann Anat.* 2009;191(6):575–85.
229. Williamson AK, Chen AC, Masuda K, Thonar EJMA, Sah RL. Tensile mechanical properties of bovine articular cartilage: Variations with growth and relationships to collagen network components. *J Orthop Res.* 2003;21(5):872–80.
230. Gannon AR, Nagel T, Bell AP, Avery NC, Kelly DJ. The changing role of the superficial region in determining the dynamic compressive properties of articular cartilage during postnatal development. *Osteoarthr Cartilage.* 2015;23(6):975–84.
231. Khan IM, Francis L, Theobald PS, Perni S, Young RD, Prokopovich P, et al. In vitro growth factor-induced bio engineering of mature articular cartilage. *Biomaterials.* 2013;34(5):1478–87.
232. Khan IM, Evans SL, Young RD, Blain EJ, Quantock AJ, Avery N, et al. Fibroblast growth factor 2 and transforming growth factor β 1 induce precocious maturation of articular cartilage. *Arthritis Rheum.* 2011;63(11):3417–27.
233. Vincent T, Hermansson M, Bolton M, Wait R, Saklatvala J. Basic FGF mediates an immediate response of articular cartilage to mechanical injury. *Proc Natl Acad Sci.* 2002;99(12):8259–64.
234. Chong K-W, Chanalaris A, Burleigh A, Jin H, Watt FE, Saklatvala J, et al. Fibroblast Growth Factor 2 Drives Changes in Gene Expression Following Injury to Murine Cartilage In Vitro and In Vivo. *Arthritis Rheum.* 2013;65(9):2346–55.
235. Alexander S, Watt F, Sawaji Y, Hermansson M, Saklatvala J. Activin A is an anticatabolic autocrine cytokine in articular cartilage whose production is controlled by fibroblast growth factor 2 and NF- κ B. *Arthritis Rheum.* 2007;56(11):3715–25.
236. Yan D, Chen D, Im H-J. Fibroblast growth factor-2 promotes catabolism via FGFR1-Ras-Raf-MEK1/2-ERK1/2 axis that coordinates with the PKC δ pathway in human articular chondrocytes. *J Cell Biochem.* 2012;113(9):2856–65.
237. Komori T. Signaling networks in RUNX2-dependent bone development. *J Cell Biochem.* 2011;112(3):750–5.

238. Egli RJ, Wernike E, Grad S, Luginbhl R. Physiological Cartilage Tissue Engineering: Effect of Oxygen and Biomechanics. *Int Rev Cel Mol Bio.* 2011;289:37–87.
239. Jeon JE, Schrobback K, Hutmacher DW, Klein TJ. Dynamic compression improves biosynthesis of human zonal chondrocytes from osteoarthritis patients. *Osteoarthr Cartilage.* 2012;20(8):906–15.
240. Tran SC, Cooley AJ, Elder SH. Effect of a mechanical stimulation bioreactor on tissue engineered, scaffold-free cartilage. *Biotechnol Bioeng.* 2011;108(6):1421–9.
241. Huey DJ, Athanasiou KA. Tension-Compression Loading with Chemical Stimulation Results in Additive Increases to Functional Properties of Anatomic Meniscal Constructs. *PLoS ONE.* 2011;6(11):e27857–9.
242. MacBarb RF, Chen AL, Hu JC, Athanasiou KA. Engineering functional anisotropy in fibrocartilage neotissues. *Biomaterials.* 2013;34(38):9980–9.
243. Elder BD, Athanasiou KA. Effects of Temporal Hydrostatic Pressure on Tissue-Engineered Bovine Articular Cartilage Constructs. *Tissue Eng Pt A.* 2009;15(5):1151–8.
244. Kelly T-AN, Roach BL, Weidner ZD, Mackenzie-Smith CR, O'Connell GD, Lima EG, et al. Tissue-engineered articular cartilage exhibits tension–compression nonlinearity reminiscent of the native cartilage. *J Biomech.* 2013;46(11):1784–91.
245. Mauck RL, Soltz MA, Wang CCB, Wong DD, Chao P-HG, Valhmu WB, et al. Functional Tissue Engineering of Articular Cartilage Through Dynamic Loading of Chondrocyte-Seeded Agarose Gels. *J Biomech Eng.* 2000;122:252–60.
246. Neumann AJ, Gardner OFW, Williams R, Alini M, Archer CW, Stoddart MJ. Human Articular Cartilage Progenitor Cells Are Responsive to Mechanical Stimulation and Adenoviral-Mediated Overexpression of Bone-Morphogenetic Protein 2. *PLoS ONE.* 2015;10(8):e0136229–17.
247. MacBarb RF, Makris EA, Hu JC, Athanasiou KA. A chondroitinase-ABC and TGF-B1 treatment regimen for enhancing the mechanical properties of tissue-engineered fibrocartilage. *Acta Biomaterialia.* 2013;9(1):4626–34.
248. Barr L, Getgood A, Guehring H, Rushton N, Henson FMD. The effect of recombinant human fibroblast growth factor-18 on articular cartilage following single impact load. *J Orthop Res.* 2014;32(7):923–7.
249. Chuang CY, Lord MS, Melrose J, Rees MD, Knox SM, Freeman C, et al. Heparan Sulfate-Dependent Signaling of Fibroblast Growth Factor 18 by

- Chondrocyte-Derived Perlecan. *Biochemistry*. 2010;49(26):5524–32.
250. Haque T, Nakada S, Hamdy RC. A review of FGF18: Its expression, signaling pathways and possible functions during embryogenesis and post-natal development. *Histol Histopathol*. 2006;22:97–105.
251. De Caro F, Bisicchia S, Amendola A, Ding L. Large Fresh Osteochondral Allografts of the Knee: A Systematic Clinical and Basic Science Review of the Literature. *Arthroscopy*. 2015;31(4):757–65.
252. Buchtova M, Oralova V, Aklian A, Masek J, Vesela I, Ouyang Z, et al. Fibroblast growth factor and canonical WNT/ β -catenin signaling cooperate in suppression of chondrocyte differentiation in experimental models of FGFR signaling in cartilage. *Biochimica et Biophysica Acta*. 2015;1852(5):839–50.
253. Israsena N, Hu M, Fu W, Kan L, Kessler JA. The presence of FGF2 signaling determines whether β -catenin exerts effects on proliferation or neuronal differentiation of neural stem cells. *Dev Biol*. 2004;268(1):220–31.
254. Zhou B, Liu Y, Kahn M, Ann DK, Han A, Wang H, et al. Interactions Between Beta-Catenin and Transforming Growth Factor-Beta Signaling Pathways Mediate Epithelial-Mesenchymal Transition and Are Dependent on the Transcriptional Co-activator cAMP-response Element-binding Protein (CREB)-binding Protein (CBP). *J Biol Chem*. 2012;287(10):7026–38.
255. Sato M. Upregulation of the Wnt/Beta-catenin Pathway Induced by Transforming Growth Factor-Beta in Hypertrophic Scars and Keloids. *Acta Derm Venereol*. 2006;86(4):300–7.
256. Yasuhara R, Ohta Y, Yuasa T, Kondo N, Hoang T, Addya S, et al. Roles of beta-catenin signaling in phenotypic expression and proliferation of articular cartilage superficial zone cells. *Lab Invest*. 2011 Oct 3;91(12):1739–52.
257. Koyama E, Shibukawa Y, Nagayama M, Sugito H, Young B, Yuasa T, et al. A distinct cohort of progenitor cells participates in synovial joint and articular cartilage formation during mouse limb skeletogenesis. *Dev Biol*. 2008;316(1):62–73.
258. Zhu M, Tang D, Wu Q, Hao S, Chen M, Xie C, et al. Activation of β -Catenin Signaling in Articular Chondrocytes Leads to Osteoarthritis-Like Phenotype in Adult β -Catenin Conditional Activation Mice. *J Bone Miner Res*. 2009;24(1):12–21.
259. Nalesso G, Thomas BL, Sherwood JC, Yu J, Addimanda O, Eldridge SE, et al. WNT16 antagonises excessive canonical WNT activation and protects cartilage in osteoarthritis. *Ann Rheum Dis*. 2016;24:S364.
260. Inui A, Iwakura T, Hari Reddi A. Regulation of lubricin/superficial zone

- protein by Wnt signalling in bovine synoviocytes. *J Tissue Eng Regen Med.* 2013;10(2):172–7.
261. Murphy MK, Huey DJ, Reimer AJ, Hu JC, Athanasiou KA. Enhancing Post-Expansion Chondrogenic Potential of Costochondral Cells in Self-Assembled Neocartilage. *PLoS ONE.* 2013;8(2):e56983.
262. Revell CM, Reynolds CE, Athanasiou KA. Effects of Initial Cell Seeding in Self Assembly of Articular Cartilage. *Ann Biomed Eng.* 2008;36(9):1441–8.
263. Mesallati T, Buckley CT, Kelly DJ. Engineering articular cartilage-like grafts by self-assembly of infrapatellar fat pad-derived stem cells. *Biotechnol Bioeng.* 2014;111(8):1–13.
264. Shepherd D, Seedhom BB. Thickness of human articular cartilage in joints of the lower limb. *Ann Rheum Dis.* 1998;58:27–34.
265. Bahney CS, Hu DP, Taylor AJ, Ferro F, Britz HM, Hallgrímsson B, et al. Stem Cell-Derived Endochondral Cartilage Stimulates Bone Healing by Tissue Transformation. *J Bone Miner Res.* 2014;29(5):1269–82.
266. Fisher MB, Henning EA, Söegaard NB, Dodge GR, Steinberg DR, Mauck RL. Maximizing cartilage formation and integration via a trajectory-based tissue engineering approach. *Biomaterials.* 2014;35(7):2140–8.
267. Khan IM, Gilbert SJ, Singhrao SK, Duance VC, Archer CW. Cartilage Integration: Evaluation of the Reasons for Failure of Integration During Cartilage Repair. *Eur Cells Mater.* 2008;16:26–39.
268. Nemoto H, Watson D, Masuda K. Transplantation of Tissue-Engineered Cartilage in an Animal Model (Xenograft and Autograft): Construct Validation. In: *Methods in Molecular Biology*; vol. 1340. Doran PM, editor. *Cartilage Tissue Engineering.* London: Humana Press; 2015. pp. 247–59.
269. Fisher MB, Belkin NS, Milby AH, Henning EA, Bostrom M, Kim M, et al. Cartilage Repair and Subchondral Bone Remodeling in Response to Focal Lesions in a Mini-Pig Model: Implications for Tissue Engineering. *Tissue Eng Pt A.* 2015;21(3-4):850–60.
270. Mauck RL, Nicoll SB, Seyhan SL, Ateshian GA, Hung CT. Synergistic Action of Growth Factors and Dynamic Loading for Articular Cartilage Tissue Engineering. *Tissue Eng.* 2004;9(4):597–611.
271. Kisiday JD, Jin M, DiMicco MA, Kurz B, Grodzinsky AJ. Effects of dynamic compressive loading on chondrocyte biosynthesis in self-assembling peptide scaffolds. *J Biomech.* 2004;37(5):595–604.
272. Waldman SD, Spiteri CG, Gryn timer MD, Pilliar RM, Kandel RA. Long-Term

- Intermittent Compressive Stimulation Improves the Composition and Mechanical Properties of Tissue-Engineered Cartilage. *Tissue Eng.* 2004;10(9/10):1323–31.
273. Natenstedt J, Kok AC, Dankelman J, Tuijthof GJ. What quantitative mechanical loading stimulates in vitro cultivation best? *J Exp Orthop.* 2015;2(1):1–15.
274. Marx V. Is super-resolution microscopy right for you? *Nat Rev Rheumatol.* 2013;10(12):1157–63.
275. Huang B, Bates M, Zhuang X. Super-Resolution Fluorescence Microscopy. *Annu Rev Biochem.* 2009;78(1):993–1016.
276. Suleiman H, Zhang L, Roth R, Heuser JE, Miner JH, Shaw AS, et al. Nanoscale protein architecture of the kidney glomerular basement membrane. *eLife.* 2013;2:e01149.
277. Früh SM, Ries J, Schoen I, Vogel V. Molecular architecture of native fibronectin fibrils. *Nat Commun.* 2015;6:1–10.
278. Chaudhary R, Campbell KR, Tilbury KB, Vanderby R Jr., Block WF, Kijowski R, et al. Articular cartilage zonal differentiation via 3D Second-Harmonic Generation imaging microscopy. *Connect Tissue Res.* 2015;56(2):76–86.
279. Chen X, Nadiarynkh O, Plotnikov S, Campagnola PJ. Second harmonic generation microscopy for quantitative analysis of collagen fibrillar structure. *Nat Protoc.* 2012;7(4):654–69.
280. Paddock S. Confocal Reflection Microscopy: The “Other” Confocal Mode. *BioTechniques.* 2002;32(2):274–8.